MATHEMATICAL MORPHOLOGY IN GEOSCIENCES AND GISci

B.S. DAYA SAGAR

http://www.isibang.ac.in/~bsdsagar

Systems Science and Informatics Unit (SSIU)

Indian Statistical Institute-Bangalore Centre

INDIAN STATISTICAL INSTITUTE

Bangalore Centre

Systems Science and Informatics Unit (SSIU)

29th September 2014

Centre for Earth & Space Sciences, UoH, Hyderabad

FOUNDING FATHERS OF

MATHEMATICAL MORPHOLOGY

Georges Matheron Jean Serra

My Connection Degree

First degree separation with Jean Serra

Two-degree separation with Georges Matheron
(through SVLN Rao and Jean Serra)

SVLN Rao (v. 31, no. 2, *Mathematical Geosciences; Associate Editor for MG 1975-77*).

Motivation

To understand the dynamical behavior of a phenomenon or a process, development of a good **spatiotemporal model** is essential. To develop a good spatiotemporal model, well-**analyzed** and well-**reasoned information** that could be **extracted / retrieved** from spatial and/or temporal data are important ingredients.

Mathematical Morphology is one of the better choices to deal with all these key aspects mentioned.

Mathematical Morphology in Spatial Informatics

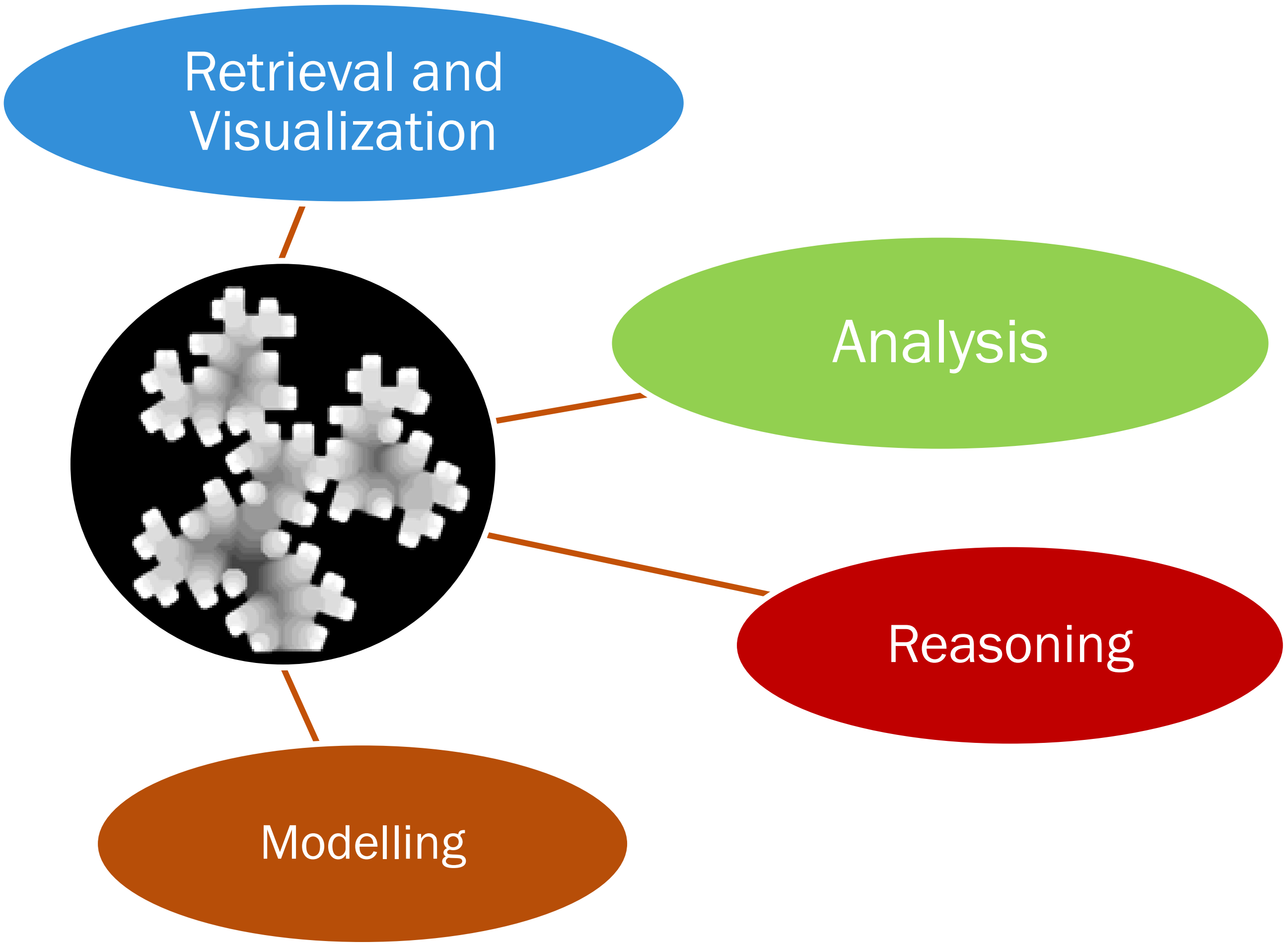

Outline

Basic description of Multivalued Functions (e.g.: Terrestrial Data)

Mathematical Morphology in Image Analysis and Spatial Informatics

Retrieval of unique phenomena (e.g. Networks), Analysis and quantitative characterization of unique phenomena and processes via various metrics

Spatial interpolation, Spatio-temporal modeling, spatial reasoning, spatial information visualization

Digital Elevation Models

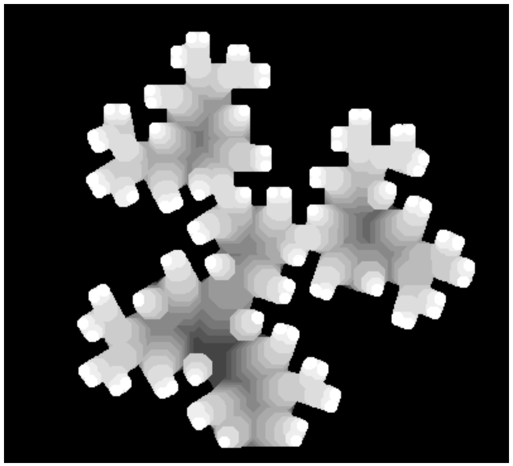

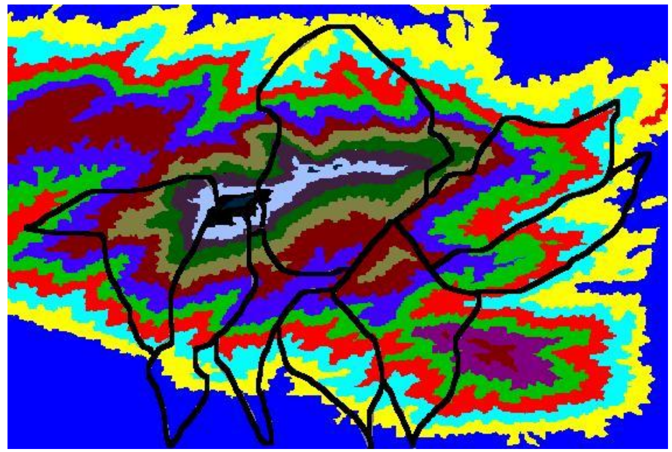

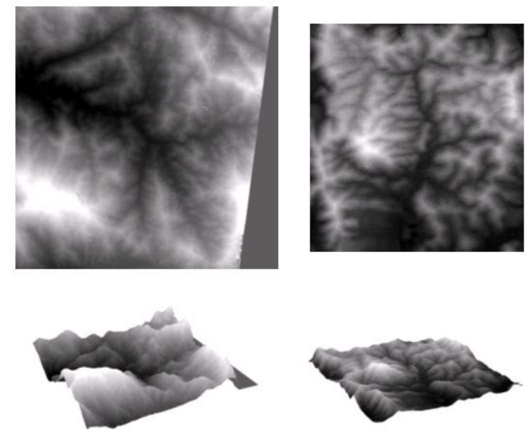

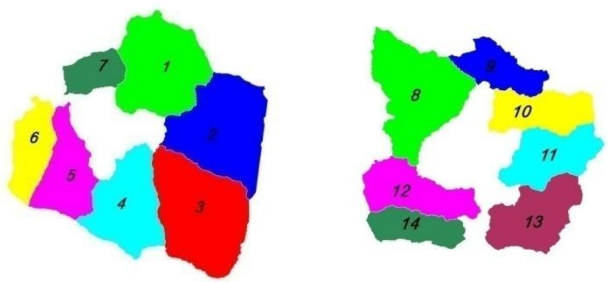

I. Mathematical Morphology

Binary Mathematical Morphology

Grayscale Morphology

Mathematical Morphology: Recent Advances

- Graph Mathematical Morphology
- Adaptive Mathematical Morphology

Concepts, Techniques & Tools

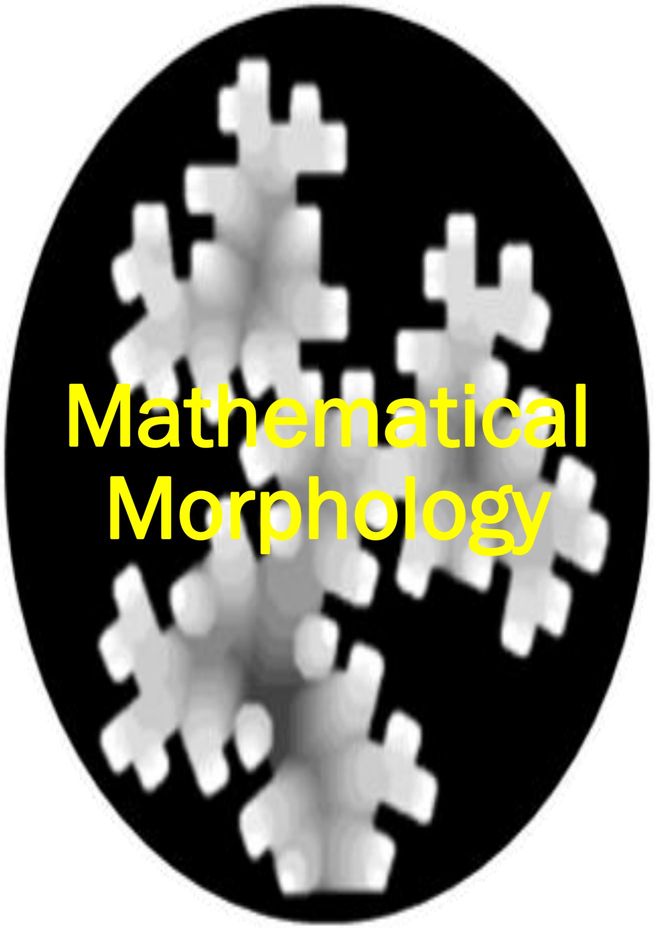

- Morphological Skeletonization
- Multiscale operations, Hierarchical segmentation
- Recursive Morphological Pruning
- Hit-or-Miss Transformation
- Morphological Thinning
- Morphological Reconstruction
- Watersheds
- Morphological shape decomposition
- Granulometries
- Hausdorff dilation (erosion) distance
- Morphological interpolation
- Directional Distances
- SKIZ and WSKIZ

Mathematical Morphological Operations

The mathematical morphological transformations useful to develop elegant algorithms to address the challenges in relation to Image Analysis and Spatial Informatics include:

- Morphological Erosion
- Morphological Dilation
- Morphological Opening
- Morphological Closing
- Multiscale Morphological Operations
- Hit-or-Miss Transformation
- Morphological Thinning , Thickening, Pruning
- Geodesic Morphological Operations
- Morphological Skeletonization
- Skeletonization by Zones of Influence
- Weighted Skeletonization by Zones of Influence
- Granulometries and Anti-Granulometries
- Morphological Distances
- Hausdorff Dilation Distances
- Hausdorff Erosion Distances
- Morphological Interpolations and Extrapolations
- The implementations of the aforementioned transformations binary, grayscale, graph and geodesic domains

Spatial Data : Various Representations

Functions (DEMs, Satellite Images, Microscopic Images etc)

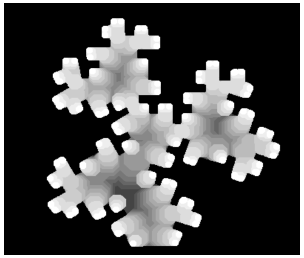

Sets (Thresholded Elevation regions, Binary images decomposed from images)

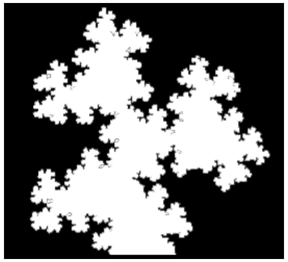

Skeletons (Unique topological networks)

Basic Transformations

- Mathematical Morphology
  - Dilation
  - Erosion
  - Opening
  - Closing

Mathematical Morphology (cont)

Binary MM

- Binary erosion transformation of *X* by structuring element, *B*
  - the set of points *s* such that the translated B_x is contained in the original set *X*, and is equivalent to intersection of all the translates.
  - $X \ominus B = \{x: B_x \subseteq X\} = \bigcap_{b \in B} X_{-b}$
- Binary dilation transformation of *X* by *B*
  - the set of all those points *s* such that the translated B_x intersects *X*, and is equivalent to the union of all translates.
  - $X \oplus B = \{x: B_x \cap X \not\subseteq \emptyset\} = \bigcup_{b \in B} X_b$
- The dilation with an elementary structuring template expands the set with a uniform layer of elements, while the erosion operator eliminates a layer from the set.
- Multiscale erosions and dilations are

  - $(X \ominus B) \ominus B \ominus \ldots \ominus B = (X \ominus nB)$,

  - $(X \oplus B) \oplus B \oplus \ldots \oplus B = (X \oplus nB)$,

  where $nB = B \oplus B \oplus \ldots \oplus B$ and *n* is the number of transformation cycles.

Mathematical Morphology (cont)

Binary MM (cont)

- By employing erosion and dilation of *X* by *B*, opening and closing transformations are further represented as:
  - $X \circ B = ((X \ominus B) \oplus B))$
  - $X \bullet B = ((X \oplus B) \ominus B))$
- After eroding *X* by *B*, the resultant eroded version is dilated to achieve the opened version of *X* by *B*.
- Similarly, closed version of *X* by *B* is obtained by first performing dilation on *X* by *B* and followed by erosion on the resultant dilated version.
- Multiscale opening and closing transformations are implemented by performing erosions and dilations recursively as shown below.

  - $(X \circ nB) = [(X \ominus nB) \oplus nB)]$,

  - $(X \bullet nB) = [(X \oplus nB) \ominus nB)]$,

  where *n* is the number of transformations cycles.

Mathematical Morphology (cont)

Greyscale MM

- Greyscale dilation and erosion operations - expansion and contractions respectively
- Let *f*(*x*,*y*) be a function on Z^2, and *B* be a fixed structuring element of size one. The erosion of *f*(*x*) by *B* replaces the value of *f* at a pixel (*x*, *y*) by the minima values of the image in the window defined by the structuring template *B*

$$(f \ominus B)(x,y) = \min_{(i,j)\in B} \{ f(x+i, y+j) \}$$

- The dilation of *f*(*x*) by *B* replaces the value of *f* at a pixel (*x*, *y*) by the maxima values of the image in the window defined by the structuring template *B*

$$(f \oplus B)(x,y) = \max_{(i,j)\in B} \{ f(x-i, y-j) \}$$

- In other words, ($f \ominus B$) and ($f \oplus B$) can be obtained by computing *minima* and *maxima* over a moving template *B*, respectively.
- Erosion is the dual of dilation :
  - Eroding foreground pixels is equivalent to dilating the background pixels.

Mathematical Morphology (cont)

Grey-scale MM (cont)

- Opening and closing are both based on the dilation and erosion transformations.
- Opening of *f* by *B* is achieved by eroding *f* and followed by dilating with respect to *B*, $(f \circ B) = [(f \ominus B) \oplus B]$,
- Closing of *f* by *B* is defined as the dilation of *f* by *B* followed by erosion with respect to B, $(f \bullet B) = [(f \oplus B) \ominus B]$,
- Opening eliminates specific image details smaller than *B*, removes noise and smoothens the boundaries from the inside, whereas closing fills holes in objects, connects close objects or small breaks and smoothens the boundaries from the outside.
- Multiscale opening and closing can be performed by increasing the size (scale) of the structuring template *nB*, where $n = 0, 1, 2, \ldots, N$. These multiscale opening and closing of *f* by *B* are mathematically represented as:

  $(f \circ nB) = \{[(f \ominus B) \ominus B \ominus \ldots \ominus B] \oplus B \oplus B \oplus \ldots \oplus B\} = [(f \ominus nB) \oplus nB]$,

  $(f \bullet nB) = \{[(f \oplus B) \oplus B \oplus \ldots \oplus B] \ominus B \ominus B \ominus \ldots \ominus B\} = [(f \oplus nB) \ominus nB]$,

  at scale $n = 0, 1, 2, \ldots, N$.
- Performing opening and closing iteratively by increasing the size of *B* transforms the function *f*(x,y) into lower resolutions correspondingly.

Mathematical Morphology (cont)

- Multiscale opening and closing of *f* by *nB* effect spatially distributed greyscale regions in the form of smoothing of contours to various degrees. The shape and size of *B* control the shape of smoothing and the scale respectively.
- Important problems like feature detection and characterisation often require analysing greyscale functions at multiple spatial resolutions. Recently, non-linear filters have been used to obtain images at multi-resolution due to their robustness in preserving the fine details.
- Advantages of mathematical morphology transformations
  - popular in object recognition and representation studies.
  - The non-linearity property in preserving the fine details.

Effect of Dilation using 3X3 structuring element

0	0	0	0	0	0	0	0	0	0	0	0	0	0	0	0
0	0	0	0	0	0	0	0	0	0	0	0	0	0	0	0
0	0	0	1	1	1	0	0	0	0	0	0	0	0	0	0
0	0	1	1	1	1	1	0	0	0	0	0	0	0	0	0
0	0	1	1	1	1	1	0	0	0	0	1	1	1	0	0
0	0	1	1	1	1	0	0	0	0	1	1	1	1	0	0
0	0	0	1	1	0	0	0	0	1	1	1	1	1	0	0
0	0	0	0	0	0	0	0	1	1	1	1	1	0	0	0
0	0	0	0	0	0	0	1	1	1	1	1	0	0	0	0
0	0	0	0	0	0	1	1	1	1	1	0	0	0	0	0
0	0	0	0	0	1	1	1	1	1	0	0	0	0	0	0
0	0	0	0	1	1	1	1	1	0	0	0	0	0	0	0
0	0	0	0	1	1	1	1	1	1	1	1	0	0	0	0
0	0	0	0	1	1	1	1	1	1	1	1	0	0	0	0
0	0	0	0	0	1	1	1	1	1	1	0	0	0	0	0
0	0	0	0	0	0	0	0	0	0	0	0	0	0	0	0

→

0	0	0	0	0	0	0	0	0	0	0	0	0	0	0	0
0	0	1	1	1	1	1	0	0	0	0	0	0	0	0	0
0	1	1	1	1	1	1	1	0	0	0	0	0	0	0	0
0	1	1	1	1	1	1	1	0	0	1	1	1	1	1	0
0	1	1	1	1	1	1	1	0	1	1	1	1	1	1	0
0	1	1	1	1	1	1	1	1	1	1	1	1	1	1	0
0	1	1	1	1	1	1	1	1	1	1	1	1	1	1	0
0	0	1	1	1	1	1	1	1	1	1	1	1	1	1	0
0	0	0	0	0	1	1	1	1	1	1	1	1	1	0	0
0	0	0	0	1	1	1	1	1	1	1	1	1	0	0	0
0	0	0	1	1	1	1	1	1	1	1	1	0	0	0	0
0	0	0	1	1	1	1	1	1	1	1	1	1	0	0	0
0	0	0	1	1	1	1	1	1	1	1	1	1	0	0	0
0	0	0	1	1	1	1	1	1	1	1	1	1	0	0	0
0	0	0	1	1	1	1	1	1	1	1	1		0	0	0
0	0	0	0	1	1	1	1	1	1	1	1	0	0	0	0

Steps in Dilation of *X* by *B*

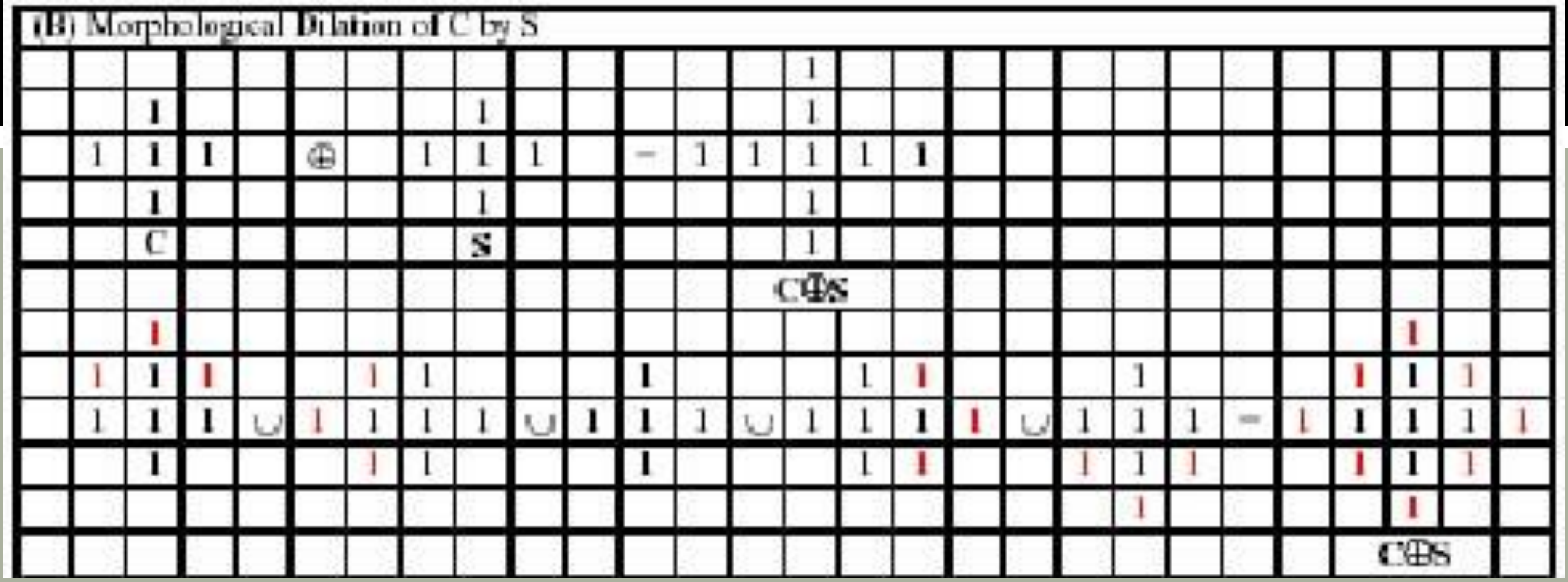

Effect of Erosion using 3X3 structuring element

0	0	0	0	0	0	0	0	0	0	0	0	0	0	0	0
0	0	0	0	0	0	0	0	0	0	0	0	0	0	0	0
0	0	0	1	1	1	0	0	0	0	0	0	0	0	0	0
0	0	1	1	1	1	1	0	0	0	0	0	0	0	0	0
0	0	1	1	1	1	1	0	0	0	0	1	1	1	0	0
0	0	1	1	1	1	0	0	0	0	1	1	1	1	0	0
0	0	0	1	1	0	0	0	0	1	1	1	1	1	0	0
0	0	0	0	0	0	0	0	1	1	1	1	1	0	0	0
0	0	0	0	0	0	0	1	1	1	1	1	0	0	0	0
0	0	0	0	0	0	1	1	1	1	1	0	0	0	0	0
0	0	0	0	0	1	1	1	1	1	0	0	0	0	0	0
0	0	0	0	1	1	1	1	1	0	0	0	0	0	0	0
0	0	0	0	1	1	1	1	1	1	1	1	0	0	0	0
0	0	0	0	1	1	1	1	1	1	1	1	0	0	0	0
0	0	0	0	0	1	1	1	1	1	1	0	0	0	0	0
0	0	0	0	0	0	0	0	0	0	0	0	0	0	0	0

→

0	0	0	0	0	0	0	0	0	0	0	0	0	0	0	0
0	0	0	0	0	0	0	0	0	0	0	0	0	0	0	0
0	0	0	0	0	0	0	0	0	0	0	0	0	0	0	0
0	0	0	0	1	0	0	0	0	0	0	0	0	0	0	0
0	0	0	1	1	0	0	0	0	0	0	0	0	0	0	0
0	0	0	0	0	0	0	0	0	0	0	0	1	0	0	0
0	0	0	0	0	0	0	0	0	0	0	1	0	0	0	0
0	0	0	0	0	0	0	0	0	0	1	0	0	0	0	0
0	0	0	0	0	0	0	0	0	1	0	0	0	0	0	0
0	0	0	0	0	0	0	0	1	0	0	0	0	0	0	0
0	0	0	0	0	0	0	1	0	0	0	0	0	0	0	0
0	0	0	0	0	0	1	1	0	0	0	0	0	0	0	0
0	0	0	0	0	1	1	1	0	0	0	0	0	0	0	0
0	0	0	0	0	0	1	1	1	1	0	0	0	0	0	0
0	0	0	0	0	0	0	0	0	0	0	0	0	0	0	0
0	0	0	0	0	0	0	0	0	0	0	0	0	0	0	0

Steps in Erosion of *X* by *B*

(A) Morphological Erosion of C by S

	1						1							0													
1	1	1		⊖		1	1	1		=			0	1	0												
	1						1							0													
	C						S							C⊖S													
	0				1				1				1				1				0						
1	1	1	∩	0	1	1	∩	1	1	1	∩	1	1	0	∩	1	1	1	−	0	1	0					
	1				1				1				1				0				0						
																					C⊕S						

Effect of Opening using 3X3 structuring element

0	0	0	0	0	0	0	0	0	0	0	0	0	0	0	0
0	0	0	0	0	0	0	0	0	0	0	0	0	0	0	0
0	0	0	1	1	1	0	0	0	0	0	0	0	0	0	0
0	0	1	1	1	1	1	0	0	0	0	1	1	1	0	0
0	0	1	1	1	1	1	0	0	0	1	1	1	1	0	0
0	0	1	1	1	1	0	0	0	1	1	1	1	1	0	0
0	0	0	1	1	0	0	0	1	1	1	1	1	0	0	0
0	0	0	0	0	0	0	1	1	1	1	1	0	0	0	0
0	0	0	0	0	0	1	1	1	1	1	0	0	0	0	0
0	0	0	0	0	1	1	1	1	1	0	0	0	0	0	0
0	0	0	0	1	1	1	1	1	0	0	0	0	0	0	0
0	0	0	0	1	1	1	1	1	1	1	1	0	0	0	0
0	0	0	0	1	1	1	1	1	1	1	1	0	0	0	0
0	0	0	0	0	1	1	1	1	1	1	0	0	0	0	0
0	0	0	0	0	0	0	0	0	0	0	0	0	0	0	0

→

0	0	0	0	0	0	0	0	0	0	0	0	0	0	0	0
0	0	0	0	0	0	0	0	0	0	0	0	0	0	0	0
0	0	0	1	1	1	0	0	0	0	0	0	0	0	0	0
0	0	1	1	1	1	0	0	0	0	0	1	1	1	0	0
0	0	1	1	1	1	0	0	0	0	1	1	1	1	0	0
0	0	1	1	1	1	0	0	0	1	1	1	1	1	0	0
0	0	0	0	0	0	0	0	1	1	1	1	1	0	0	0
0	0	0	0	0	0	0	1	1	1	1	1	0	0	0	0
0	0	0	0	0	0	1	1	1	1	1	0	0	0	0	0
0	0	0	0	0	1	1	1	1	1	0	0	0	0	0	0
0	0	0	0	1	1	1	1	1	0	0	0	0	0	0	0
0	0	0	0	1	1	1	1	1	1	1	0	0	0	0	0
0	0	0	0	1	1	1	1	1	1	1	0	0	0	0	0
0	0	0	0	0	1	1	1	1	1	1	0	0	0	0	0
0	0	0	0	0	0	0	0	0	0	0	0	0	0	0	0

Steps in Opening of *X* by *B*

(C) Morphological Opening of C by S

1	1	1					1						0	0	0					1						1	
1	1	1		$\ominus$		1	1	1		=			0	1	0		$\oplus$		1	1	1		=		1	1	1
1	1	1					1						0	0	0					1						1	
	C						S							$C\ominus S$						S						$C\ominus S\oplus S$	

Effect of Closing using 3X3 structuring element

0	0	0	0	0	0	0	0	0	0	0	0	0	0	0	0
0	0	1	1	0	0	0	0	0	0	1	1	0	0	0	0
0	0	1	1	0	0	0	0	0	1	1	0	0	0	0	0
0	0	0	0	0	0	0	0	1	1	1	0	0	0	0	0
0	0	0	0	0	0	0	0	1	1	0	0	0	0	1	0
0	0	0	0	0	0	0	0	1	0	0	0	1	1	1	0
0	0	0	1	1	1	1	0	1	0	0	1	1	1	0	0
0	0	1	1	1	1	0	1	1	1	1	1	1	0	0	0
0	1	1	1	1	0	0	0	1	0	0	0	0	0	0	0
0	1	0	0	0	1	0	0	0	1	0	0	0	0	0	0
0	1	0	0	0	0	1	0	1	1	0	0	0	0	0	0
0	1	0	0	0	0	0	1	1	1	0	0	0	0	0	0
0	1	1	0	0	0	0	1	1	1	0	1	0	0	0	0
0	1	1	1	0	0	0	1	1	0	0	0	0	0	0	0
0	0	1	1	1	1	1	1	0	0	0	0	0	0	0	0
0	0	0	0	0	0	0	0	0	0	0	0	0	0	0	0

0	0	0	0	0	0	0	0	0	0	0	0	0	0	0	0
0	0	1	1	0	0	0	0	0	0	1	1	0	0	0	0
0	0	1	1	0	0	0	0	0	1	1	0	0	0	0	0
0	0	0	0	0	0	0	0	1	1	1	0	0	0	0	0
0	0	0	0	0	0	0	0	1	1	1	0	0	0	1	0
0	0	0	0	0	0	0	0	1	1	1	1	1	1	1	0
0	0	0	1	1	1	1	1	1	1	1	1	1	1	0	0
0	0	1	1	1	1	1	1	1	1	1	1	1	0	0	0
0	1	1	1	1	1	1	1	1	1	0	0	0	0	0	0
0	1	0	0	0	1	1	1	1	1	0	0	0	0	0	0
0	1	0	0	0	0	1	1	1	1	0	0	0	0	0	0
0	1	0	0	0	0	0	1	1	1	0	0	0	0	0	0
0	1	1	0	0	0	0	1	1	1	1	1	0	0	0	0
0	1	1	1	0	0	0	1	1	0	0	0	0	0	0	0
0	0	1	1	1	1	1	1	0	0	0	0	0	0	0	0
0	0	0	0	0	0	0	0	0	0	0	0	0	0	0	0

Steps in Closing of *X* by *B*

(D) Morphological Closing of C by S

											1	1	1														
1	1	1				1				1	1	1	1	1					1				1	1	1		
1	0	1	⊕		1	1	1		=	1	1	1	1	1		⊖		1	1	1	=		1	1	1		
1	1	1				1				1	1	1	1	1					1				1	1	1		
	C					S					1	1	1						S					C			
												C⊕S												C⊕S⊖S			

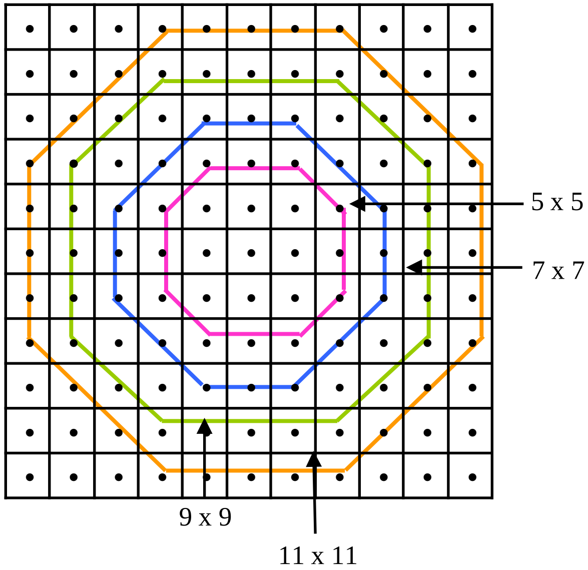

Octagonal symmetric structuring elements of various primitive sizes ranging from 5 × 5 to 11 × 11. These primitive sizes can be considered as B.

Important phases of Research related to Image Analysis

I. Information Retrieval
II. Information Analysis
III. Information Reasoning
IV. Information Modelling and Simulation
V. Information Visualization

Is there a single mathematical field that can address Research related to Digital Images?

Deal Images with Mathematical Morphology!

II.I NETWORKS EXTRACTION &THEIR PROPERTIES

Networks extraction and their properties : Sub-basins delineation

- Geomorphologic basin is an area outlined by a topographic boundary that diverts water flow to stream networks flowing into a single outlet.
- DEM is an useful source for watershed and network extraction.
- Hydrologic flow is modelled using eight-direction pour point model (Puecker et. al., 1975).

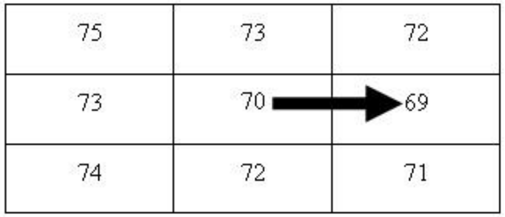

- The two topologically significant networks, include Channel & Ridge networks.
- The paths of these extracted networks are the crenulations in the elevation contours.
- Crenulations can be isolated from DEMs by using nonlinear morphological transformations.

Network Extraction: Binary Morphology-Based

Step-1:

Threshold decomposition of f(x,y)

Step 2:

Skeletonization

Step 3:

Systematic logical union and difference to extract network within each spatially distributed region and Union of network(s) obtained

Equations for Network Extraction

$$f^t = \begin{cases} 1 & \text{if} \quad f(x,y) \geq t \\ 0 & \text{if} \quad f(x,y) < t \quad \text{where} \quad 0 \leq f(x,y) \leq 255 \end{cases}$$

$$f^t = X_t; f^{t+1} = X_{t+1}; \cdots; f^N = X$$

$$Sk_n(X_t) = (X_t \ominus nB) \setminus (X_t \ominus nB) \circ B \qquad n = 0, 1, 2, \cdots, N$$

$$Sk(X_t) = \bigcup_{n=0}^{N} Sk_n(X_t)$$

$$CH(f) = \bigcup_{t=1}^{255} \left(\left(Sk(X_t) \cup X_{t+1} \right) \setminus X_{t+1} \right)$$

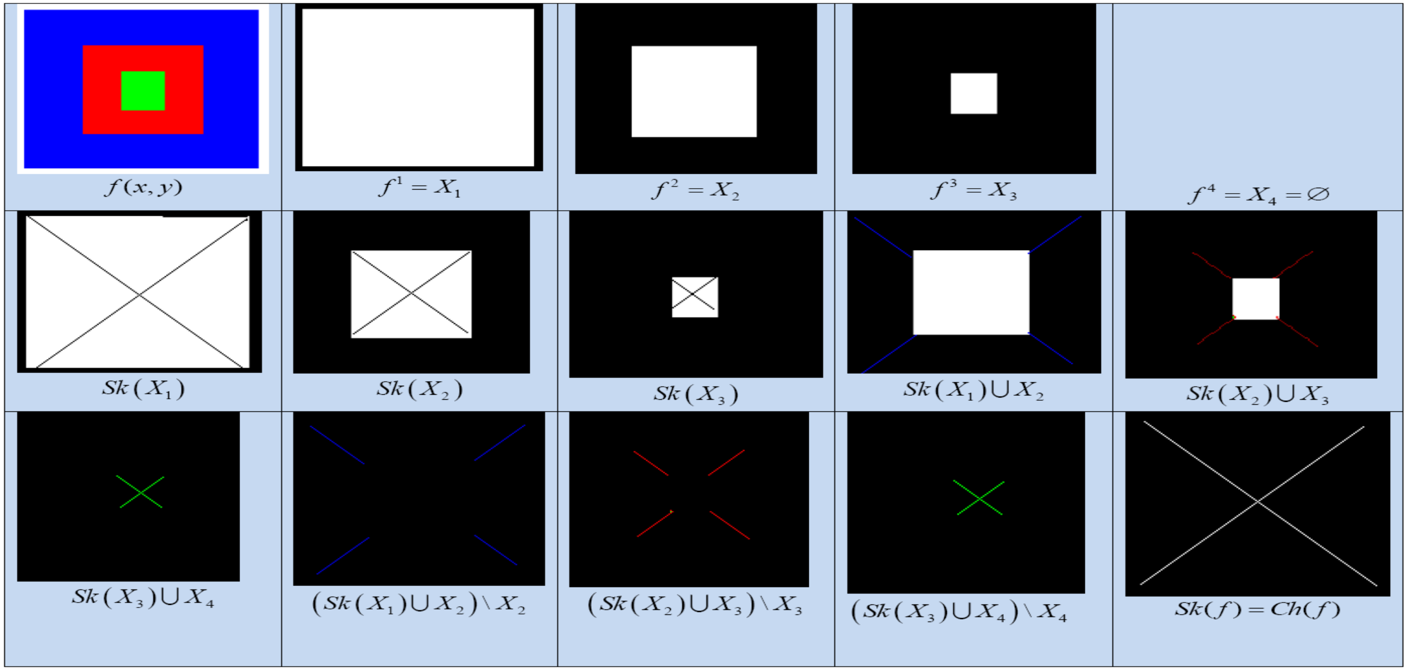

Networks extraction: Grayscale Morphology-Based

- The DEM, *f* is first eroded by B_n with n=1, 2,…,N, and the eroded DEM is opened by *B* of the smallest size. The opened version of each eroded image is subtracted from the corresponding eroded image to produce the *n*th level subsets of the ridge network. Union of these subsets of level n = 0 to N gives the ridge network for the DEM.

$$\mathrm{RID}_{n}^{i}(f) = [(f \ominus B_{n}^{i}) \setminus \{[(f \ominus B_{n}^{i}) \ominus B_{1}^{i}] \oplus B_{1}^{i}\}]$$

$$\mathrm{RID}(f) = \bigcup_{\substack{n=0 \\ i=1}}^{\substack{4 \\ N}} [\mathrm{RID}_{n}^{i}(f)]$$

Networks extraction and their properties

- DEM, *f* is first dilated by B_n and the dilated *f* is closed by *B* of the smallest size. The closed version of each dilated image is subtracted from the corresponding dilated image to produce the *n*th level subsets of the channel network. Union of these subsets of level $n = 0$ to N gives the channel network for the DEM.

$$\mathrm{CH}_n^i(f) = [(f \oplus \mathrm{B}_n^i) \setminus \{[(f \oplus \mathrm{B}_n^i) \oplus \mathrm{B}_1^i] \ominus \mathrm{B}_1^i\}]$$

$$\mathrm{CH}(f) = \bigcup_{\substack{n=0 \\ i=1}}^{\substack{4 \\ N}} [\mathrm{CH}_n^i(f)]$$

- 1-D structuring elements of primitive size

1
1
1

1	1	1

1		
	1	
		1

		1
	1	
1		

Networks extraction and their properties

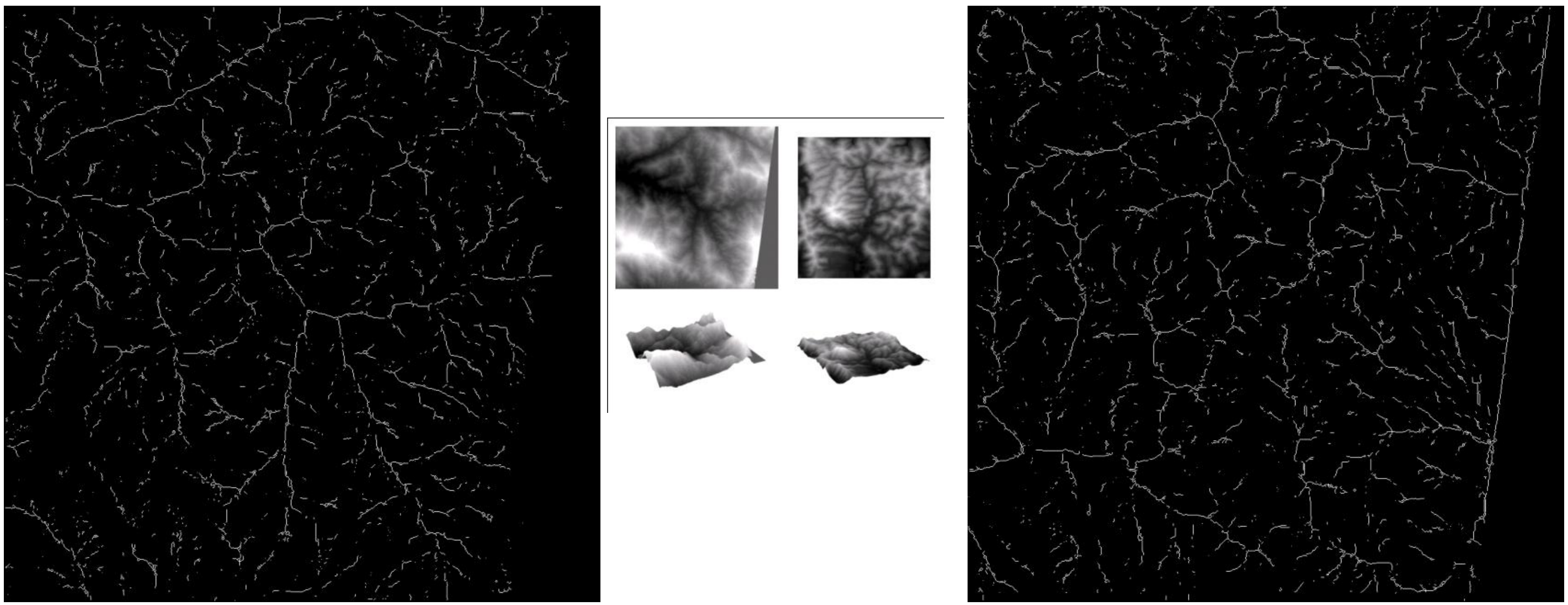

(a) Ridge networks, and (b) channel networks extracted from Cameron Highlands DEM.

Networks extraction and their properties

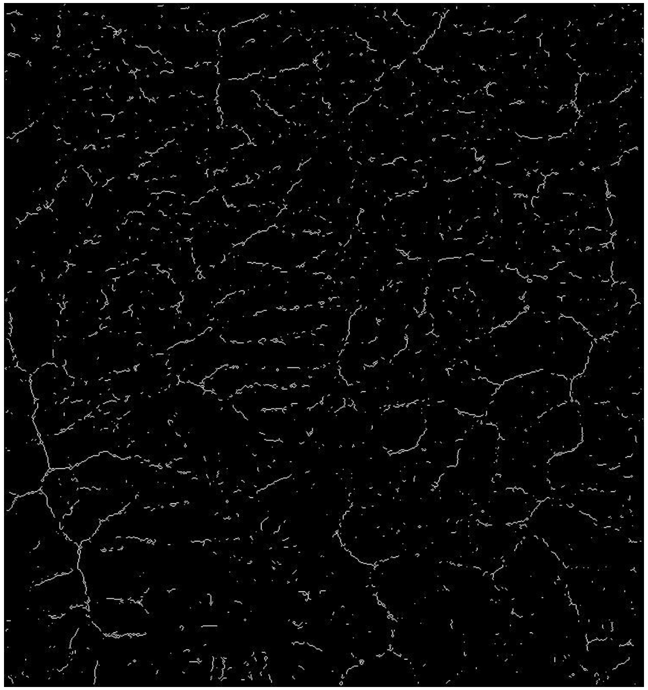

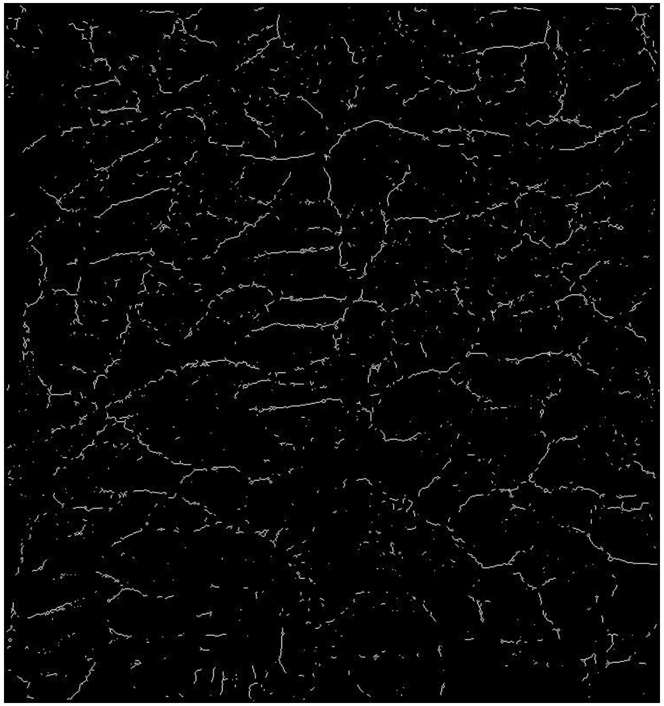

(a) Ridge networks, and (b) channel networks extracted from Petaling DEM.

Algorithm

- Algorithm is to extract singular networks such as channel and ridge connectivity networks from DEMs.
- Sub watershed boundary in DEM is automatically generated by considering channel and ridge connectivity networks.
- Mathematical morphology transformations such as dilation, erosion, opening and closing are used in this algorithm.

- Step-1:

$$CH_e(M) = \varepsilon^{e}_{;}(M) \, / \, \gamma^{1}_{;}\{\varepsilon^{e}_{;}(M)\}$$

$$e = 0, 1, 2, \ldots, N$$

- Step-2:

$$CH(M) = \bigcup_{e=0}^{N} CH_e(M)$$

$$e = 0, 1, 2, \ldots, n$$

- Step-3:

$$RID_e(M) = \varepsilon^{e}_{;}\{(CH(M))^c\} \, // \, \gamma^{1}_{;}\{\varepsilon^{e}_{;}\{(CH(M))^c\}\}$$

- Step-4:

$$RID(M) = \bigcup_{e=1}^{N} RID_e(M)$$

$$e = 0, 1, 2, \ldots, n$$

- Step-5:

$$CH(M) \cup RID(M)$$

Decomposed basins and networks

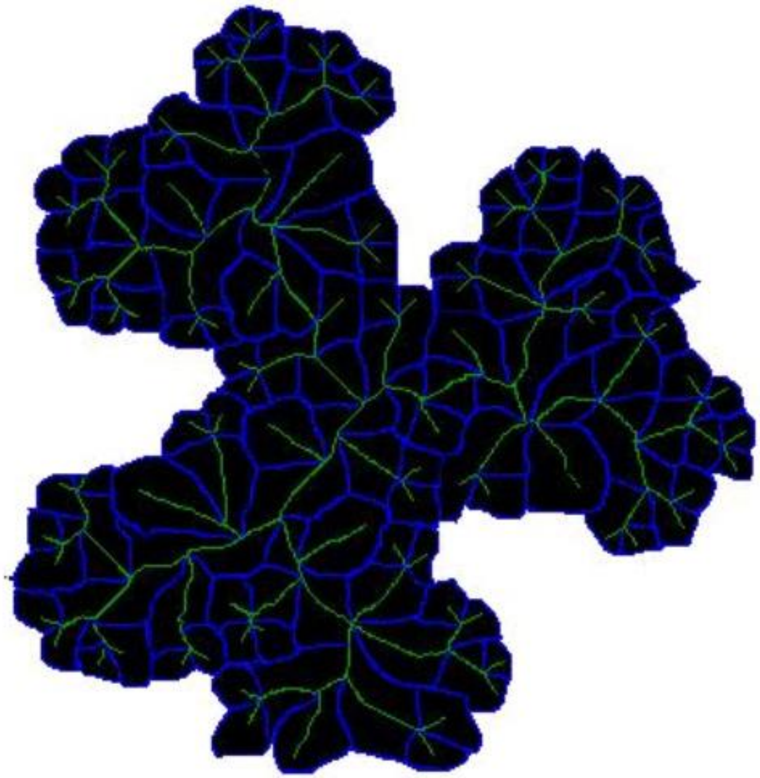

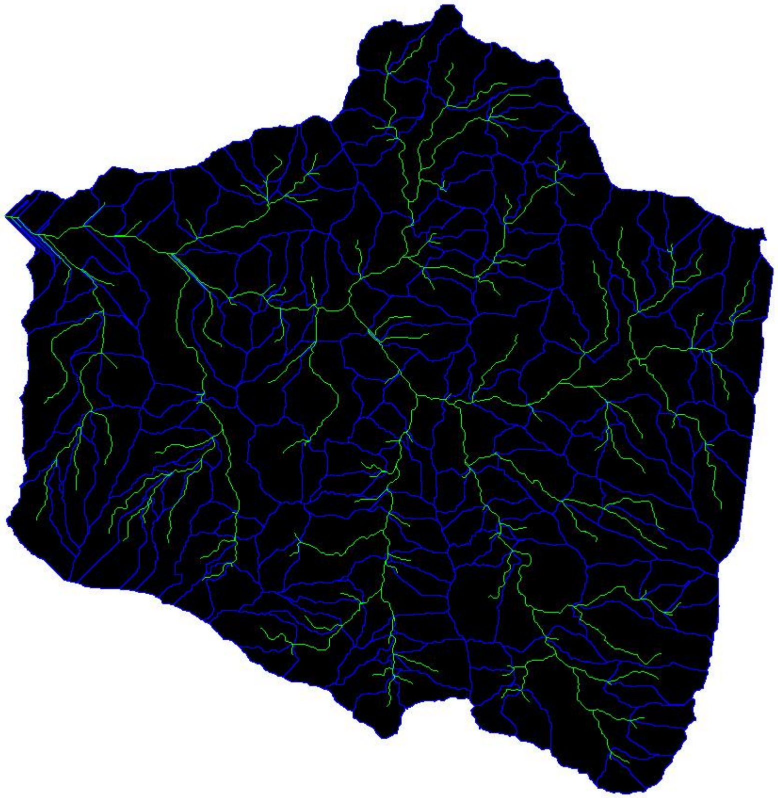

Channel Network of Gunung Ledang Region

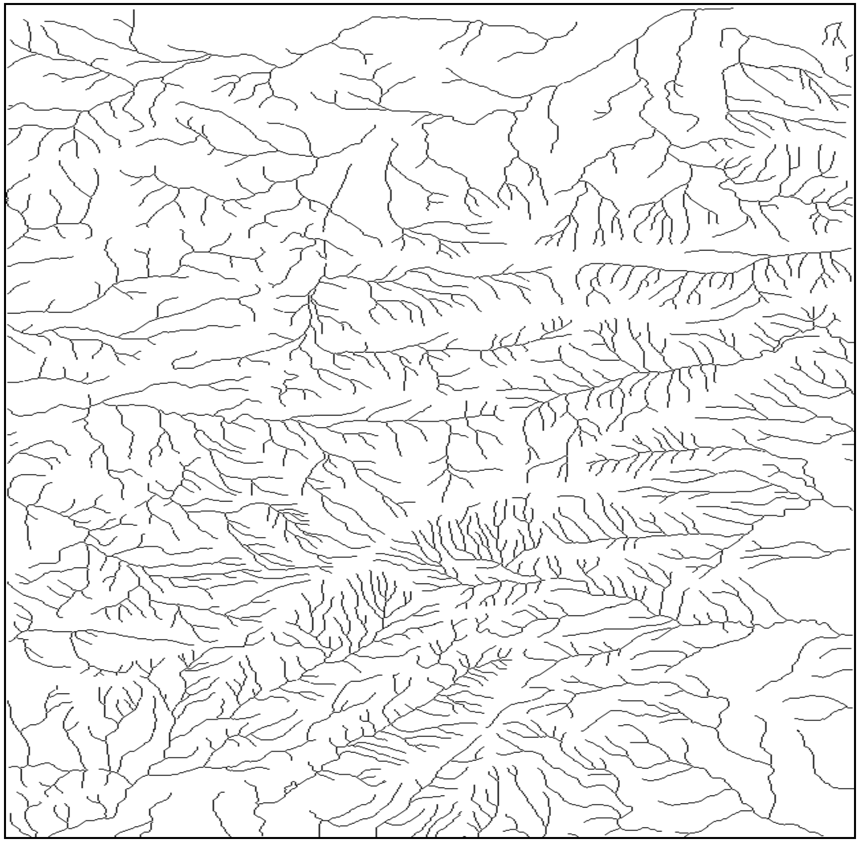

Ridge Network of Gunung Ledang Region

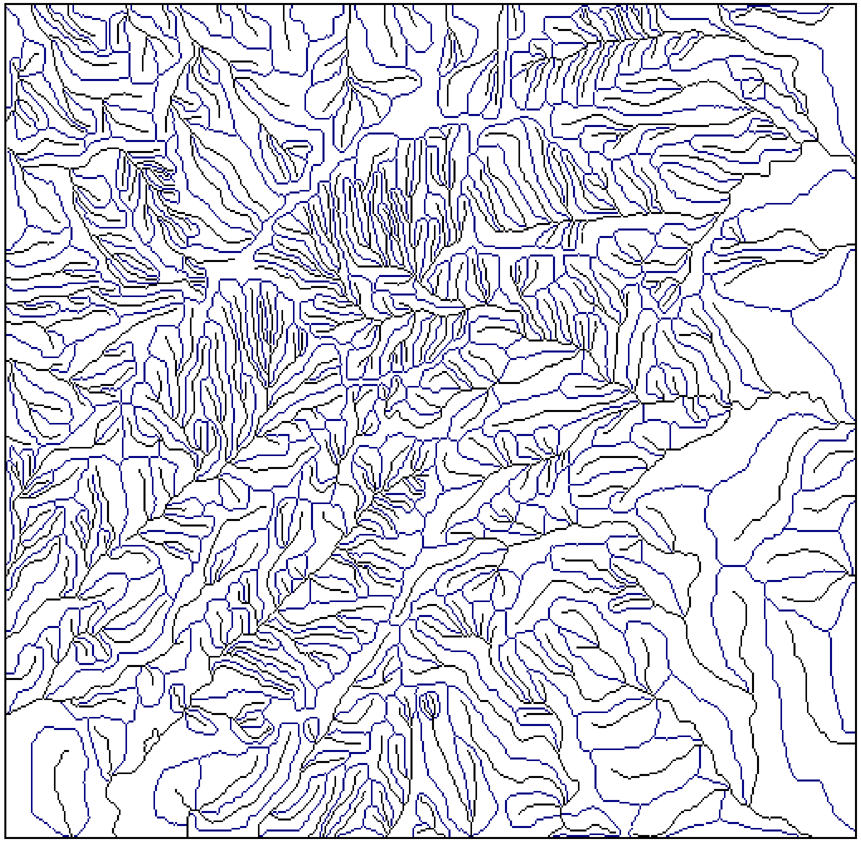

Networks : Binary Vs Grayscale

Binary Morphology

Binary morphology-based network extraction is:

- more stable,
- more accurate, and
- computationally expensive

Gray-scale Morphology

Grayscale-based network extraction—

- may not be accurate like binary-morphology based—
  - generates network that yields disconnections some times, but
- computationally not expensive.

II.II. Terrestrial Analysis

Scale invariance and Power-laws in networks

Shape-dependant power-laws

Granulometric analysis

II.II.I. Scale Invariant Power-laws: Morphometry and Allometry of Networks

First step in drainage basin analyses is the classification of stream orders by Horton-Strahler's ordering system (Horton, 1945; Strahler, 1957). The order of the whole tree is defined to be the order of the root. This ordering system has been found to correlate well with important basin properties in a wide range of environments.

This figure shows a sample network classified based on Horton-Strahler's ordering system.

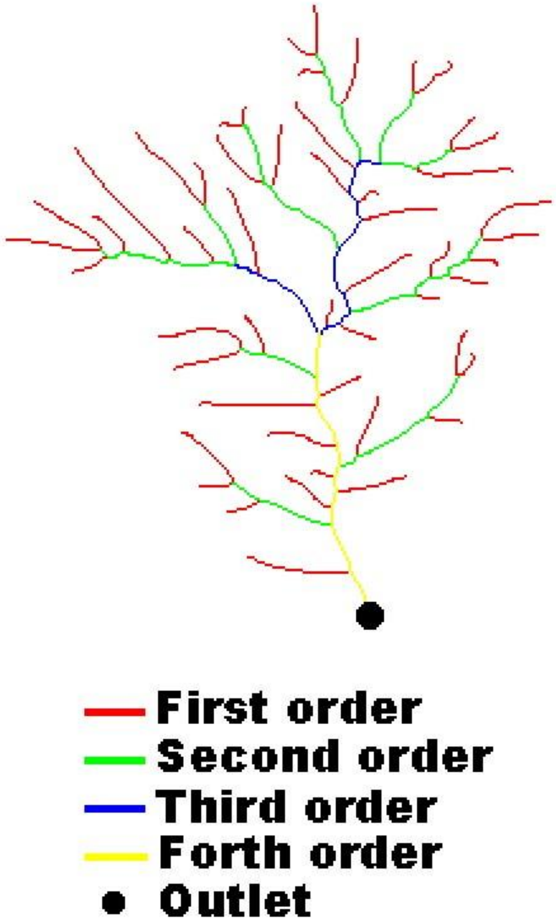

Model network.

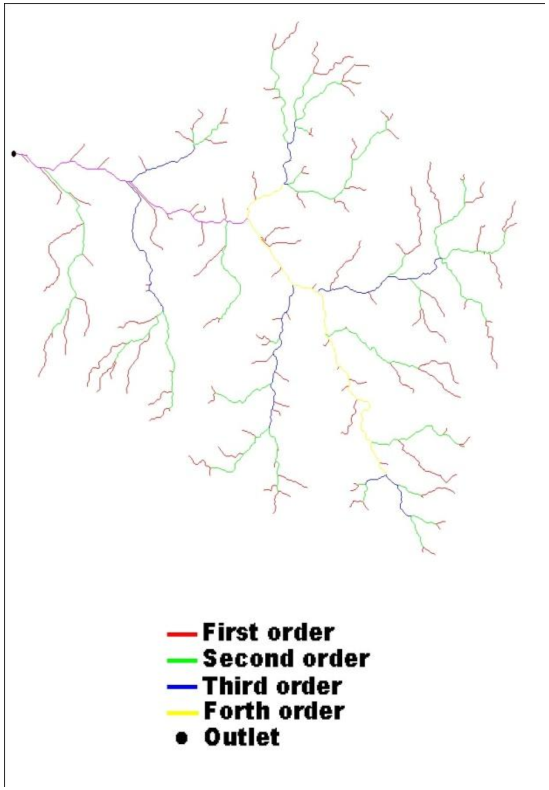

Cameron Highland channel network.

Scale Invariant Power-laws: Two Topological Quantities

- Two topological quantities bifurcation ratio (R_b) and length ratio (R_l)

$$R_b = \frac{N_i}{N_{i+1}} \qquad R_l = \frac{L_i}{L_{i-1}}$$

Networks extraction and their properties : Morphometry

- Besides these two ratios, the universal similarity of stream network can be shown through Hack's law and Hurst's law as follows:

- Hack's Law: $L_{mc} \propto A^{h}$

  where A is the area of basin with main channel length L_{mc}.

- Hurst's law: $L_{\perp} \propto L_{\parallel}^{H}$

  where $L_{||}$ is the longitudinal length and L transverse length respectively.

Allometric power-laws

- Allometric power-laws are derived between the basic measures such as basin area, basin perimeter, channel length, longitudinal length and transverse length
- Observed that these power-laws are of universal type as they exhibit similar scaling relationships at all scales.

Existing allometric power-laws: Decomposed basins & networks

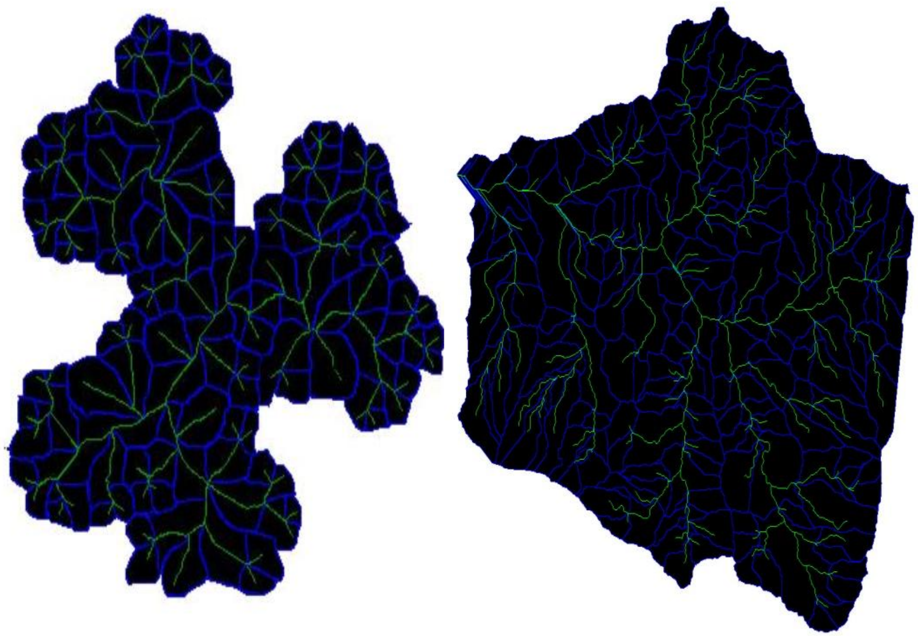

Existing allometric power-laws : Decomposed basins and networks

The number of decomposed sub-basins of respective orders from the simulated 6th order F-DEM include:

- two 5th
- five 4th
- ten 3rd
- thirty six 2nd, and
- eighty six 1st order basins.

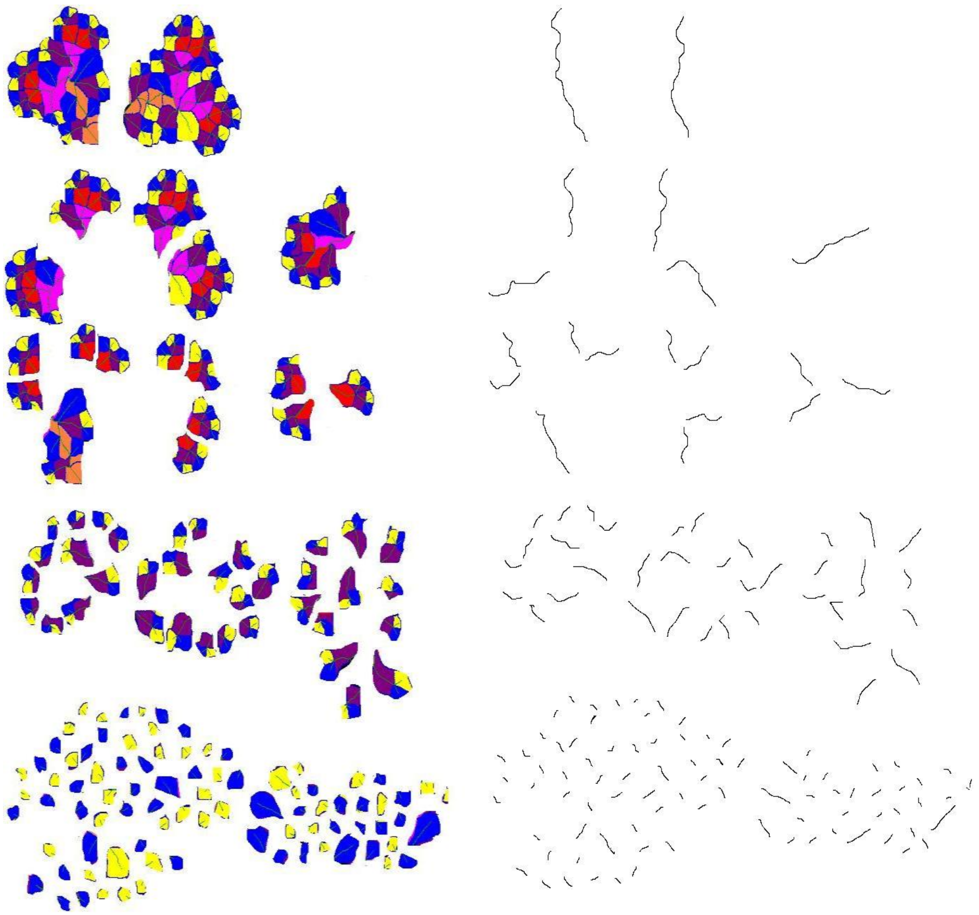

Existing allometric power-laws :

Decomposed basins and networks


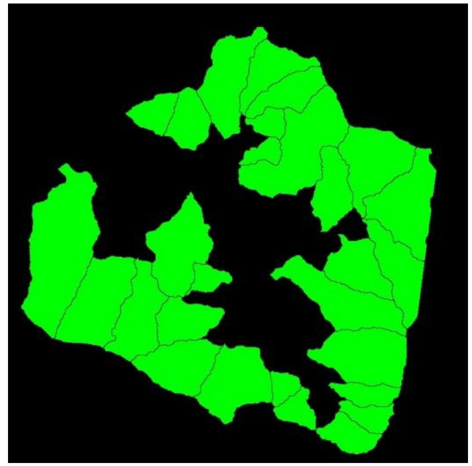
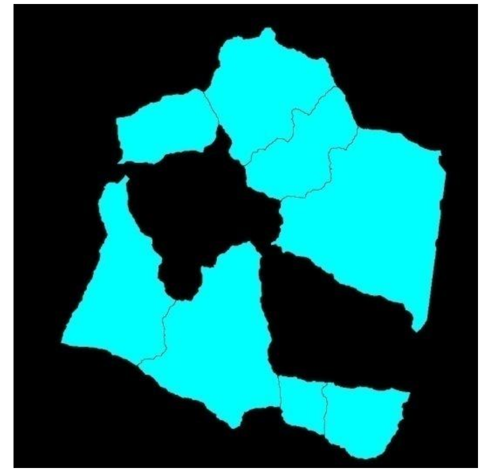

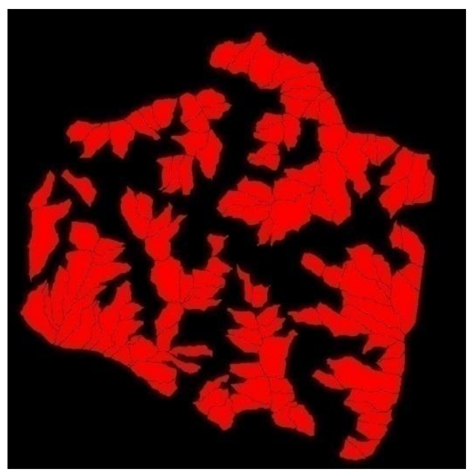

Decomposed sub-basins are

- two 4th
- eight 3rd
- twenty-eight 2nd, and
- one hundred twenty-four 1st

order basins.

Existing allometric power-laws : Basic Measures

Basic measures for a basin, (a) basin area, (b) total channel length, (c) main channel length, (d) basin perimeter, (e) longitudinal length and (f) transverse length.

Scale Invariant allometric power-laws

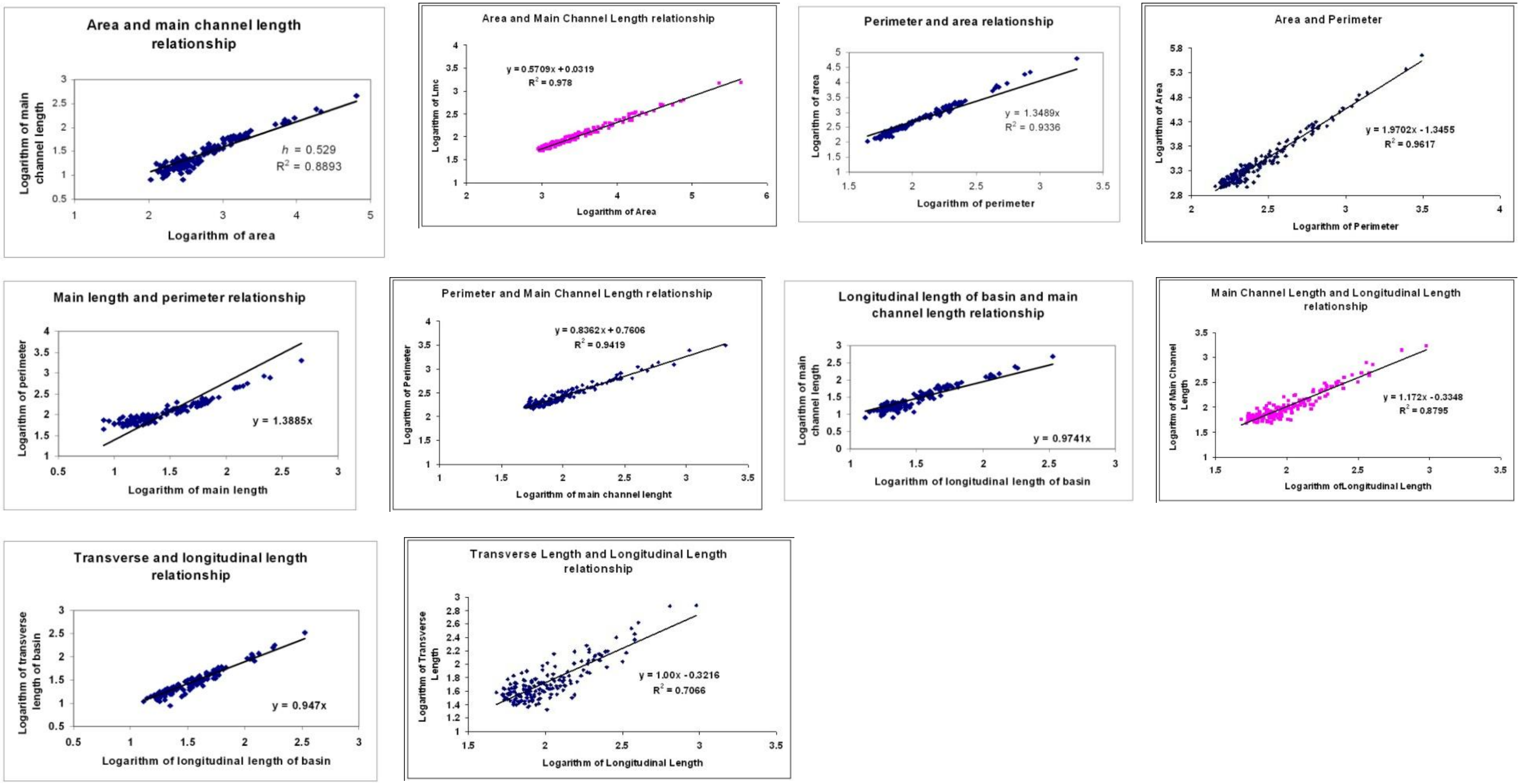

Allometric relationships among various areal and length parameters for all sub-basins of F-DEM and TOPSAR DEM.

Scale Invariant allometric power-laws
F-DEM TOPSAR DEMs

Relations	Notations	For all orders	Basin's order 1	2	3	4	5	6
A and L_{mc}	h	0.53	0.502	0.56	0.56	0.55	0.55	0.56
A and P	α	1.35	1.31	1.36	1.41	1.44	1.48	1.46
P and L_{mc}	β	1.39	1.51	1.32	1.28	1.26	1.23	1.23
L_{mc} and L_{ll}	-	0.97	0.92	1.01	1.04	1.03	0.94	0.95
$L_{\perp}$ and L_{ll}	H	0.95	0.94	0.94	0.96	0.98	0.94	0.98
2h	D_{Lmc}	1.06	1.00	1.11	1.11	1.10	1.10	1.12
$2/\alpha$	D_p	1.48	1.53	1.47	1.42	1.39	1.35	1.37
$1+\frac{D_{Lmc}}{1+H}$	-	1.55	1.52	1.57	1.59	1.56	1.57	1.57

Relations	Notations	For all orders	Basin's order 1	2	3	4	5
A and L_{mc}	h	0.57	0.60	0.57	0.50	0.58	0.56
A and P	α	1.97	1.62	1.78	1.78	1.69	1.62
P and L_{mc}	β	0.84	0.78	0.92	0.88	1.09	1.05
L_{mc} and L_{ll}	-	1.17	0.75	1.00	0.92	1.02	1.08
$L_{\perp}$ and L_{ll}	H	1.00	0.39	0.53	0.68	1.00	0.97
2h	D_{Lmc}	1.14	1.20	1.14	1.00	1.16	1.12
$2/\alpha$	D_p	1.02	1.23	1.12	1.12	1.18	1.23
$1+\frac{D_{Lmc}}{1+H}$	-	1.57	1.86	1.74	1.60	1.58	1.57

Existing allometric power-laws : Scaling laws

Our results shown for basins derived from F-DEM and TOPSAR DEM are in good accord with power-laws derived from Optimal Channel Networks (Maritan et. al., 2002) and Random Self-Similar Networks (Veitzer and Gupta 2000) and certain natural river basins.

Novel scaling relationships between travel-time channel networks, convex hulls and convexity measures

Network topology and watershed geometry are important features in terrain characterization.

Travel-time networks are sequence of networks generated by removing the extremities of the network iteratively. Hit-or-Miss transformation and Thinning transformations is used in generating travel-time network. Half-plane closing-based algorithm (Soille, 2005) is employed to generate convex hulls for these travel-time networks.

Length of the travel-time network and area of the corresponding convex hull are used to derive new scaling exponents.

Proposed scaling relationships : Travel-time networks

- The process of deleting the end points from the networks is named as pruning.
- To decompose the stream network subsets from n = 1 to N, structuring template of B_1 and B_2 are decomposed into various subsets, B_n^i where $i = 1,2,\ldots,8$ and $n = 1,2$

- Both structuring templates are disjointed into eight directions. The intersecting portion of eroded S and eroded Sc by disjointed templates $\{B_1^k\}$ and $\{B_2^k\}$ $k = 1,2,\ldots,8$ respectively are computed to derive pruned version of S.
- The X's in the structuring templates signifies the 'don't care' condition – it doesn't matter whether the pixel in that location has a value of 0 or 1.

$$B_1^1 = \begin{matrix} 1 & 0 & 0 \\ 0 & 1 & 0 \\ 0 & 0 & 0 \end{matrix} \quad B_1^2 = \begin{matrix} 0 & 0 & 1 \\ 0 & 1 & 0 \\ 0 & 0 & 0 \end{matrix} \quad B_1^3 = \begin{matrix} 0 & 0 & 0 \\ 0 & 1 & 0 \\ 0 & 0 & 1 \end{matrix} \quad B_1^4 = \begin{matrix} 0 & 0 & 0 \\ 0 & 1 & 0 \\ 1 & 0 & 0 \end{matrix}$$

$$B_1^5 = \begin{matrix} X & 1 & X \\ 0 & 1 & 0 \\ 0 & 0 & 0 \end{matrix} \quad B_1^6 = \begin{matrix} 0 & 0 & X \\ 0 & 1 & 1 \\ 0 & 0 & X \end{matrix} \quad B_1^7 = \begin{matrix} 0 & 0 & 0 \\ 0 & 1 & 0 \\ X & 1 & X \end{matrix} \quad B_1^8 = \begin{matrix} X & 0 & 0 \\ 1 & 1 & 0 \\ X & 0 & 0 \end{matrix}$$

$$B_2^1 = \begin{matrix} 0 & 1 & 1 \\ 1 & 0 & 1 \\ 1 & 1 & 1 \end{matrix} \quad B_2^2 = \begin{matrix} 1 & 1 & 0 \\ 1 & 0 & 1 \\ 1 & 1 & 1 \end{matrix} \quad B_2^3 = \begin{matrix} 1 & 1 & 1 \\ 1 & 0 & 1 \\ 1 & 1 & 0 \end{matrix} \quad B_2^4 = \begin{matrix} 1 & 1 & 1 \\ 1 & 0 & 1 \\ 0 & 1 & 1 \end{matrix}$$

$$B_2^5 = \begin{matrix} X & 0 & X \\ 1 & 0 & 1 \\ 1 & 1 & 1 \end{matrix} \quad B_2^6 = \begin{matrix} 1 & 1 & X \\ 1 & 0 & 0 \\ 1 & 1 & X \end{matrix} \quad B_2^7 = \begin{matrix} 1 & 1 & 1 \\ 1 & 0 & 1 \\ X & 0 & X \end{matrix} \quad B_2^8 = \begin{matrix} X & 1 & 1 \\ 0 & 0 & 1 \\ X & 1 & 1 \end{matrix}$$

Proposed scaling relationships : Travel-time networks

- Mathematically,
  $S * B = (S \ominus B_1^k) \cap (S^c \ominus B_2^k)$ where $B = B_1^k \cup B_2^k$
- By subtracting $(S * B)$ from S, a pruned version of S is obtained and expressed as
- $S_1 = S \otimes \{B\}$ where, $S \otimes \{B\} = S - (S * B))$
- $\{B\}$ is the sequence of $\{(B_1^1, B_1^2, \cdots, B_1^8), (B_2^1, B_2^2, \cdots, B_2^8)\}$
- After pruning of S in first pass with B_1, the process continue with pruning with B_2 and so on until S is pruned in the last pass with B_8.
  $S \otimes \{B\} = ((\cdots((S \otimes B^1) \otimes B^2) \cdots) \otimes B^8)$
- The whole process removes the first-encountered open pixels of S and produces S_1.
- Repeating the same process on S_1 will produce S_2 . The process is repeated until no further changes occur, where the closed outlet is reached.

Proposed scaling relationships : Convex hull

Convex hull is the smallest convex set that contains all the points of the network.

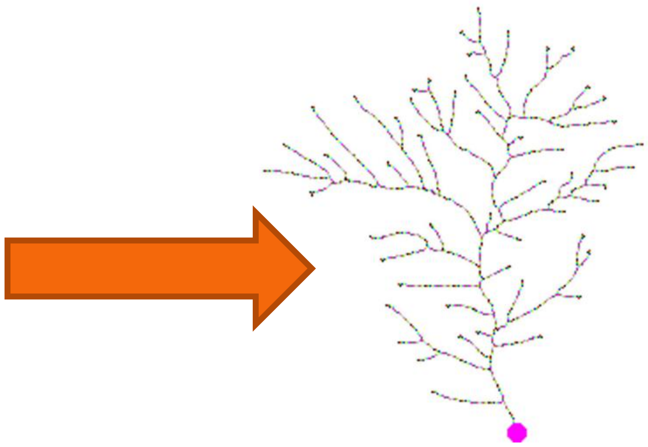

Since convex hull represents the basin of network, convex hulls of the travel-time networks are generated.

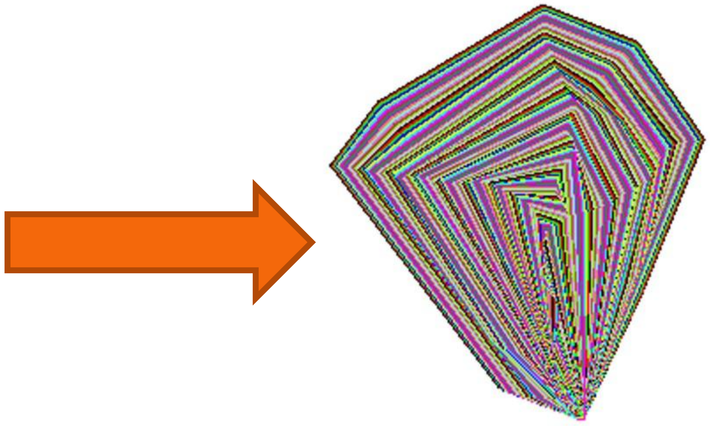

Proposed scaling relationships : Pruned network and convex hull

Properties of the pruned network:

1. $S = \bigcup_{n=0}^{N-1} (S_n - S_{n+1})$

2. $S_N \subset S_{N-1} \subset \cdots \subset S_2 \subset S_1 \subset S$

3. $S, S_1, S_2, \cdots, S_N$ obtained by iterative **pruning.**

The final convex polygon containing all the points of S yields C(S).

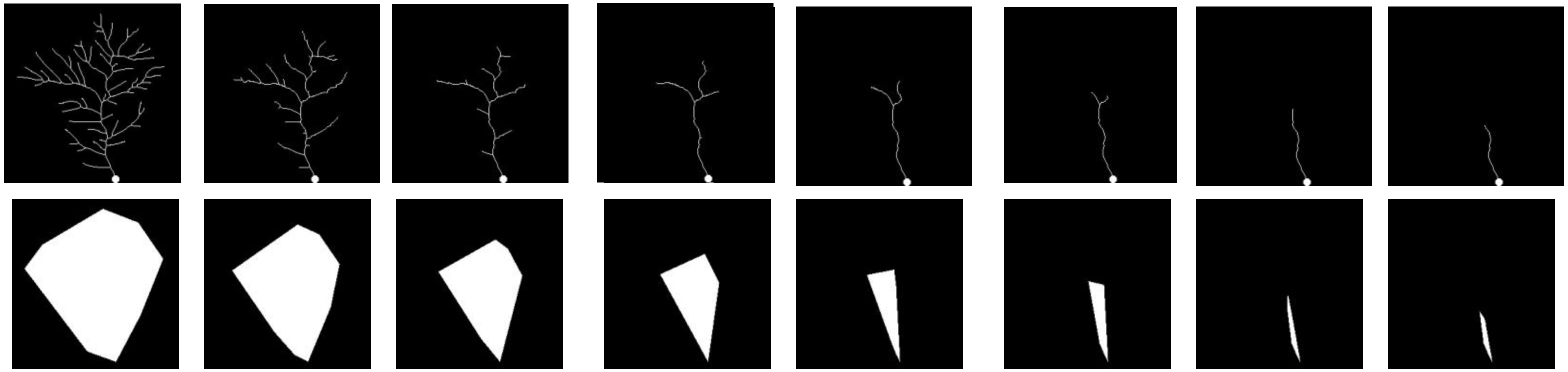

Proposed scaling relationships

- Network – pruning – network length = S_n
- Convex hull computed – convex hull area = $C(S_n)$
- Convexity measures, CM = ratio between the areas of S_n and $C(S_n)$.

$$L(S_n) \sim A[C(S_n)]^{\alpha}$$

$$CM(S_n) \sim \frac{1}{L(S_n)^{\beta}}$$

$$CM(S_n) \sim \frac{1}{A[C(S_n)]^{\lambda}}$$

Graph of lengths of the sequential pruned networks versus the corresponding areas of convex hulls.

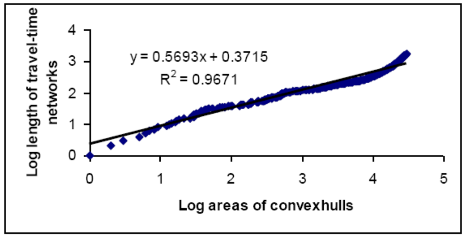

Relationship between channel lengths and convexity measures.

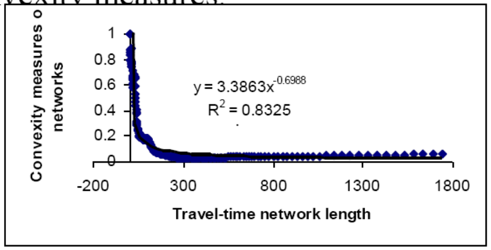

Relationship between areas of convex hulls and convex measures.

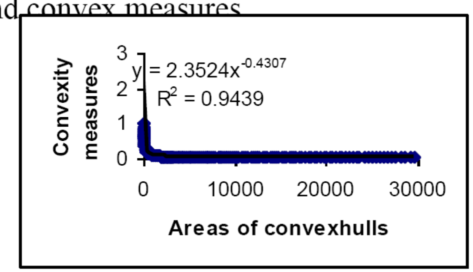

Proposed scaling relationships

- Sample basin
- Simulated F-DEM basins
- Cameron basins
- Petaling basins

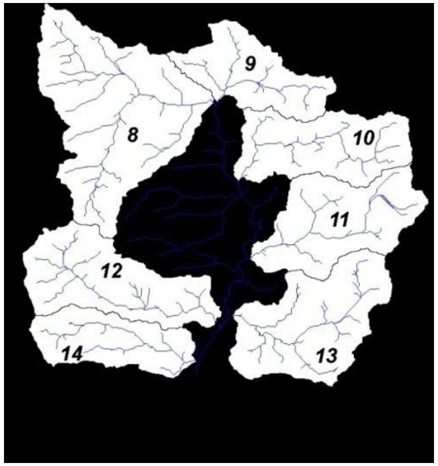

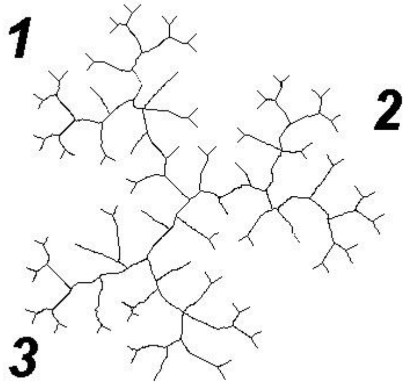

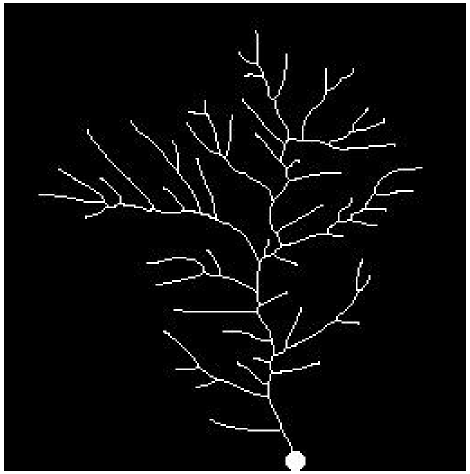

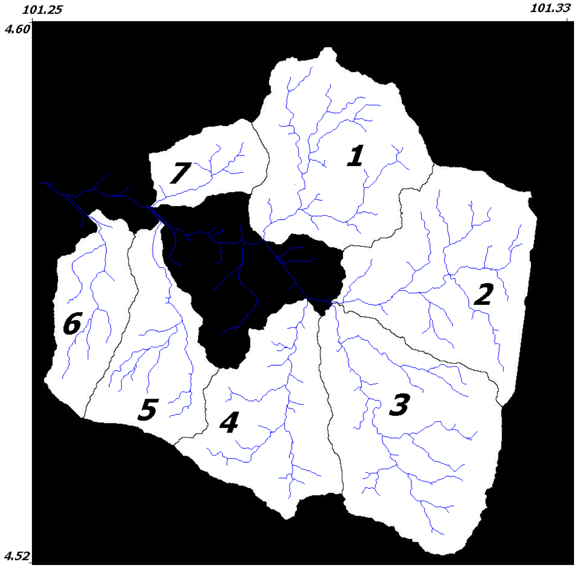

Proposed scaling relationships

Network	α, (R^2)	σ, R^2	λ, R^2	R_b	R_l	*h*	*H*
Sample	0.5693, (0.9671)	0.6988, (0.8325)	0.4307, (0.9439)	3.84	1.66	-	-
Basin 1 (Cameron)	0.5777, (0.9883)	0.7109, (0.9358)	0.4223, (0.9783)	3.60	2.21	0.5414	0.9714
Basin 2 (Cameron)	0.5774, (0.9925)	0.7189, (0.9586)	0.4226, (0.9861)	4.35	2.25	0.5561	1
Basin 3 (Cameron)	0.5799, (0.9934)	0.7131, (0.963)	0.4201, (0.9875)	3.31	2.39	0.5612	0.9256
Basin 4 (Cameron)	0.5521, (0.9835)	0.7814, (0.92)	0.4479, (0.9752)	4.47	3.18	0.5671	0.9506
Basin 5 (Cameron)	0.5798, (0.9905)	0.7083, (0.9469)	0.4202, (0.982)	3.31	2.16	0.5766	0.9162
Basin 6 (Cameron)	0.5819, (0.9865)	0.6955, (0.925)	0.4181, (0.9743)	4.00	2.64	0.5746	0.8597
Basin 7 (Cameron)	0.5885, (0.9887)	0.68, (0.9348)	0.4115, (0.9772)	2.82	2.39	0.5548	0.895
Basin 1 (Petaling)	0.5462, (0.969)	0.7741, (0.8561)	0.4538, (0.9557)	5.00	2.57	0.5568	0.9319
Basin 2 (Petaling)	0.5393, (0.9899)	0.8357, (0.9532)	0.4607, (0.9863)	4.00	3.51	0.5828	0.8623
Basin 3 (Petaling)	0.5198, (0.9852)	0.8953, (0.9367)	0.4802, (0.9827)	4.24	3.30	0.597	0.9019
Basin 4 (Petaling)	0.5592, (0.9938)	0.7771, (0.9684)	0.4408, (0.99)	4.24	2.96	0.5807	0.8902
Basin 5 (Petaling)	0.5729, (0.9906)	0.729, (0.9492)	0.4271, (0.9832)	4.79	3.96	0.5844	0.8704
Basin 6 (Petaling)	0.5547, (0.9872)	0.7798, (0.937)	0.4453, (0.9804)	4.89	3.42	0.5713	0.9116
Basin 7 (Petaling)	0.6059, (0.9929)	0.6387, (0.9551)	0.3941, (0.9834)	3.60	3.39	0.5865	0.8312

Allometric power-laws between travel-time channel networks, convex hulls, and convexity measures for model network, networks of Hortonian fractal DEM, and networks of fourteen basins of Cameron Highlands and Petaling region.

Proposed scaling relationships

These proposed scaling exponents are shown for basins derived from simulated F-DEM and TOPSAR DEMs.

These exponents are scale-independent.

At macroscopic level, these exponents complement with other existing scaling coefficients can be used to identify commonly sharing generic mechanisms in different river basins.

II.II.II. Scale Invariant But Shape Dependent Power-laws

Objectives

To propose morphology based method via fragmentation rules to compute scale invariant but shape-dependent measures of non-network space of a basin.

To make comparisons between morphometry based parameters / dimensions and dimensions derived for non-network space.

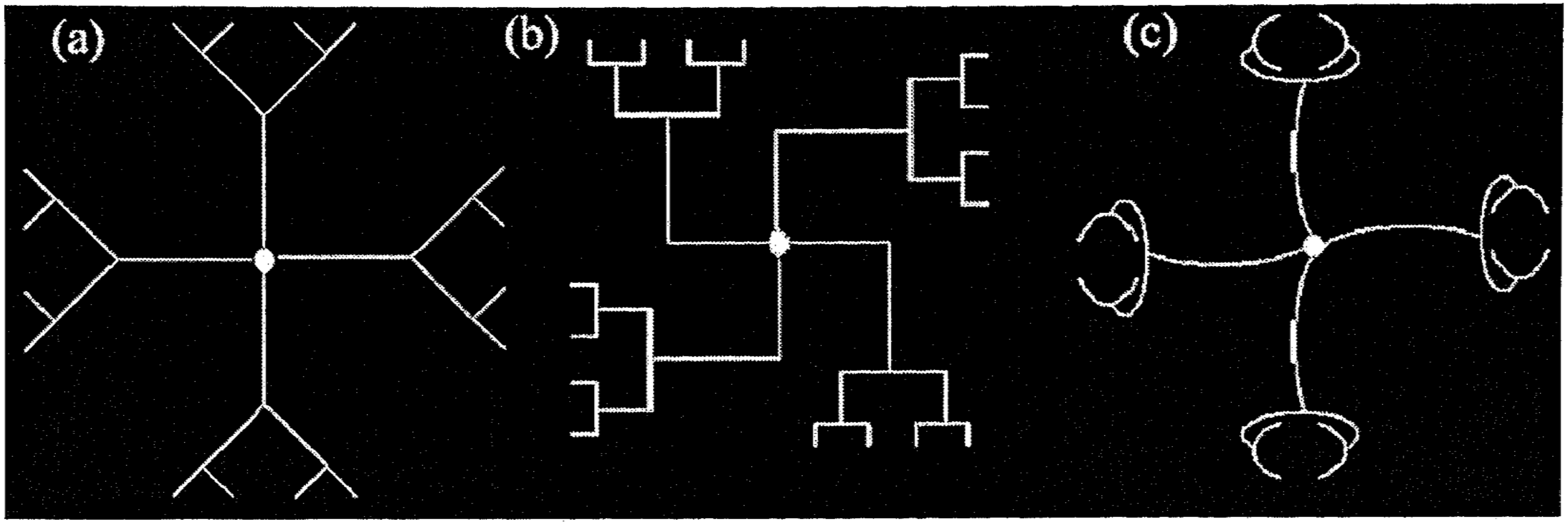

Topologically Invariant networks with variant geometric organization

Proposed Technique

Step1: Channel network is traced from topographic map.

Step2: Channel network is dilated and eroded iteratively until the entire basin is filled up with white space. This step is to generate catchment boundary automatically. Dilation followed by erosion is called structural closing, which will smoothen the image.

Step3: Generate the basin with channel network and non-network space with boundary by subtracting the channel network from the catchment boundary achieved in Step2.

Step4: Structural opening (erosion followed by dilation) is performed recursively in basin achieved in Step3 to fill the entire basin of non-network space with varying size of octagons.

Step5: Assign unique color for each size of octagons.

Step6: Compute morphometry for the basin.

Step7: Compute shape dependent dimension.

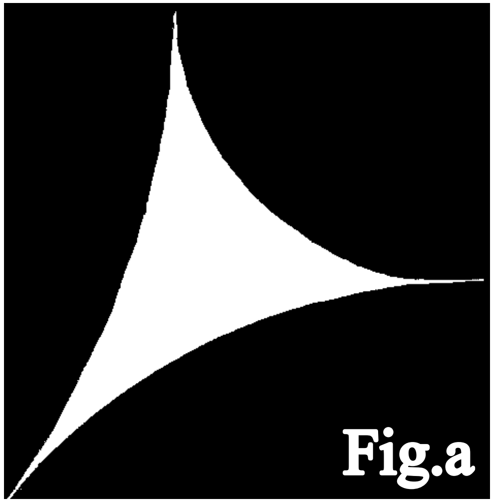

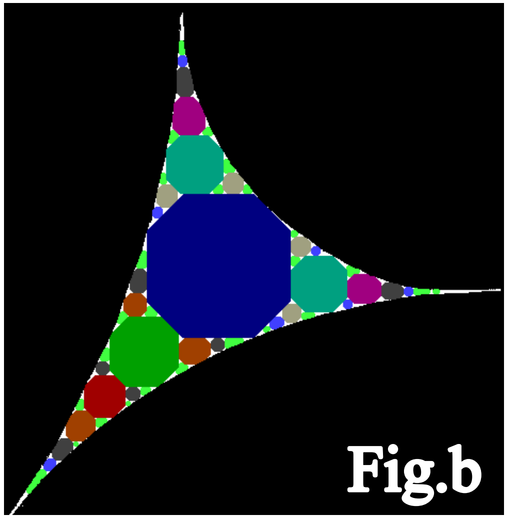

Power law relationship

- As per the previous fig. the slopes of the best-fit lines (α_N and α_A) for number-radius and area-radius relationships yield 2.37 and 1.34.
- These slope values of the best-fit lines provide shape dependent dimensions as $D_N = \alpha_N - 1$ and $D_A = \alpha_A$.
- As in previous Fig., D_N and D_A for non-network space yield 1.37 and 1.34.
- A Power-law relationship is shown in earlier Fig. with an exponent value 1.79 between the area and number of NODs observed with increasing radius of structuring template.

(a) Appollonian Space, and (b) after decomposition by means of octagon.

Algorithm Implementation:

Step 1: **Channel network of sub basin 1**

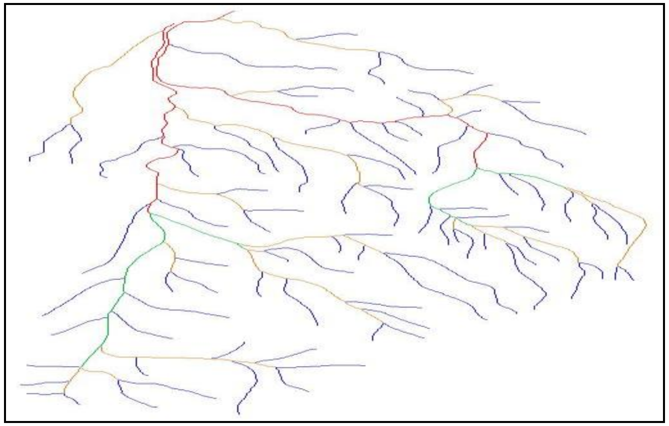

Step 2: **Close-Hull Generation**

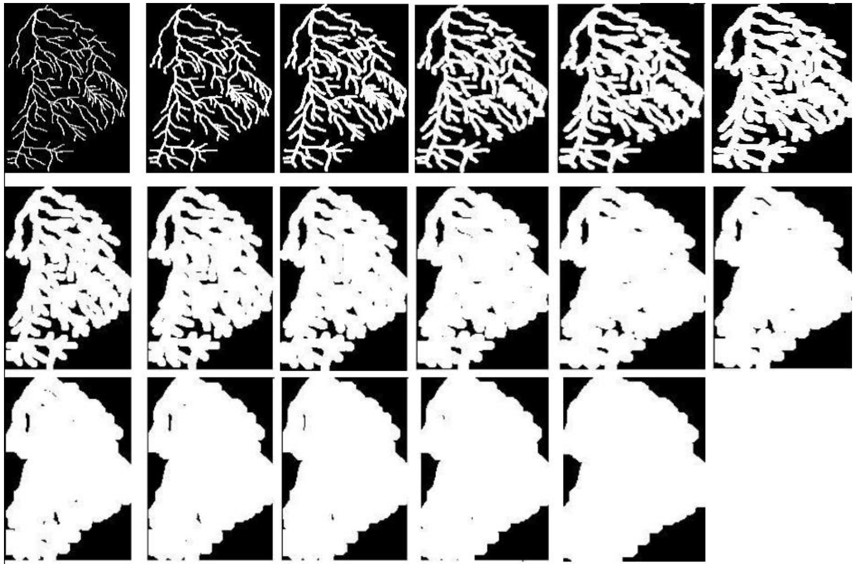

Iterative dilation of channel network of basin 1

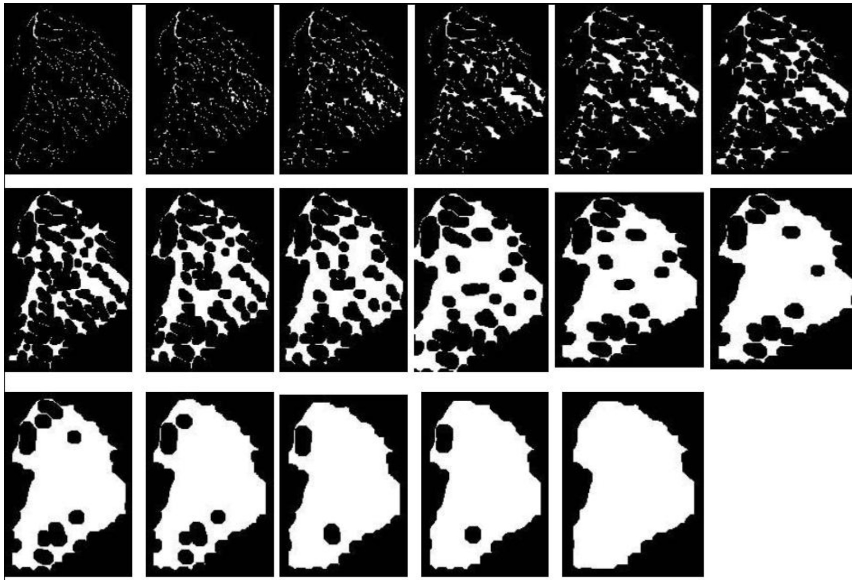

Iterative erosion applied to previous Fig

Step 3: Non-network space of basin 1

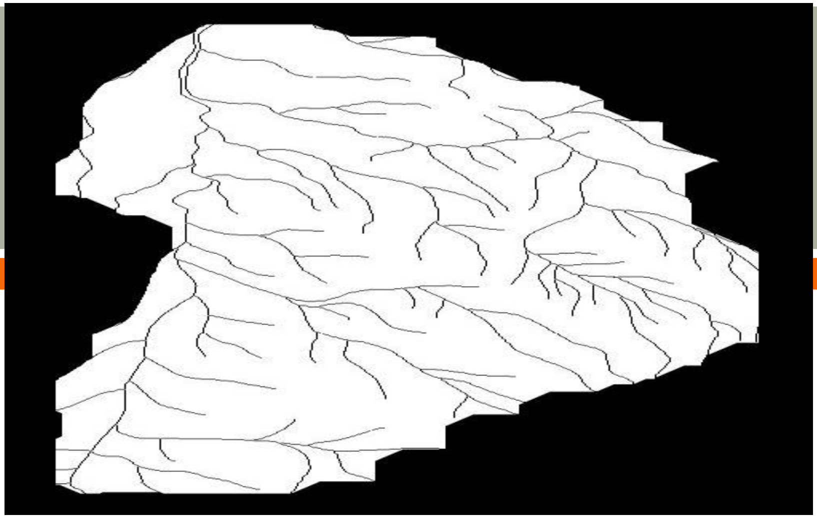

Iterative erosion applied to step-3 Fig.

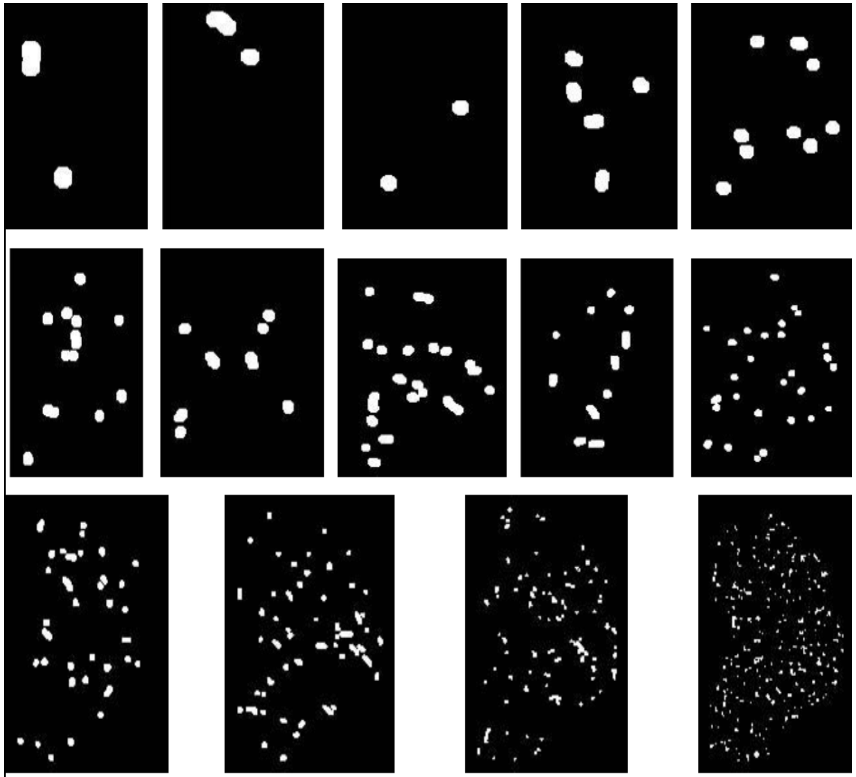

Iterative erosion applied to previous Fig.

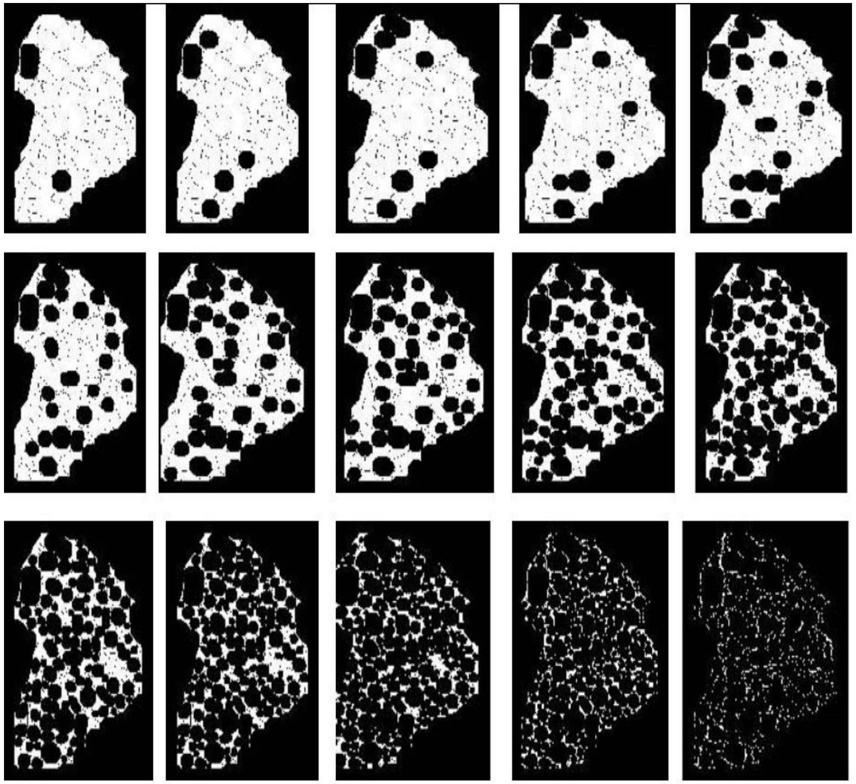

Iterative dilation applied to previous Fig.

Step 4: Non-Network Space Decomposition

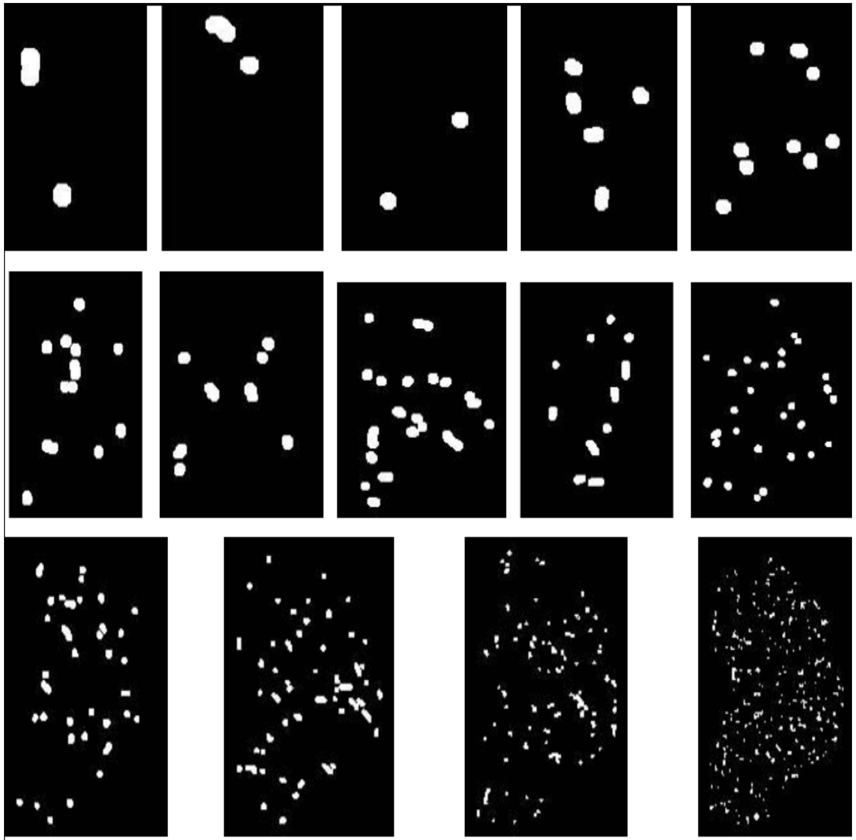

Iterative erosion applied to previous Fig.

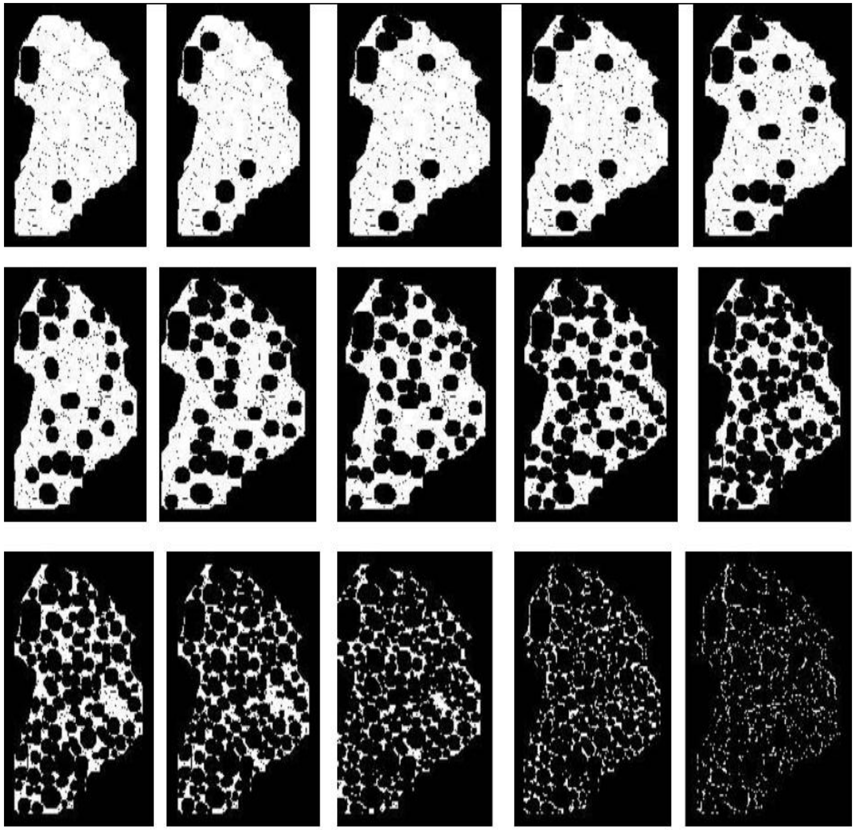

Iterative dilation applied to previous Fig.

Decomposition of Non-network space in to non-overlapping disks of octagon shape of several sizes for basin 1

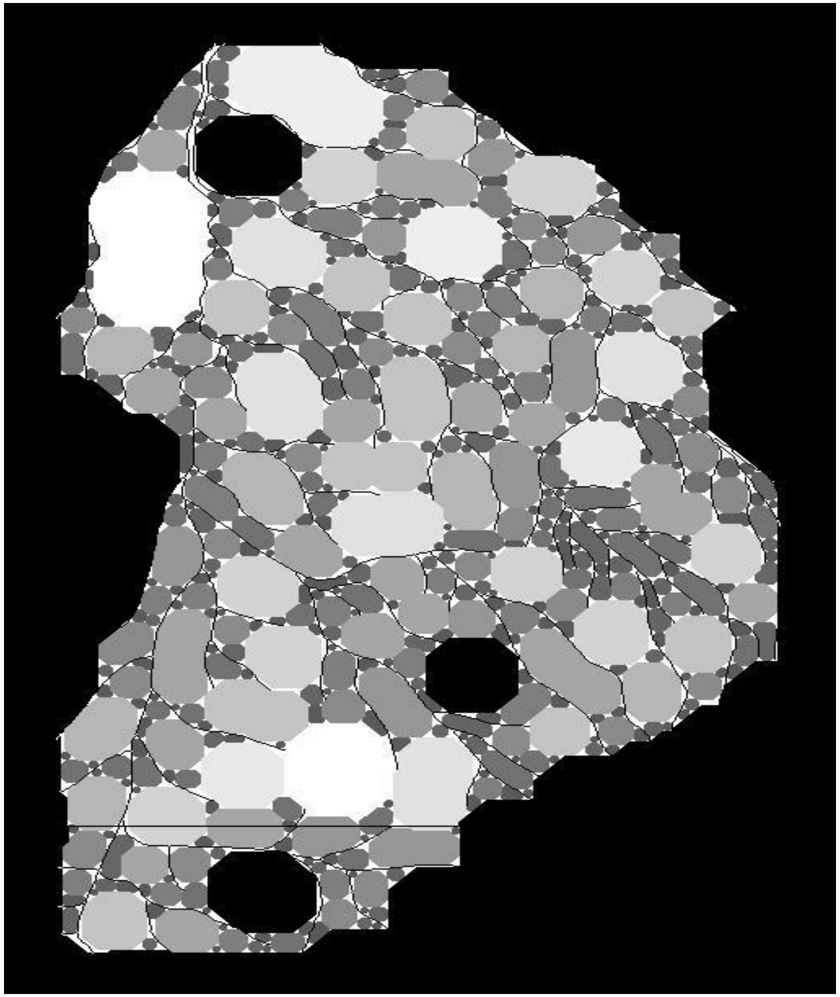

Non-Network Spaces Packed with Non-Overlapping Disks of basins 2 to 8

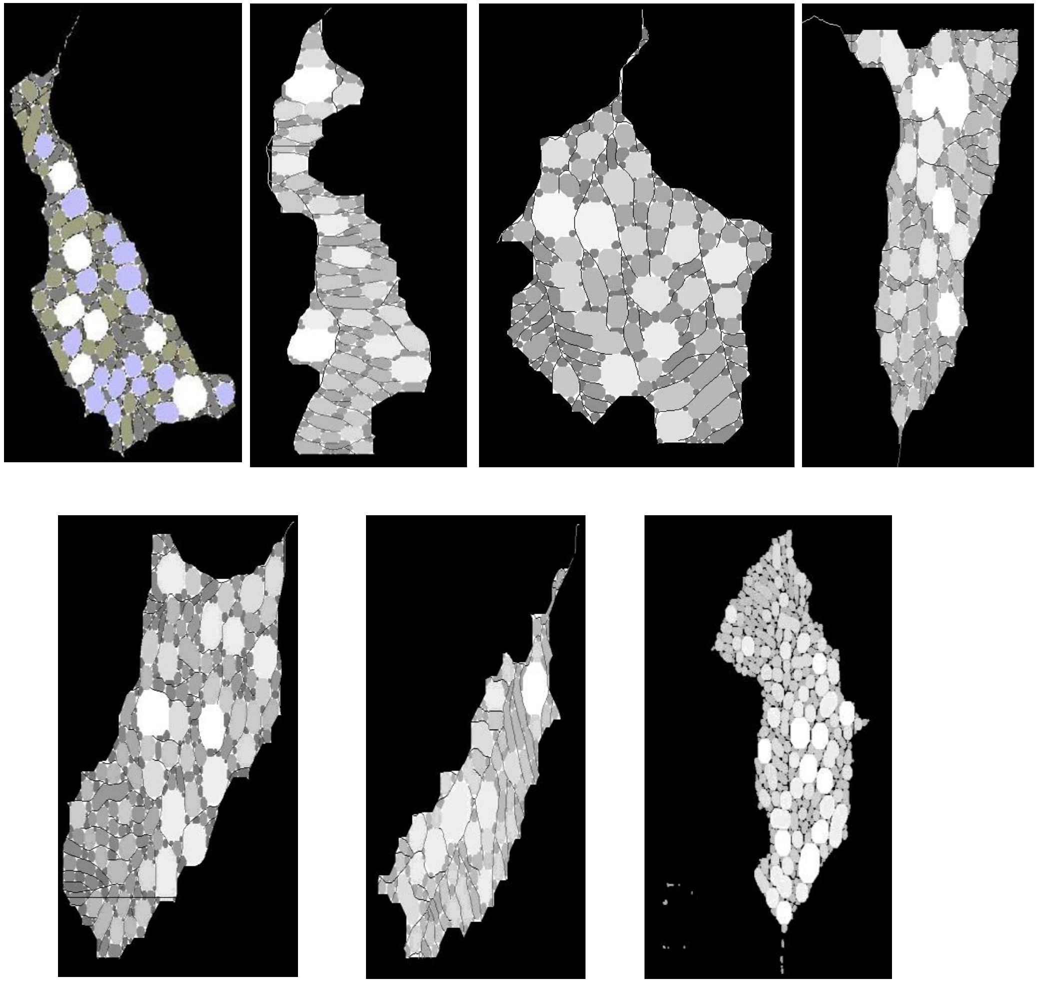

Dimensions derived from morphometry of network and non network space

Morphometric parameter computations achieved through decomposition of non-network space

Basin #	Network FD	Log R_S/ Log R_N	R vs A	R vs N	A vs N
1	1.83	1.93	1.34	2.06	1.50
2	0.86	1.63	1.33	1.23	1.59
3	0.98	1.41	1.02	1.87	1.80
4	2.07	2.01	1.43	2.17	1.52
5	1.73	1.90	1.34	1.94	1.43
6	1.84	2.04	1.13	1.87	1.63
7	1.33	1.61	1.23	2.08	1.70
8	1.65	2.06	1.61	2.38	1.49

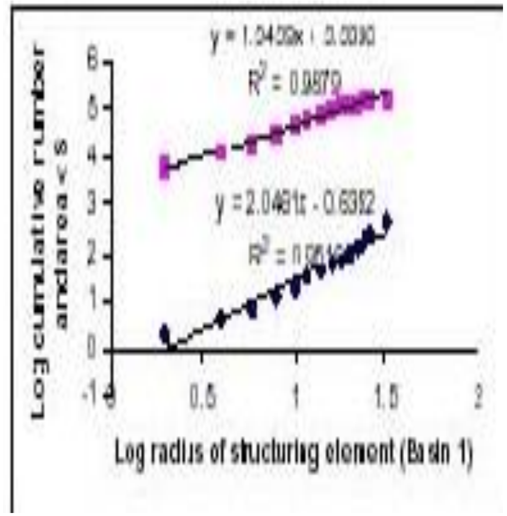

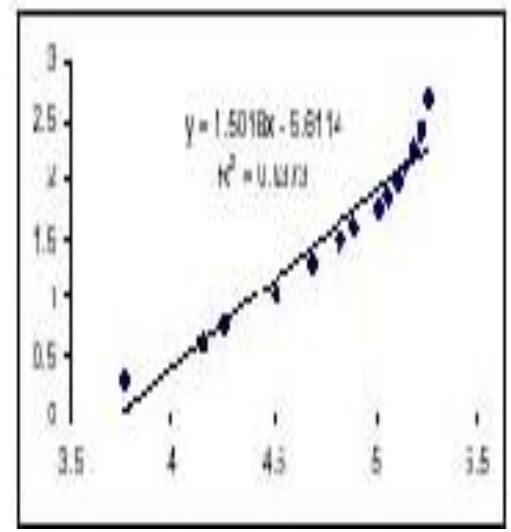

Basin number versus varied dimensions derived from morphometry of networks and non-network spaces

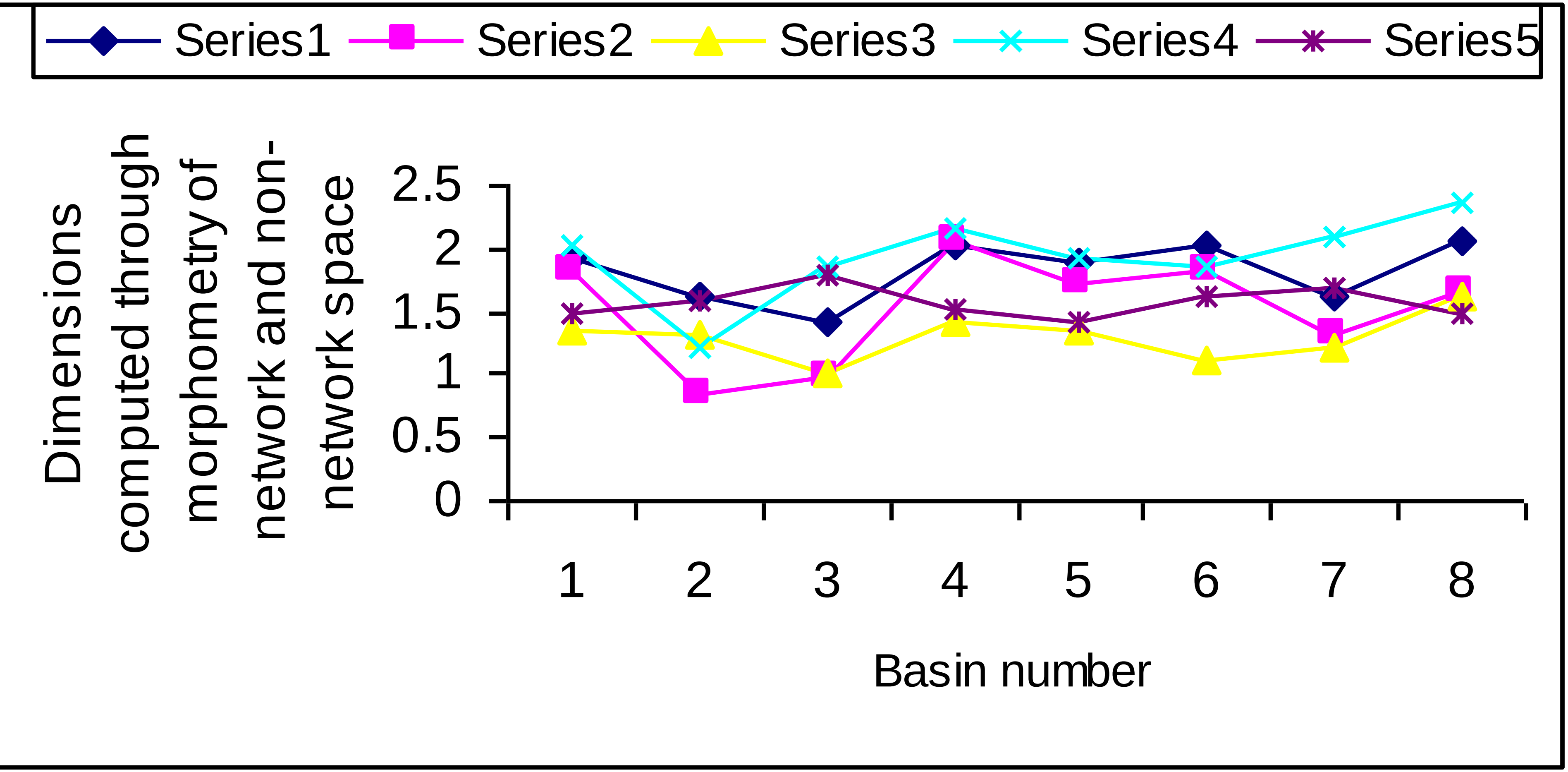

II.II.III. Granulometric analysis of digital topography

Granulometric analysis

Morphological multiscaling transformations are shown to be a potential tool in deriving meaningful terrain roughness indexes.

Consider two different basins of two different physiographic setups (fluvial and tidal) that possess similar topological quantities, i.e., their networks may be topologically similar to each other. But the processes involved therein may be highly contrasting due to their different physiographic origins. Under such circumstances, the results that exhibit similarities in terms of topological quantities and scaling exponents would be insufficient to make an appropriate relationship with involved processes.

Therefore, granulometric approach is proposed to derive shape-size complexity measures of basins. This approach is based on probability distribution functions computed for both protrusions and intrusions (in other words *supremums* and *infimums*) of various degrees of sub-basins.

This granulometry-based technique is tested on sub-basins with various sizes and shapes decomposed from DEMs of two distinct geomorphic regions.

Granulometric Analysis

- Multi-scale opening till completely black
- Multi-scale closing till completely white
- Subtraction
- Probability function

$$PS_f(-n,B) = A[(f \bullet B_n) - (f \bullet B_{n-1})], 1 \leq n \leq K$$

$$PS_f(+n,B) = A[(f \circ B_n) - (f \circ B_{n+1})], 0 \leq n \leq N$$

$$ps(n,f) = \frac{A(f \circ B_n) - A(f \circ B_{n+1})}{A(f \circ B_0)}, n = 0,1,2,\ldots,N$$

$$ps(-n,f) = \frac{A(f \bullet B_n) - A(f \bullet B_{n-1})}{A(f \bullet B_K) - A(f \bullet B_0)}, n = 1,2,\ldots,K$$

- Average size

$$AS(f/B) = \sum_{n=0}^{N} nps(n,f)$$

- Average roughness

$$H(f/B) = -\sum_{k=0}^{n} ps(n,f) \log ps(n,f)$$

Anti(Granulometric) Analysis

Multiscale opening/closing by rhombus

- Scale 1 , 40, 80, 120, 160

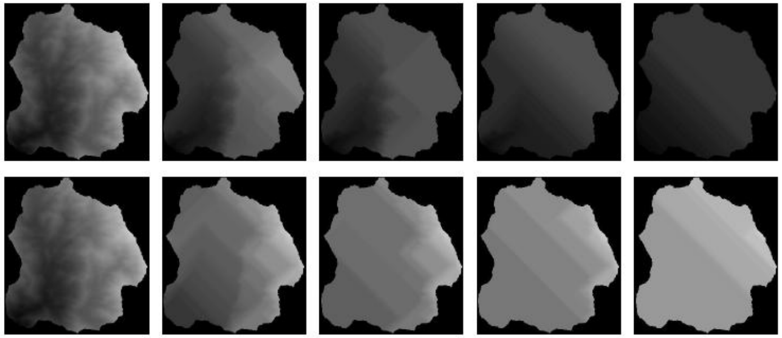

Multiscale opening/closing by octagon

- Scale 1 , 30, 60, 90, 120

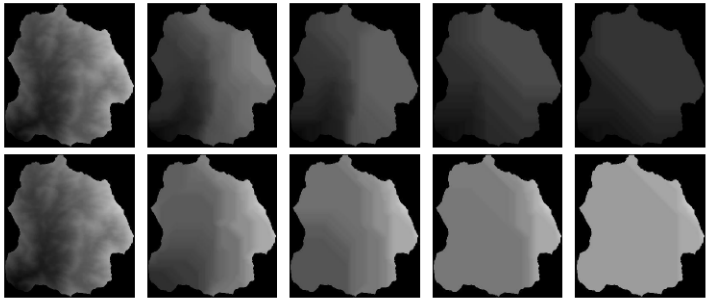

Multiscale opening/closing by square

- Scale 1 , 20, 40, 60, 80

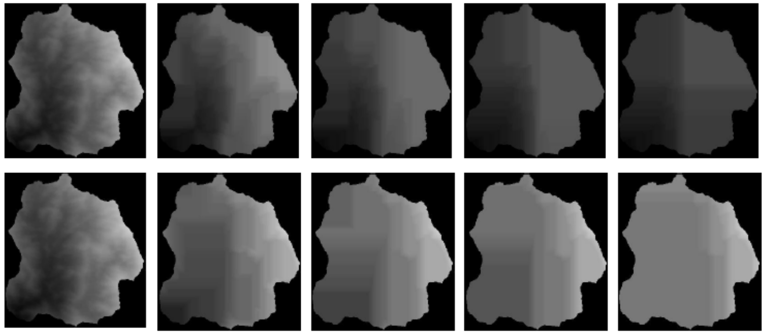

Granulometric analysis : Basin wise analysis

- Average size – 14 sub-basins
- Average roughness – 14 sub-basins

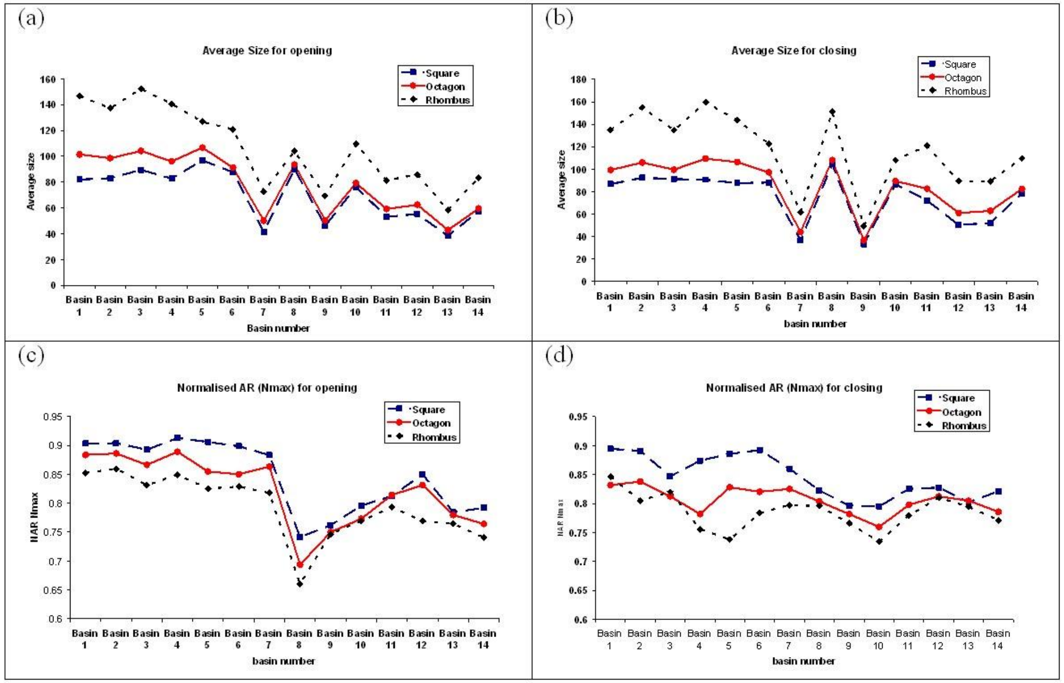

Granulometric Analysis : Basin wise analysis

The number of iterations required to make each sub-basin either become darker or brighter depends on the size, shape, origin, orientation of considered primitive template used to perform multiscale openings or closings, and also on the size of the basin and its physiographic composition. More opening/closing cycles are needed when structuring element rhombus is used, and it is followed by octagon and square.

Mean roughness indicates the shape-content of the basins. If the shape of SE is geometrically similar to basin regions, the average roughness result possesses lower analytical values. If the topography of basin is very different from the shape of SE, high roughness value is produced, which indicates that the basin is rough relative to that SE. In general, all basins are rougher relative to square shape as highest roughness indices are derived when square is used as SE.

A clear distinction is obvious between the Cameron and Petaling basins. Generally, roughness values of Cameron basins are significantly higher than that of Petaling basins.

The terrain complexity measures derived granulometrically are scale-independent, but strictly shape-dependent. The shape dependent complexity measures are sensitive to record the variations in basin shape, topology, and geometric organisation of hillslopes.

Granulometric analysis of basin-wise DEMs is a helpful tool for defining roughness parameters and other morphological/topological quantities.

III. Mathematical Morphology in GISci

Spatial Interpolations

Spatial Reasoning

- Strategic set identification
- Directional Spatial Relationship
- Spatial-Interactions
- Point-to-Polygon Conversion

III.I. Spatial Interpolations

VISUALIZATION OF SPATIO-TEMPORAL BEHAVIOUR OF DISCRETE MAPS VIA GENERATION OF RECURSIVE MEDIAN ELEMENTS

<u>Outline</u>

Mathematical Morphological Transformations employed include:

Hausdorff Dilation, Hausdorff Erosion, Morphological Median Element Computation, and Morphological Interpolation.

Objectives

To show relationships between the layers depicting noise-free phenomenon at two time periods.

To relate connected components of layers of two time periods via FOUR possible categories of spatial relationships of THREE groups.

To propose a framework to generate recursive interpolations via median set computations.

To demonstrate the validity of the framework on epidemic spread.

THREE Groups and FOUR Categories??

Three groups are conceived by checking the intersection properties between the corresponding connected components.

Four categories under the above three groups are visualized via logical relationships and Hausdorff erosion and Hausdorff dilation distances.

What are these Hausdorff distances?

What basics do we require to know to compute these distances?

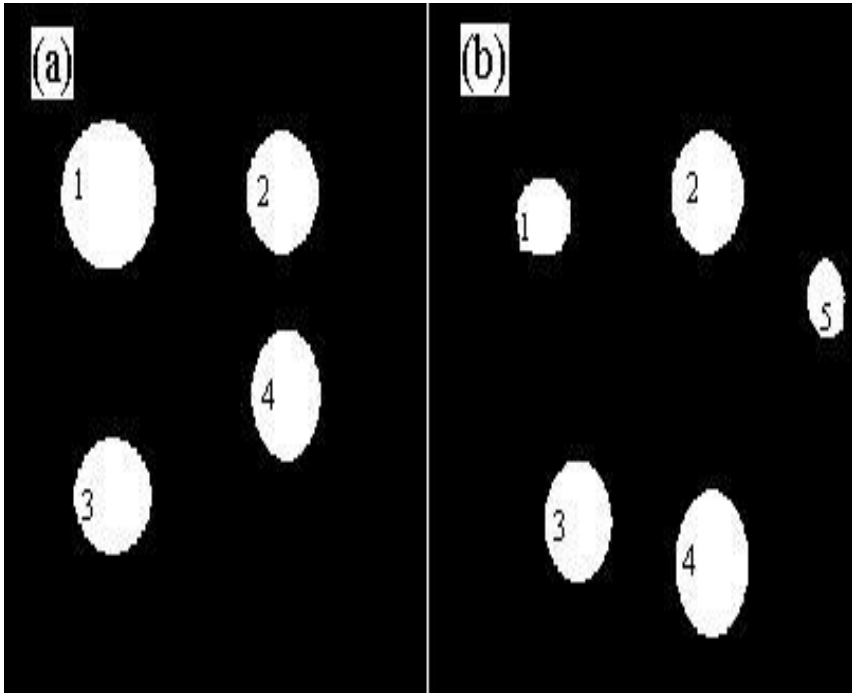

Spatial Relationships Between Sets and Their Categorization

- *Ordered sets*.

semi-ordered sets, if subsets of X^t (resp. X^{t+1}) are only partially contained in the other set X^{t+1} (resp. X^t).

Whereas, (X^t) and (X^{t+1}) are considered as *disordered sets* if there exists an empty set while taking the intersection of (X^t) and (X^{t+1}) (or) of their corresponding subsets.

Description of categories via logical relations

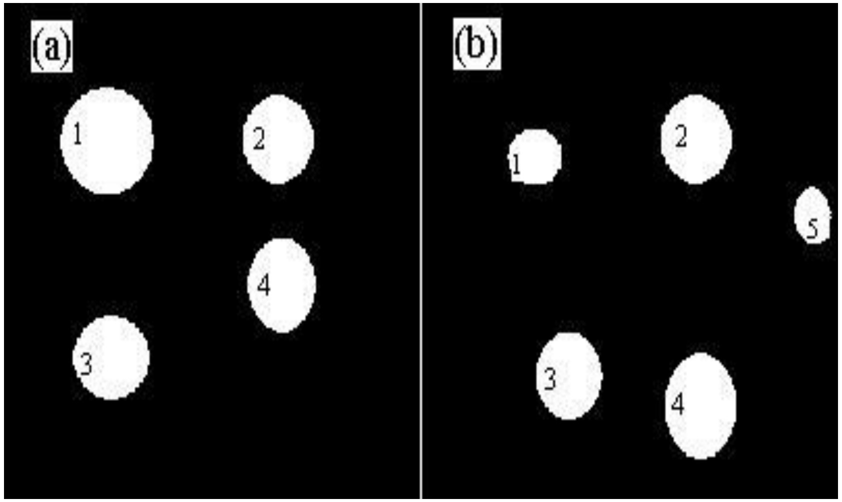

Categories via Hausdorff Erosion and Dilation Distances

TABLE 1. CATEGORY-WISE HAUSDORFF DISTANCES

Group	Category	$\sigma\left(X_i^t, X_i^{t+1}\right)$	$\rho\left(X_i^t, X_i^{t+1}\right)$
I	1	0	0
I	2	≥ 1	≥ 1
II	3	Does not exist	≥ 1
III	4	Does not exist	Does not exist

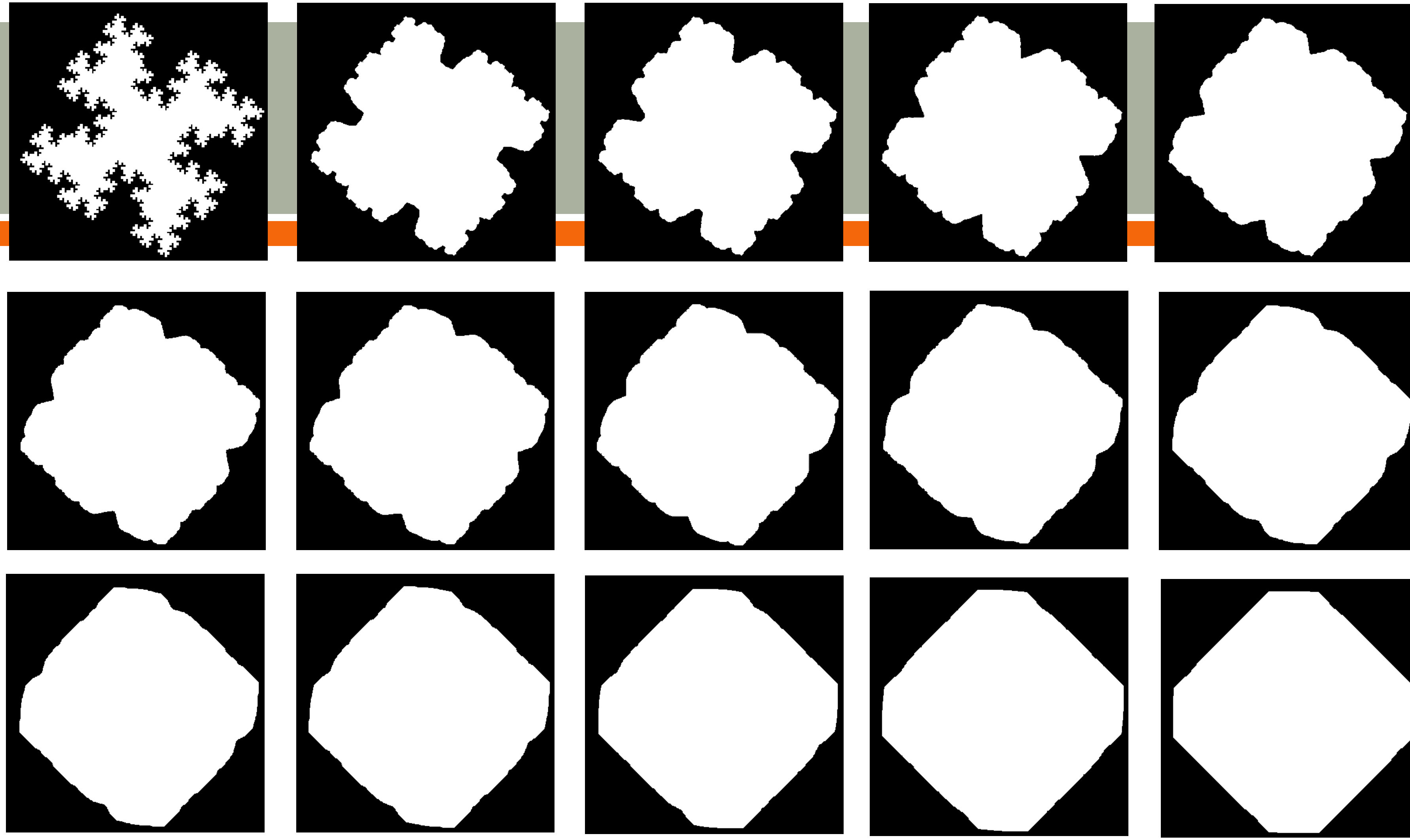

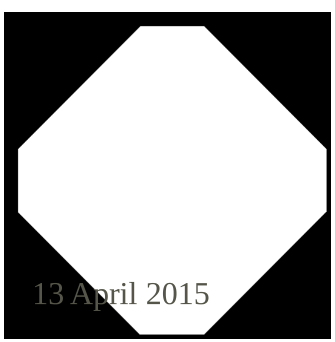

Morphological interpolation sequence of fractal M_1 and its convex hull M_{16} (left-right, then top-bottom).

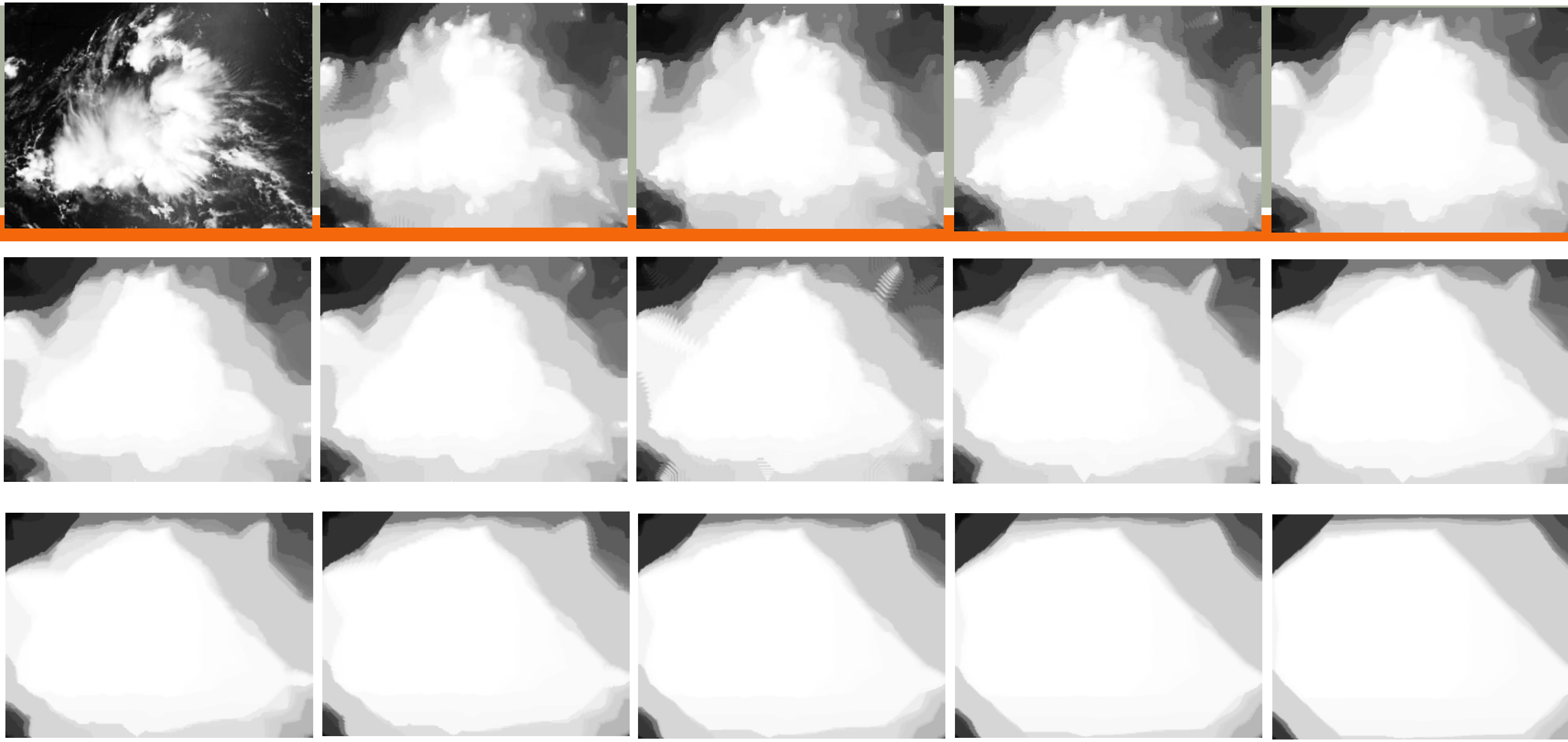

Morphological interpolation sequence of cloud field f_1 and its convex hull f_{16} (left-right, then top-bottom).

Interpolated Sequence of Lakes' Data of Two Seasons

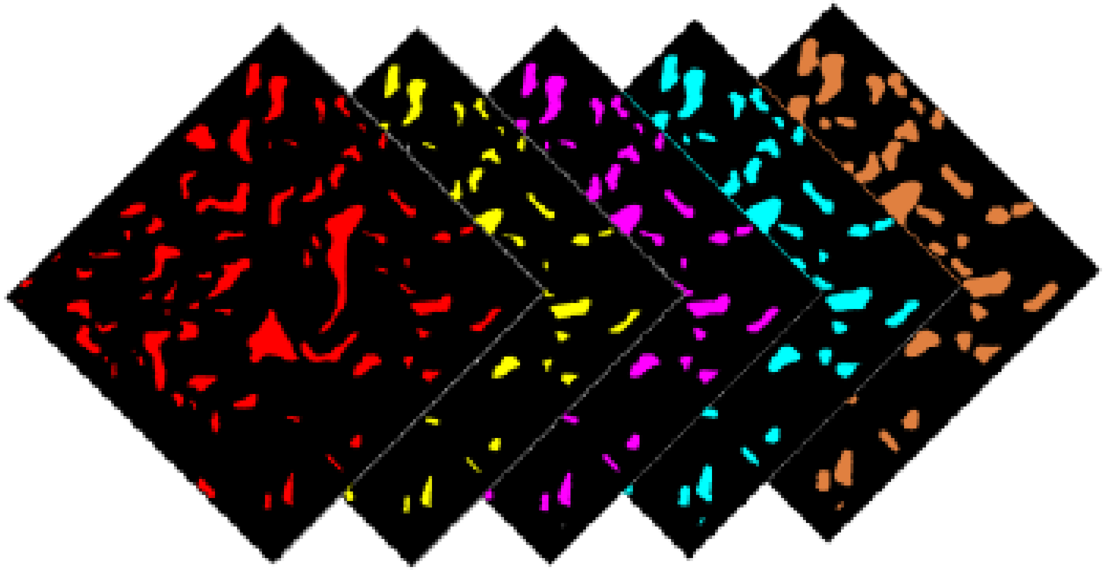

Fig. 4. A sequence of interpolated sets (slices) in between the two input slices shown in Figs. 3a, b. Equations 8(a) and 14 are used to recursively generate the interpolated slices. The layer depicting water bodies with magenta color is the median set shown in Fig. 3c.

Observed and Interpolated Epidemic Spread Maps

http://www.isibang.ac.in/~bsdsagar/AnimationOfEpidemicSpread.avi

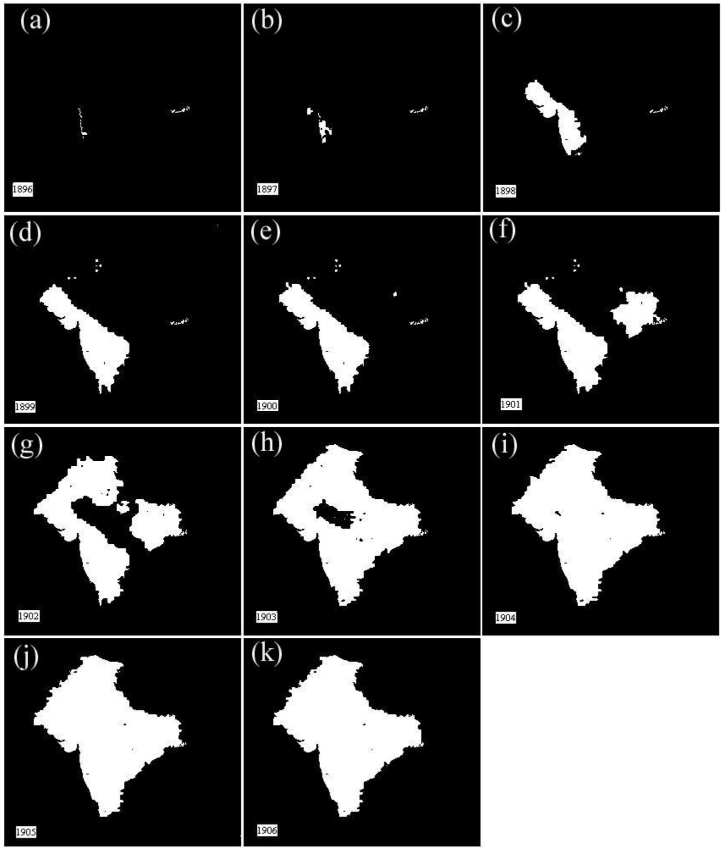

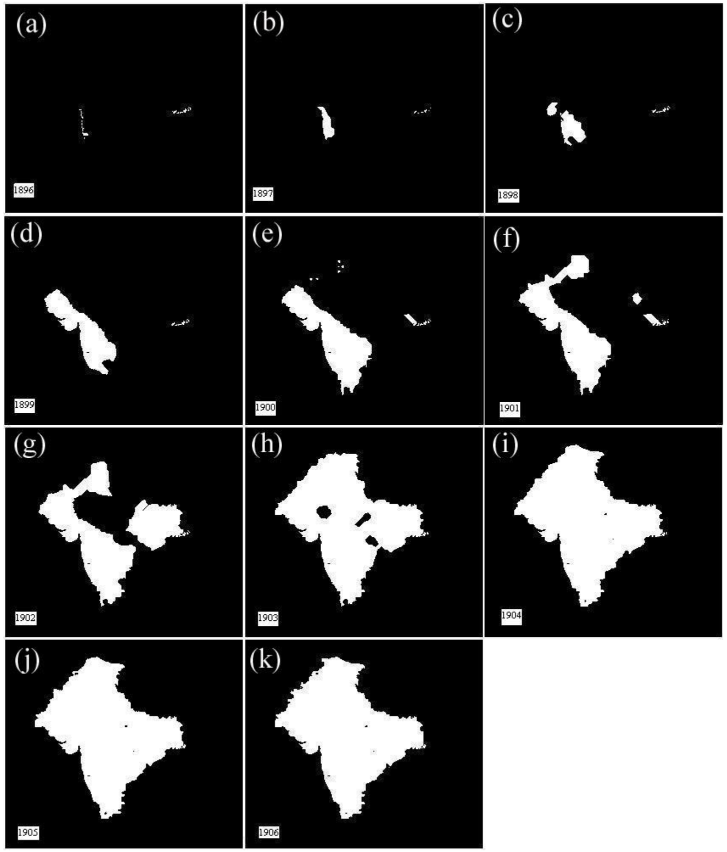

Observed and Interpolated Sequences

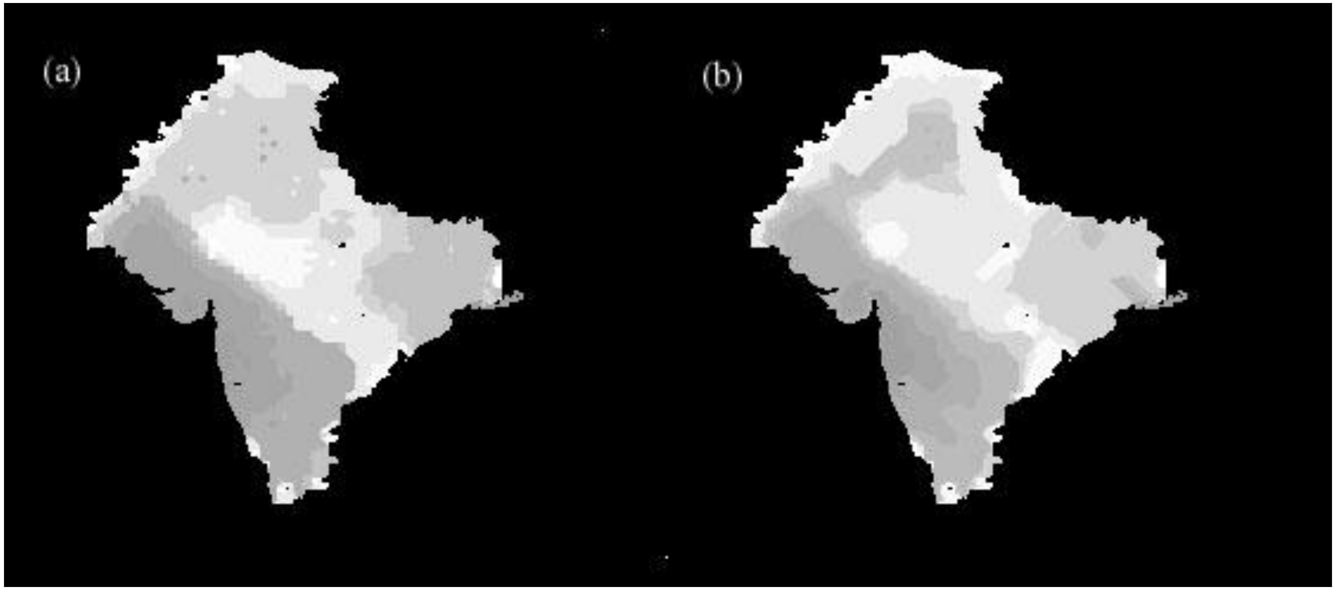

Earth Surface Transformation

Hierarchical Morphological Interpolation between landscape functions, say, f_1 and f_{256}.

f_1 f_{256}

f_{128}

f_{64} f_{192}

f_{32} f_{96} f_{160} f_{224}

$\vdots$

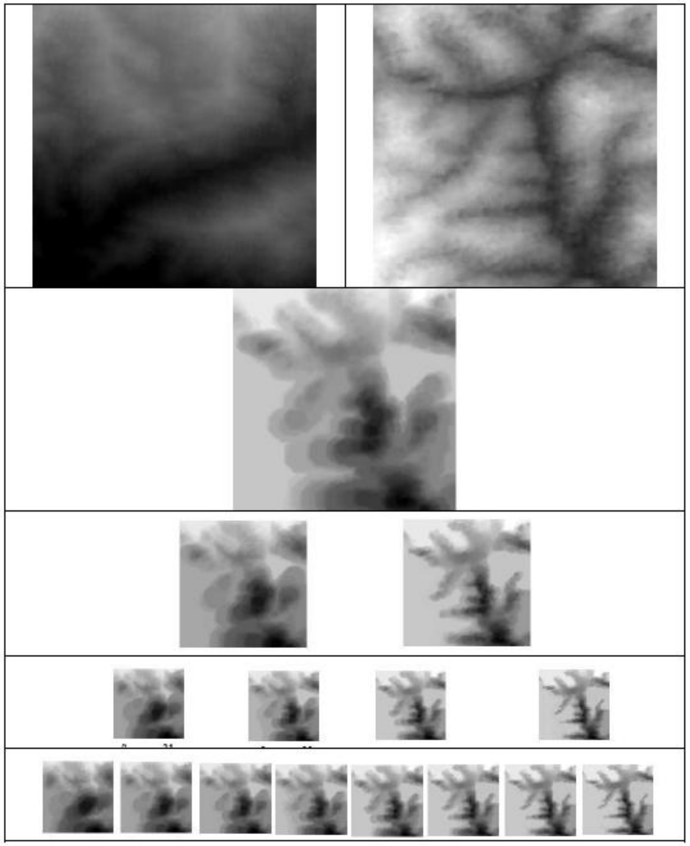

III.II. Spatial Reasoning

Strategically important set(s)

Directional spatial relationship

Point-polygon conversion

III.II.I. Strategically significant state(s)

$$H/P(A_{ij}) = -\sum_{\substack{\forall j \\ i \neq j}} \Pr\left[P(A_{ij})\log \Pr\left[P(A_{ij})\right]\right]$$

$$H/C(A_{ij}) = -\sum_{\substack{\forall j \\ i \neq j}} \Pr\left[C(A_{ij})\log \Pr\left[C(A_{ij})\right]\right]$$

$$H/d(A_{ij}) = -\sum_{\substack{\forall j \\ i \neq j}} \Pr\left[d(A_{ij})\log \Pr\left[d(A_{ij})\right]\right]$$

$$H/d(A_{ji}) = -\sum_{\substack{\forall i \\ i \neq j}} \Pr\left[d(A_{ji})\log \Pr\left[d(A_{ji})\right]\right]$$

$$\left(SH_i^P\right) = \min_{\forall i}\left\{H/P(A_{ij})\right\} \quad \left(SA_i^p\right) = \max_{\forall i}\left\{\overline{\sum_i NP(A_{ij})}\right\}$$

$$\left(SH_i^d\right) = \min_{\forall i}\left\{\min\left\{H/d(A_{ij}), H/d(A_{ji})\right\}\right\}$$

$$\left(SH_i^C\right) = \min_{\forall i}\left\{H/C(A_{ij})\right\}$$

$$\left(SA_i^d\right) = \min_{\forall i,j}\left\{\min\left[\overline{\sum_i Nd(A_{ij})}, \overline{\sum_j Nd(A_{ji})}\right]\right\}$$

$$\left(SA_i^c\right) = \max_{\forall i}\left\{\overline{\sum_i C(A_{ij})}\right\}$$

$$P(A_{ij}) = P\left[(A_i \oplus B) \cap (A_j)\right]$$

$$d(A_{ij}) = \min_{i \neq j}\left\{n : A_j \subseteq (A_i \oplus nB)\right\},$$

$$C(A_{ij}) = C(A_{ji})$$

$$= \left[\frac{\rho(A_{ij})}{\max\left[d(A_{ij}), d(A_{ji})\right]}\right]$$

$$= \left[\frac{\rho(Nd(A_{ij}))}{\max\left[Nd(A_{ij}), Nd(A_{ji})\right]}\right]$$

Matrices and Parameters

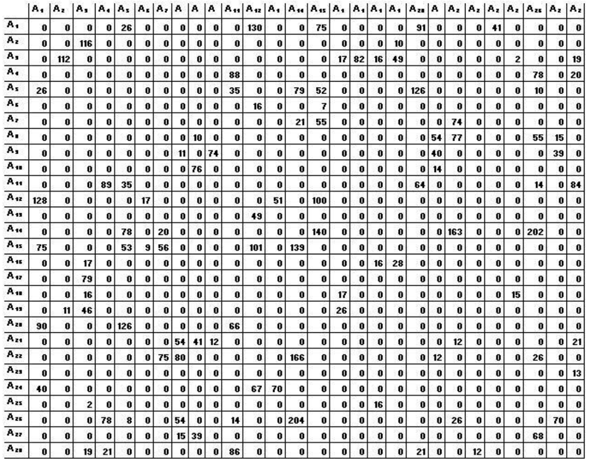

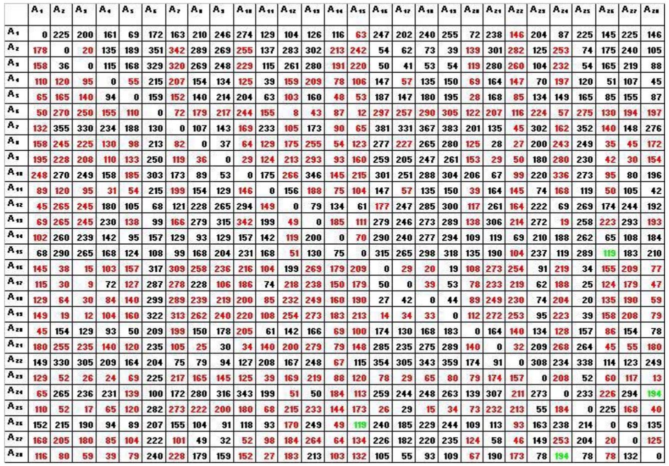

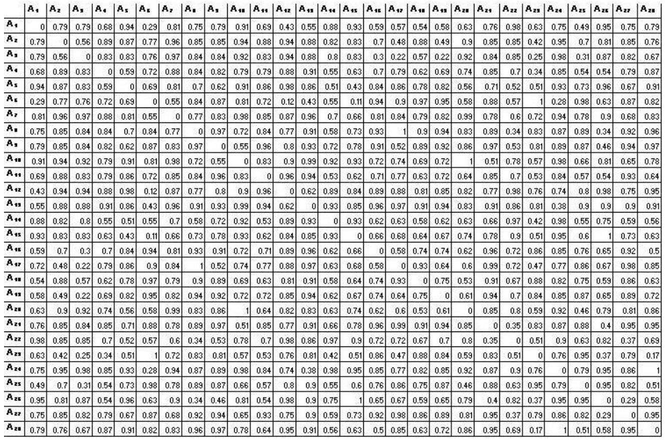

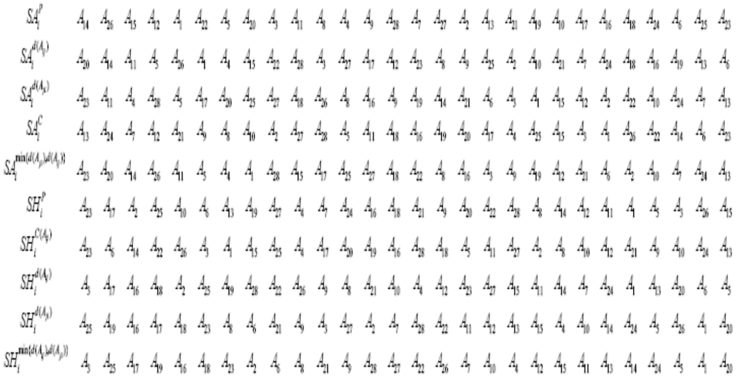

Strategically significant state(s) w.r.t 10 parameters

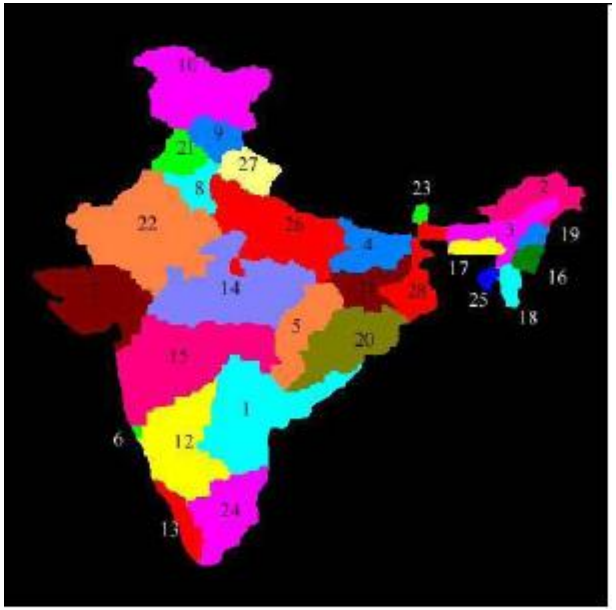

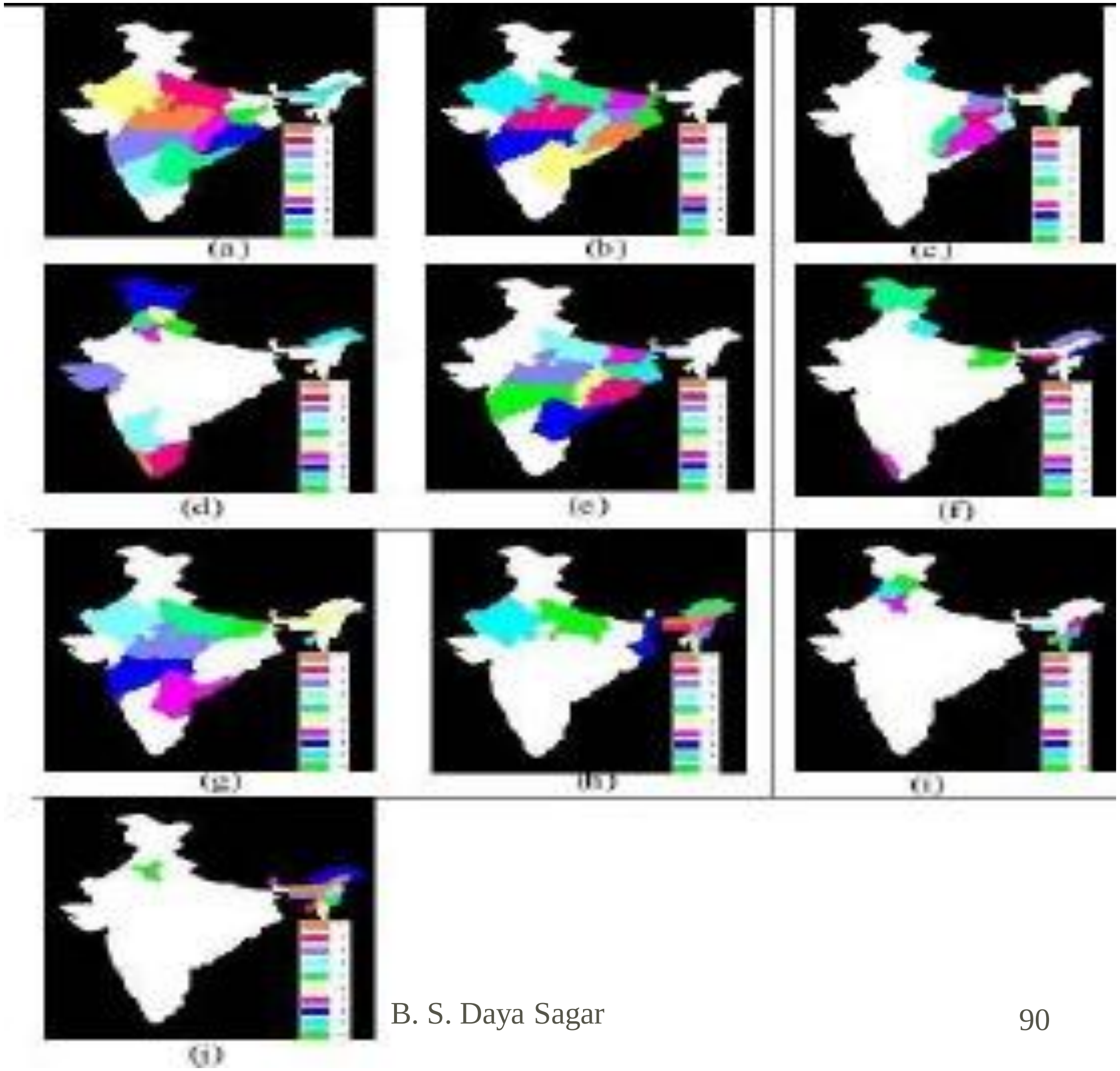

III.II.II Directional Spatial Relationship

http://www.isibang.ac.in/~bsdsagar/AnimationOfDirectionalSpatialRelationship.wmv

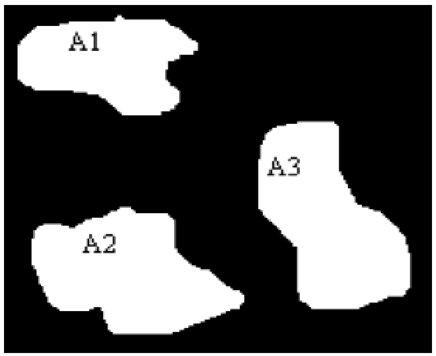

Fig. 1. (A_1, A_2, A_3) three disjoint objects possessing different directional spatial relationship.

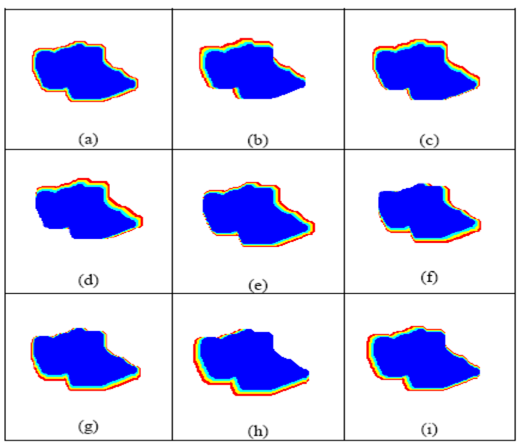

Fig. 5. Directional dilations on objects A by all nine origins. (a) $A \oplus B^0$, (b) $A \oplus B^1$, (c) $A \oplus B^2$, (d) $A \oplus B^3$, (e) $A \oplus B^4$, (f) $A \oplus B^5$, (g) $A \oplus B^6$, (h) $A \oplus B^7$, (i) $A \oplus B^8$.

$$\begin{matrix} 1 & 1 & 1 \\ 1 & (1) & 1 \\ 1 & 1 & 1 \end{matrix} \quad \begin{matrix} (1) & 1 & 1 \\ 1 & 1 & 1 \\ 1 & 1 & 1 \end{matrix} \quad \begin{matrix} 1 & (1) & 1 \\ 1 & 1 & 1 \\ 1 & 1 & 1 \end{matrix}$$
$$(B^0) \qquad (B^1) \qquad (B^2)$$

$$\begin{matrix} 1 & 1 & (1) \\ 1 & 1 & 1 \\ 1 & 1 & 1 \end{matrix} \quad \begin{matrix} 1 & 1 & 1 \\ 1 & 1 & (1) \\ 1 & 1 & 1 \end{matrix} \quad \begin{matrix} 1 & 1 & 1 \\ 1 & 1 & 1 \\ 1 & 1 & (1) \end{matrix}$$
$$(B^3) \qquad (B^4) \qquad (B^5)$$

$$\begin{matrix} 1 & 1 & 1 \\ 1 & 1 & 1 \\ 1 & (1) & 1 \end{matrix} \quad \begin{matrix} 1 & 1 & 1 \\ 1 & 1 & 1 \\ (1) & 1 & 1 \end{matrix} \quad \begin{matrix} 1 & 1 & 1 \\ (1) & 1 & 1 \\ 1 & 1 & 1 \end{matrix}$$
$$(B^6) \qquad (B^7) \qquad (B^8)$$

Fig. 3. Structuring element is shown with different possible origins. Except the first structuring element for which the origin is shown at the center, all other eight structuring elements are with other eight possible positions as origins. Those eight other structuring elements are asymmetric structuring elements as their transposes are not equivalents of their non-transposed versions.

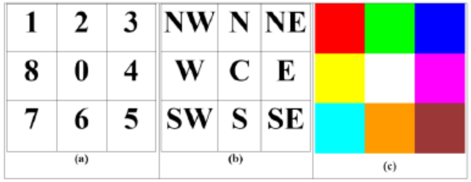

Fig. 4 Shows (a) origins of structuring element, and their corresponding directions in (b) and color codes in (c).

$$\Delta(A_i, A_j) = i \,\Big|\, \min_{\forall i} \left\{ n : A_j \subseteq \left(A_i \oplus n\hat{B}^i \right) \right\}$$

TABLE 1. DISTANCES, UNIQUE ORIGINS AND DIRECTIONS

Minimum Dilation Distances				Unique Origins				Directional Relations				Visualization of Directional Relations			
	A_1	A_2	A_3		A_1	A_2	A_3		A_1	A_2	A_3		A_1	A_2	A_3
A_1	0	53	50	A_1	0	2	1	A_1	C	N	NW	A_1			
A_2	46	0	36	A_2	6	0	7	A_2	S	C	SW	A_2			
A_3	52	49	0	A_3	5	3	0	A_3	SE	NE	C	A_3			

III.II.II. Directional Spatial Relationship

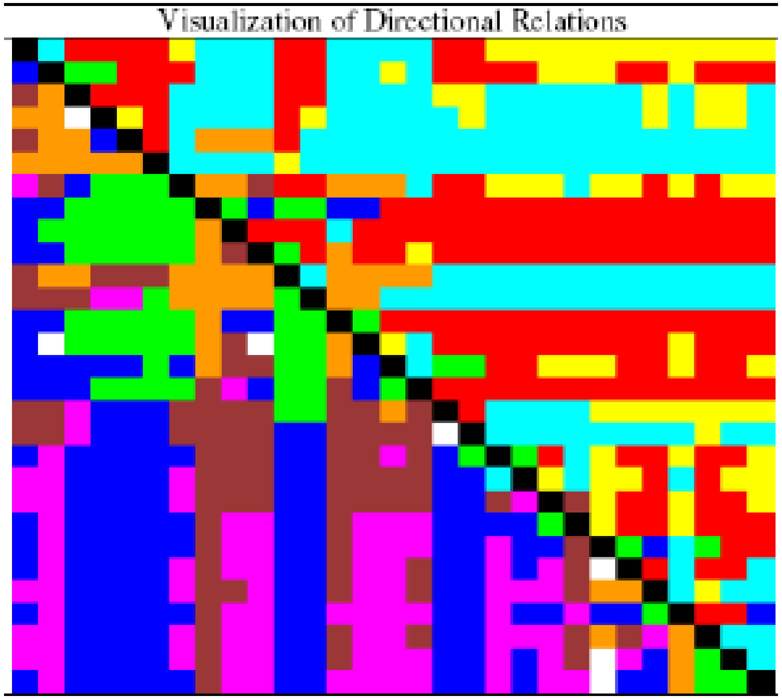

III.II.III Spatial Interactions: Gravity Models

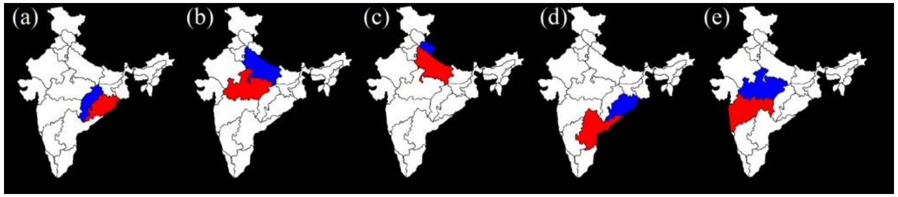

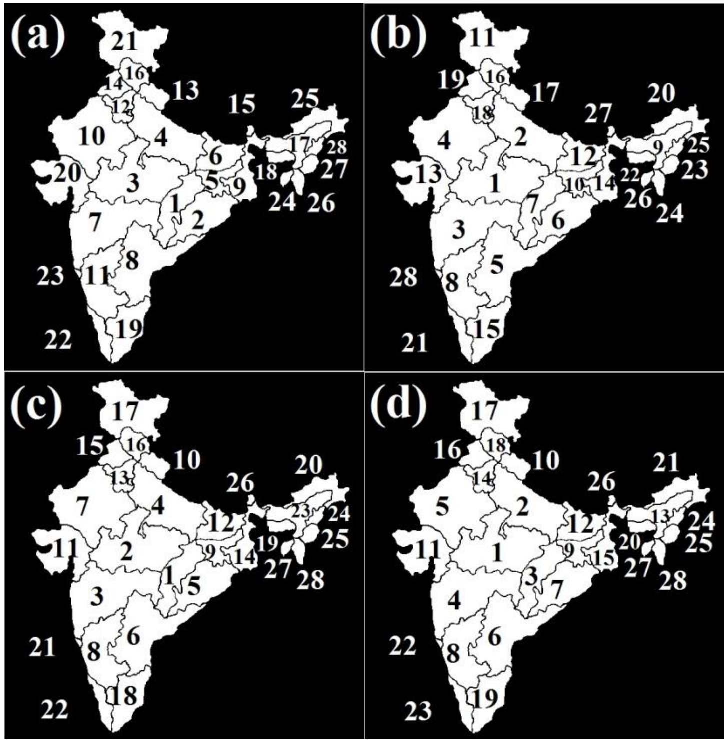

III.II.IV Spatiotemporal Visualization

To visualize point-data into polygonal data

Weighted Skeletonization by Influence Zones (WSKIZ)

Point-to-Polygon Conversion

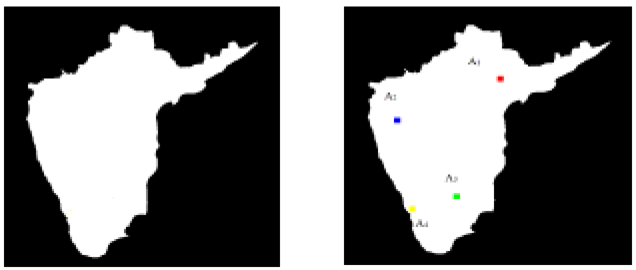

(a) (b)

Fig. 2. (a) region considered is south India, and (b) gauge-station locations (A_1, A_2, A_3, A_4).

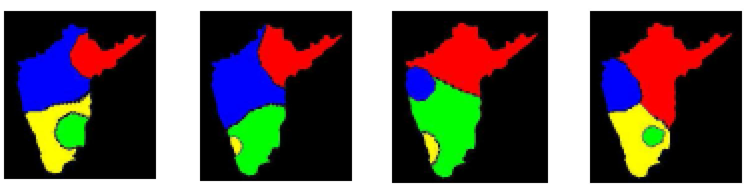

(a) (b) (c) (d)

Fig. 3. The variable strengths (in terms of propagation speeds are given as (a) $A_2 > A_4 > A_1 > A_3$, (b) $A_2 > A_1 > A_3 > A_4$, (c) $A_1 > A_3 > A_2 > A_4$, and (d) $A_1 > A_4 > A_2 > A_3$.

$$Z(A_i) = \bigcup_n \left(\delta^{n}_{\lambda_i}(A_i) \cap A\right) \setminus \bigcup_{\forall j} \left(\delta^{n}_{\lambda_j \neq i}(A_j) \cap A\right)$$

$$Z(A) = \left[\bigcup_i \left(Z(A_i)\right)\right]^C$$

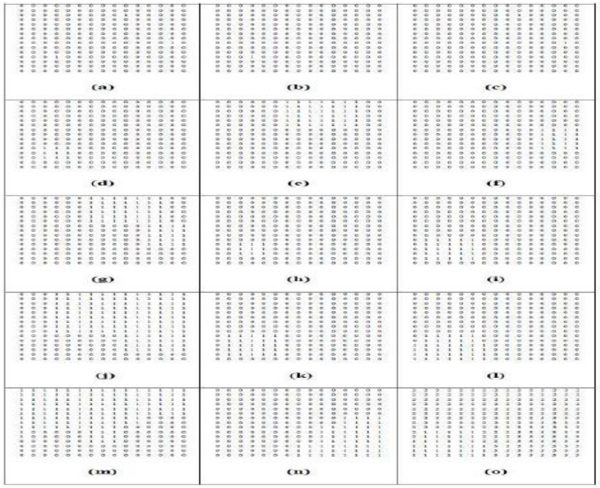

Fig. S1. (a) original map with three points (shown with 1s) for (A_1), (A_2), and (A_3), (b) i^{th} point $(A_i) = (A_1)$, (c) union of j^{th} points, $\bigcup_{\forall j, j \neq i} A_j = (A_2) \bigcup (A_3)$, (d) first cycle of dilation of i^{th} point by B (Square in shape) with the propagation speed of $\lambda = 1$, denoted by $\delta^{n=1}_{\lambda=1}(A_1)$, (e) first cycle of dilation of j^{th} point (A_2) by B with the propagation speed of $\lambda = 3$, $\delta^{n=1}_{\lambda=3}(A_2)$, (f) first cycle of dilation of i^{th} point (A_3) by B with the propagation speed of $\lambda = 2$, $\delta^{n=1}_{\lambda=2}(A_3)$, (g) union of $\delta^{n=1}_{\lambda=3}(A_2)$ and $\delta^{n=1}_{\lambda=2}(A_3)$, (h) $\delta^{n=1}_{\lambda=1}(A_1) \setminus \delta^{n=1}_{\lambda=3}(A_2) \bigcup \delta^{n=1}_{\lambda=2}(A_3)$, (i) $\delta^{n=2}_{\lambda=1}(A_1)$ (j) similarly for next iteration: $\delta^{n=2}_{\lambda=3}(A_2) \bigcup \delta^{n=2}_{\lambda=2}(A_3)$, (k) $\delta^{n=2}_{\lambda=1}(A_1) \setminus \delta^{n=2}_{\lambda=3}(A_2) \bigcup \delta^{n=2}_{\lambda=2}(A_3)$, (l) $Z(A_1) = \bigcup_n \left[\delta^{n}_{\lambda=1}(A_1) \setminus \delta^{n}_{\lambda=3}(A_2) \bigcup \delta^{n}_{\lambda=2}(A_3)\right]$, (m) similarly follow the steps from (b-l) by changing the i^{th} point from (A_1) to (A_2), and by treating (A_1) and (A_3) as j^{th} points; the $Z(A_2)$ is obtained, (n) obtained $Z(A_3)$, and (o) three zones $Z(A_1)$, $Z(A_2)$, and $Z(A_3)$ are shown with 1s, 2s, and 3s.

Point-to-Polygon Conversion

http://www.isibang.ac.in/~bsdsagar/AnimationOfPointPolygonConversion.wmv

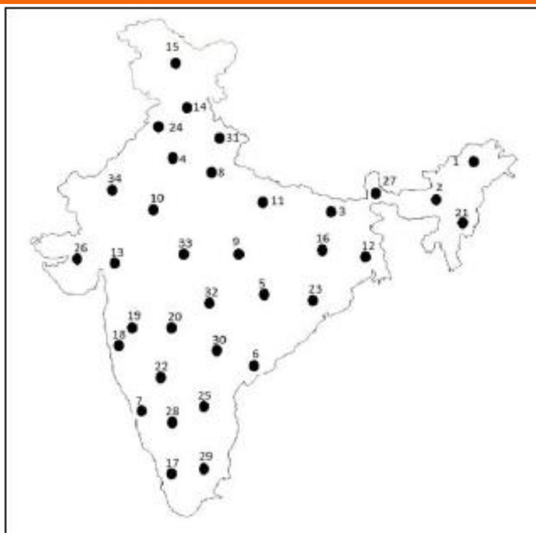

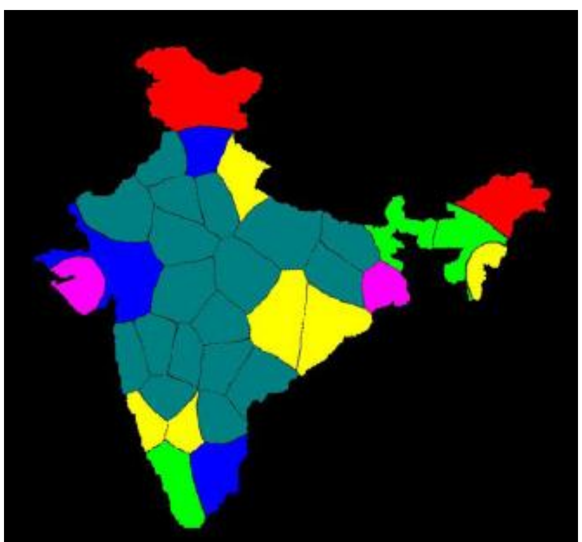

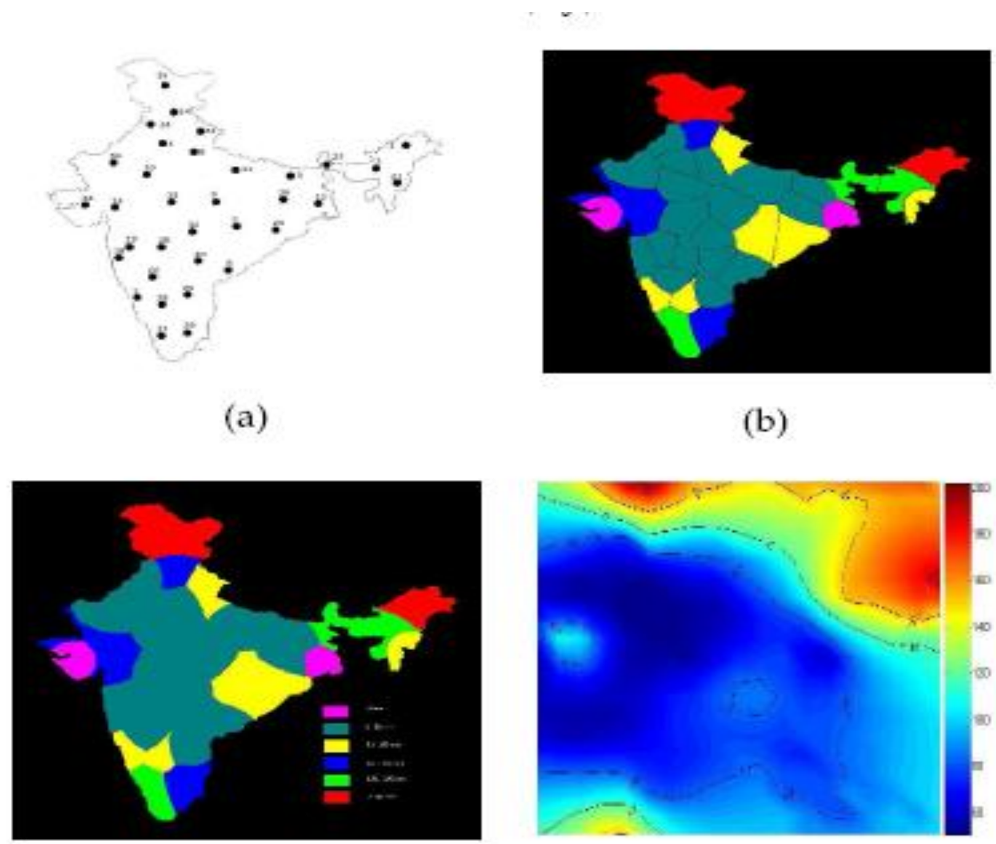

(a) (b)

(c) (d)

Fig. 4. (a) 34 points (locations) of rain-gauge stations spread over India indexed ($A_1 - A_{34}$), (b) Rainfall zonal map generated by having various possible propagation speeds, and the variable strengths in terms of propagation speeds are given according to ranks shown in Table 1, (c) broader zones obtained after merging the zones (Fig. 4b) obtained with similar propagation speeds, and (d) kriged map generated for 34 gauge station data.

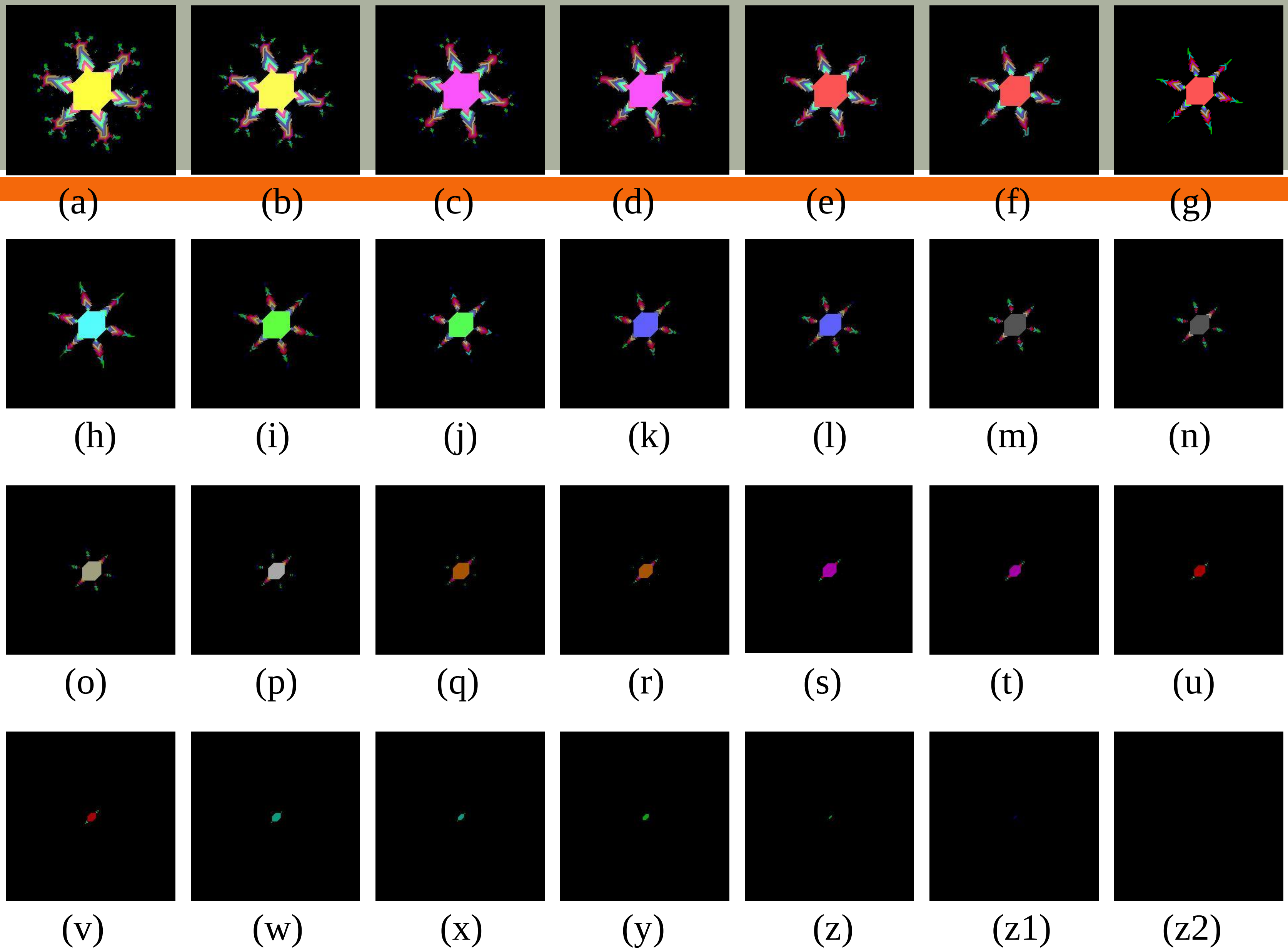

Extracting pore throat from eroded **triadic Koch curve** images by structuring element of octagon.

Top and side views of 3D model at

(a) binary pore,

(b) pore-bodies,

(c) pore-channel, and

(d) pore-throat

of **triadic Koch curve**

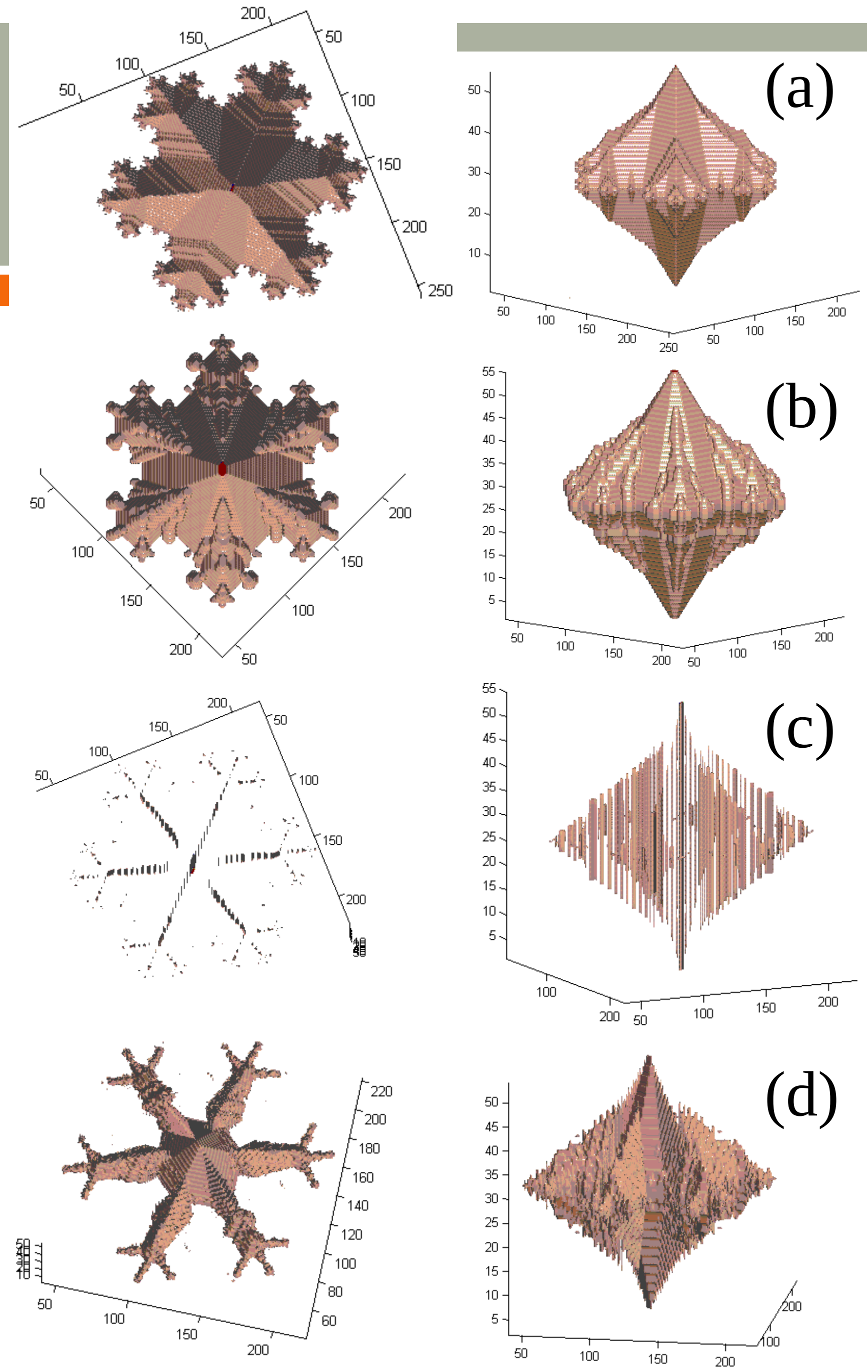

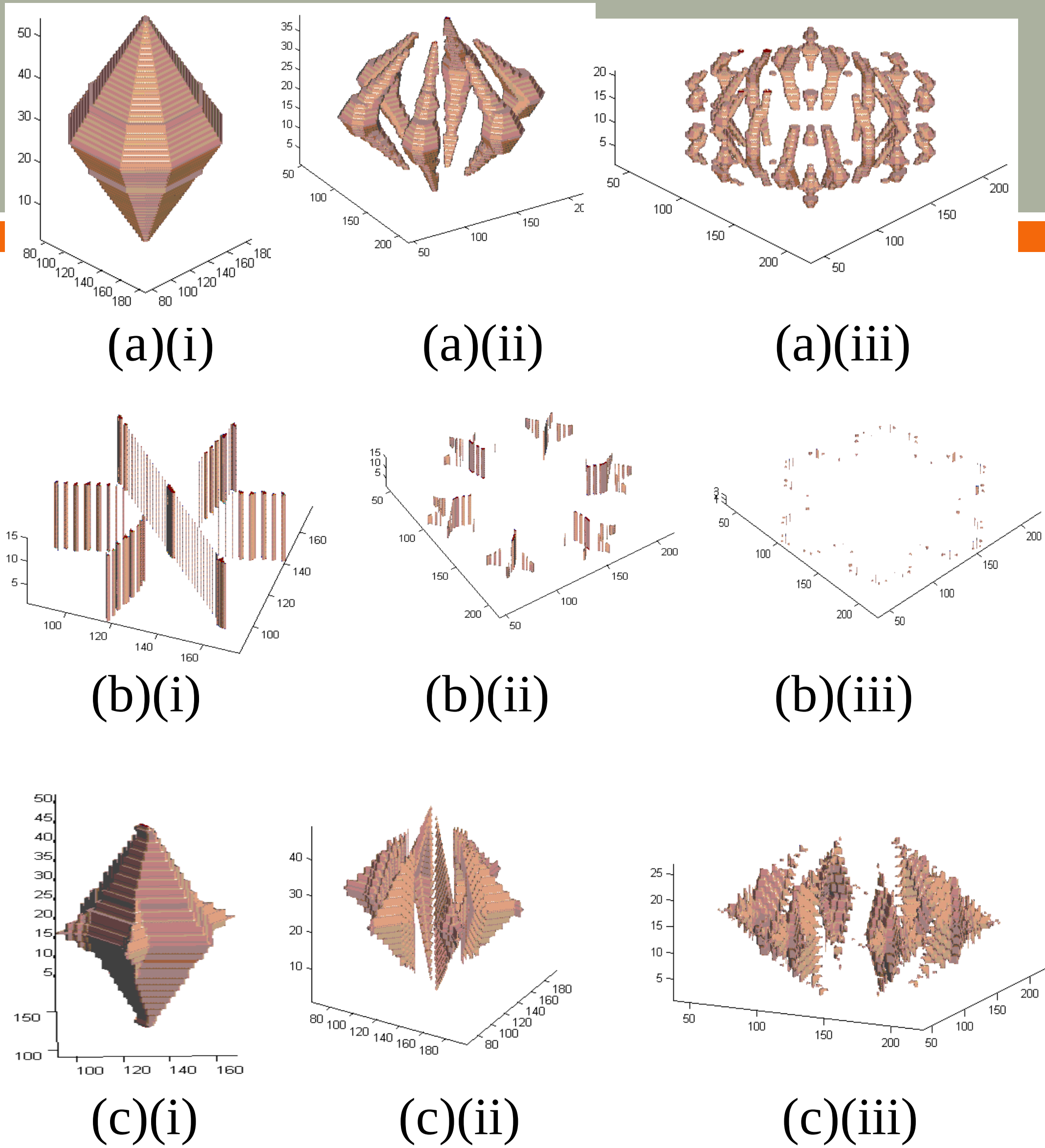

The diagram shows the order-wise isolated 3D pore quantities at (i) inner, (ii) middle and (iii) outer layers of

(a) pore bodies,

(b) pore channels, and

(c) pore throats.

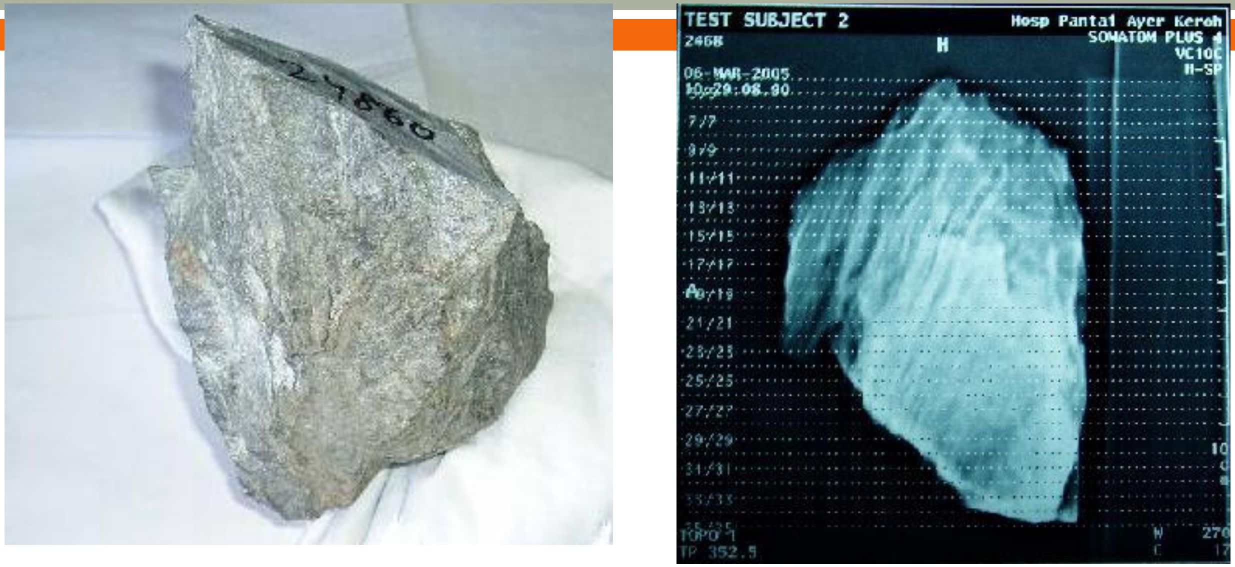

(a) (b)

(a) The photograph of schist rock sample; (b) the CT scans applied at schist rock sample

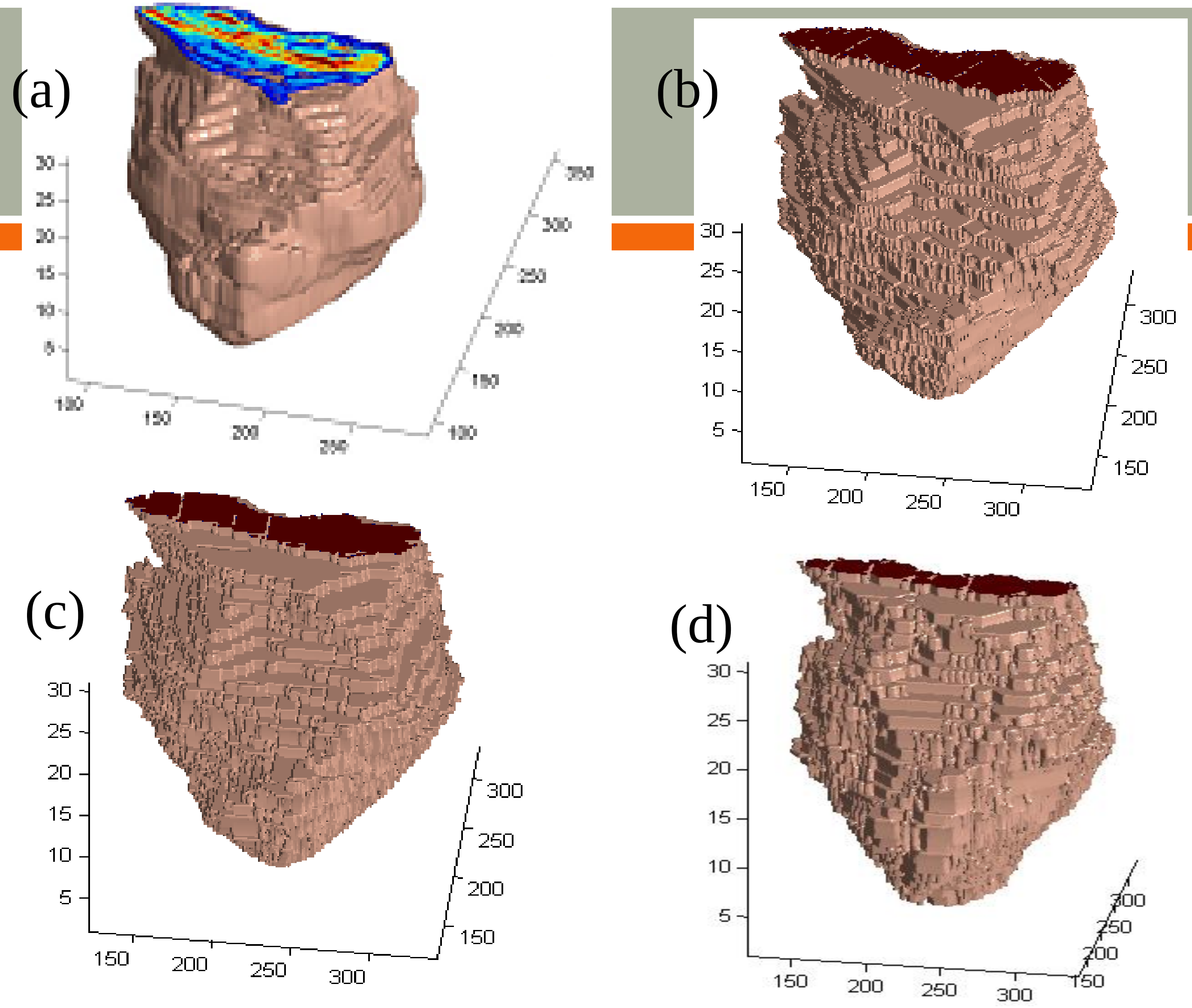

The 3D reconstruction of (a) binary schist image; non-overlapping decomposition technique by structuring elements of (b) rhombus, (c) square and (d) octagon

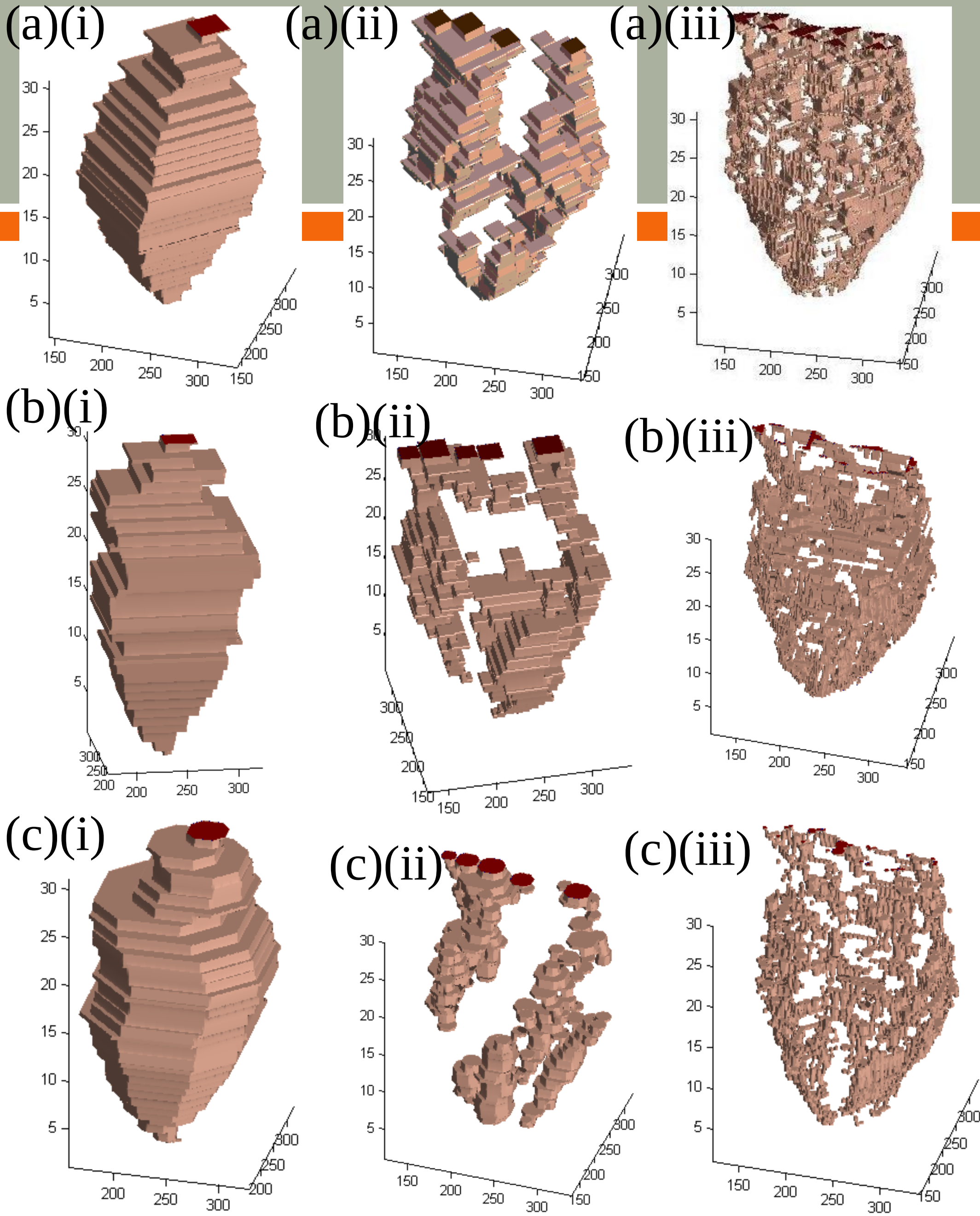

Order-wise isolated 3D rock quantities at (i) inner, (ii) middle and (iii) outer layers rock by structuring elements

(a) rhombus

(b) square, and

(c) octagon.

ACKNOWLEDGEMENTS

Support given by Bimal Roy and Sankar Pal (Current and Former Directors of Indian Statistical Institute) who created a great environment for academic research is gratefully acknowledged.

Grateful to collaborators, mentors, reviewers, examiners, friends, employers, well-wishers, and doctoral students—S. V. L. N. Rao, B. S. P. Rao, M. Venu, K. S. R. Murthy, Gandhi, Srinivas, Radhakrishnan, Lea Tien Tay, Chockalingam, Lim Sin Liang, Teo Lay Lian, Dinesh, Jean Serra, Gabor Korvin, Arthur Cracknell, Deekshatulu, Bhanu Prasad, Wolfgang-Martin Boerner, Alan Wilson, Michael Batty, Jack Schuenemeyer, Philippos Pomonis, Peter Atkinson, Hien-Teik Chuah, Laurent Najman, Jean Cousty, Christian Lantuejoul, Christer Kiselman, Alan Tan, Sankar Pal, Bimal Roy, Lim Hock, VC Koo, Rajesh, Ashok, Pratap, Rajashekhara, Saroj Meher, B. K. Sahu, K. V. Subbarao, Baldev Raj, C. Babu Rao, Sravan, Raghvendra Sharma, and several others.

Selected References

- Mandelbrot, B. B. (1982). The Fractal Geometry of Nature. Freeman, San Francisco.
- Turcotte, D. L. (1997). Fractals in Geology and Geophysics, Cambridge University Press, Cambridge.
- Matheron, G. (1975). Random Sets and Integral Geometry, John Wiley Hoboekn, New Jersey.
- Serra, J. (1982), Image Analysis and Mathematical Morphology, Academic Press, London.
- B. S. Daya Sagar, 2013, Mathematical Morphology in Geomorphology and GISci, ISBN-13: 9781439872000. Pages: 546, Publisher: Chapman & Hall

Selected References

- SAGAR, B. S. D.; VENU, M.; SRINIVAS, D. (2000): Morphological operators to extract channel networks from digital elevation models", International Journal of Remote Sensing," VOL. 21, 21-30.
- SAGAR, B. S. D.; MURTHY, M. B. R.; RAO, C. B.; RAJ, B. (2003): Morphological approach to extract ridge-valley connectivity networks from digital elevation models (DEMs), International Journal of Remote Sensing, VOL. 24, 573 – 581.
- TAY, L. T.; SAGAR, B. S. D.; CHUAH, H. T. (2005): Analysis of geophysical networks derived from multiscale digital elevation models: a morphological approach, IEEE Geoscience and Remote Sensing Letters, VOL. 2, 399-403.
- LIM, S. L.; KOO, V. C.; SAGAR, B. S. D. (2009): Computation of complexity measures of morphologically significant zones decomposed from binary fractal sets via multiscale convexity analysis, *Chaos, Solitons & Fractals*, VOL. 41, 1253–1262.
- LIM, S. L.; SAGAR, B. S. D. (2007): Cloud field segmentation via multiscale convexity analysis, *Journal Geophysical Research-Atmospheres*, VOL. 113, D13208, doi:10.1029/2007JD009369.
- SAGAR, B. S. D. (1996): Fractal relations of a morphological skeleton, Chaos, Solitons & Fractals, VOL. 7, 1871-1879.
- SAGAR, B. S. D.; TIEN, T. L. (2004): Allometric power-law relationships in a Hortonian Fractal DEM, Geophysical Research Letters, VOL. 31, L06501.
- TAY, L. T.; SAGAR, B. S. D.; CHUAH, H. T. (2006): Allometric relationships between travel-time channel networks, convex hulls, and convexity measures, Water Resources Research, VOL. 46, W06502.
- SAGAR, B. S. D. (2007): Universal scaling laws in surface water bodies and their zones of influence, Water Resources Research, VOL. 43, W02416.
- SAGAR, B. S. D.; CHOCKALINGAM, L. (2004): Fractal dimension of non-network space of a catchment basin, Geophysical Research Letters, VOL. 31, L12502.
- CHOCKALINGAM, L.; SAGAR, B. S. D. (2005): Morphometry of networks and non-network spaces, Journal of Geophysical Research, VOL. 110, B08203.
- TAY, L. T.; SAGAR, B. S. D.; CHUAH, H. T. (2007): Granulometric analysis of basin-wise DEMs: a comparative study, International Journal of Remote Sensing, VOL. 28, 3363-3378.
- SAGAR, B. S. D.; SRINIVAS, D.; RAO, B. S. P. (2001): Fractal skeletal based channel networks in a triangular initiator basin, Fractals, VOL. 9, 429-437.
- SAGAR, B. S. D.; VENU, M.; GANDHI, G.; SRINIVAS, D. (1998): Morphological description and interrelationship between force and structure: a scope to geomorphic evolution process modelling, International Journal of Remote Sensing, VOL. 19, 1341-1358.

Selected References

- SAGAR, B. S. D. (2005): Discrete simulations of spatio-temporal dynamics of small water bodies under varied streamflow discharges, Nonlinear Processes in Geophysics, VOL. 12, 31-40, 2005.
- SAGAR, B. S. D. (2010): Visualization of spatiotemporal behavior of discrete maps via generation of recursive median elements, IEEE Transactions on Pattern Analysis and Machine Intelligence, VOL. 32, 378-384.
- RAJASHEKHARA, H. M.; PRATAP VARDHAN; SAGAR, B. S. D. (2011): Generation of Zonal Map from Point Data via Weighted Skeletonization by Influence Zone, *IEEE Geoscience and Remote Sensing Letters* (Revised version under review).
- SAGAR, B. S. D.; PRATAP VARDHAN; DE, D. (2011): Recognition and visualization of strategically significant spatial sets via morphological analysis, *Computers in Environment and Urban Systems*, (Revised version under review).
- B. S. DAYA SAGAR, 2013, MATHEMATICAL MORPHOLOGY IN GEOMORPHOLOGY AND GISCI, ISBN-13: 9781439872000. PAGES: 546, PUBLISHER: CHAPMAN & HALL

A Book on Mathematical Morphology in Geomorphology and GISci
(CRC Press, Boca Raton, FL, 2013)

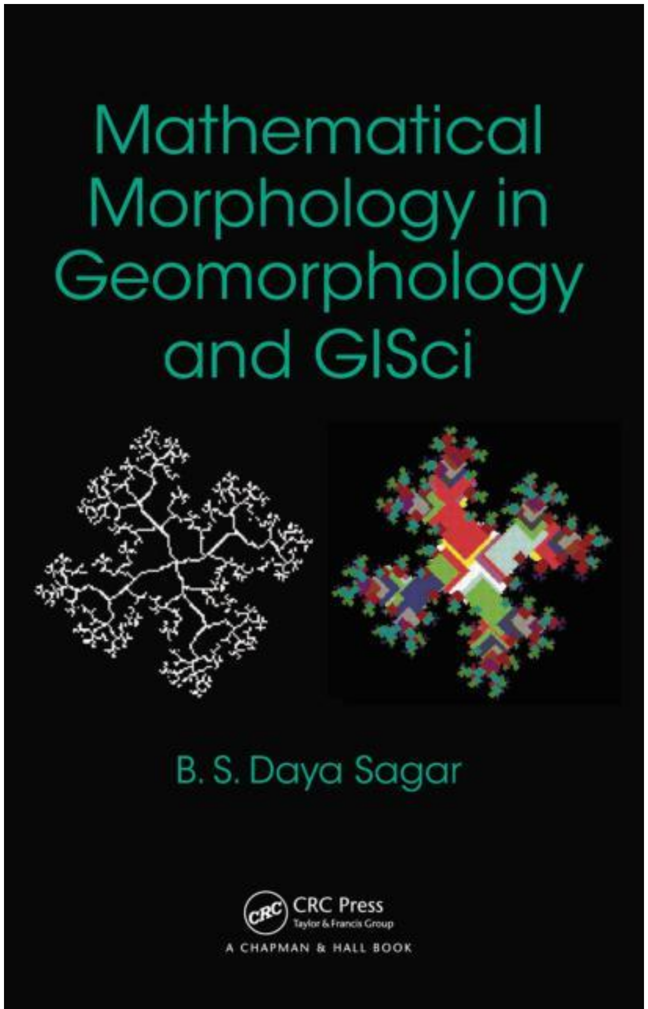

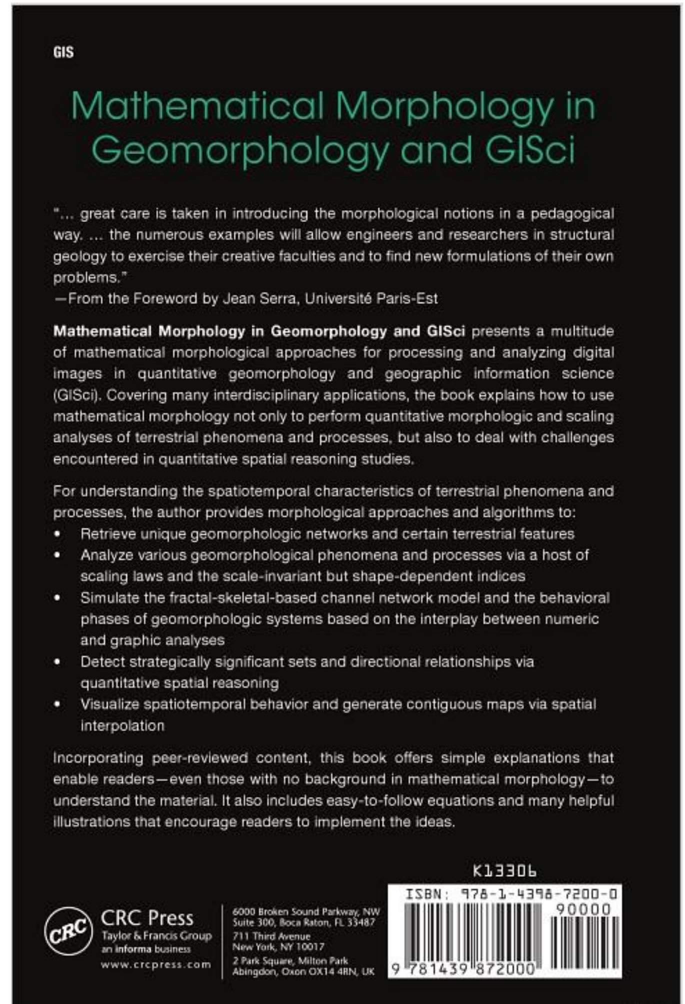
GIS

Mathematical Morphology in Geomorphology and GISci

"… great care is taken in introducing the morphological notions in a pedagogical way. … the numerous examples will allow engineers and researchers in structural geology to exercise their creative faculties and to find new formulations of their own problems."
—From the Foreword by Jean Serra, Université Paris-Est

Mathematical Morphology in Geomorphology and GISci presents a multitude of mathematical morphological approaches for processing and analyzing digital images in quantitative geomorphology and geographic information science (GISci). Covering many interdisciplinary applications, the book explains how to use mathematical morphology not only to perform quantitative morphologic and scaling analyses of terrestrial phenomena and processes, but also to deal with challenges encountered in quantitative spatial reasoning studies.

For understanding the spatiotemporal characteristics of terrestrial phenomena and processes, the author provides morphological approaches and algorithms to:

- Retrieve unique geomorphologic networks and certain terrestrial features
- Analyze various geomorphological phenomena and processes via a host of scaling laws and the scale-invariant but shape-dependent indices
- Simulate the fractal-skeletal-based channel network model and the behavioral phases of geomorphologic systems based on the interplay between numeric and graphic analyses
- Detect strategically significant sets and directional relationships via quantitative spatial reasoning
- Visualize spatiotemporal behavior and generate contiguous maps via spatial interpolation

Incorporating peer-reviewed content, this book offers simple explanations that enable readers—even those with no background in mathematical morphology—to understand the material. It also includes easy-to-follow equations and many helpful illustrations that encourage readers to implement the ideas.

K13306
CRC Press
Taylor & Francis Group
an informa business
www.crcpress.com
6000 Broken Sound Parkway, NW
Suite 300, Boca Raton, FL 33487
711 Third Avenue
New York, NY 10017
2 Park Square, Milton Park
Abingdon, Oxon OX14 4RN, UK
ISBN: 978-1-4398-7200-0
90000
9 781439 872000

Thank You

Q & A